BILAYER MEMBRANE LIPOSOME MIMICKING RED BLOOD CELL FOR DRUG DELIVERY APPLICATIONS

SUMAIRA NAEEM

FACULTY OF SCIENCE
UNIVERSITY OF MALAYA
KUALA LUMPUR

2019

BILAYER MEMBRANE LIPOSOME MIMICKING RED BLOOD CELL FOR DRUG DELIVERY APPLICATIONS

SUMAIRA NAEEM

THESIS SUBMITTED IN FULFILMENT OF THE REQUIREMENTS FOR THE DEGREE OF DOCTOR OF PHILOSOPHY

DEPARTMENT OF CHEMISTRY
FACULTY OF SCIENCE
UNIVERSITY OF MALAYA
KUALA LUMPUR

2019

UNIVERSITY OF MALAYA

ORIGINAL LITERARY WORK DECLARATION

Name of Candidate: **SUMAIRA NAEEM**

Matric No: **SHC130001**

Name of Degree: **DOCTOR OF PHILOSOPHY**

Title of Thesis: **BILAYER MEMBRANE LIPOSOME MIMICKING RED BLOOD CELL FOR DRUG DELIVERY APPLICATIONS.**

Field of Study: **PHYSICAL CHEMISTRY**

I do solemnly and sincerely declare that:

(1) I am the sole author/writer of this Work;
(2) This Work is original;
(3) Any use of any work in which copyright exists was done by way of fair dealing and for permitted purposes and any excerpt or extract from, or reference to or reproduction of any copyright work has been disclosed expressly and sufficiently and the title of the Work and its authorship have been acknowledged in this Work;
(4) I do not have any actual knowledge nor do I ought reasonably to know that the making of this work constitutes an infringement of any copyright work;
(5) I hereby assign all and every rights in the copyright to this Work to the University of Malaya ("UM"), who henceforth shall be owner of the copyright in this Work and that any reproduction or use in any form or by any means whatsoever is prohibited without the written consent of UM having been first had and obtained;
(6) I am fully aware that if in the course of making this Work I have infringed any copyright whether intentionally or otherwise, I may be subject to legal action or any other action as may be determined by UM.

Candidate's Signature Date:

Subscribed and solemnly declared before,

Witness's Signature Date:

Name:

Designation:

BILAYER MEMBRANE LIPOSOME MIMICKING RED BLOOD CELL FOR DRUG DELIVERY APPLICATIONS

ABSTRACT

The advancement of research in colloidal systems has led to the increased application of this technology in more effective and targeted drug delivery. The first closed bilayer phospholipid system, the liposome system, has been making steady progress in achieving many desirable parameters such as drug loading, size-controlling measures, stability longer circulation half-lives, triggered release and in overcoming obstacles to cellular and tissue uptake of drugs with improved biodistribution *in vitro* and *in vivo*. The current study focused on preparing liposomes which could mimic certain characteristics of red blood cell bilayer membranes to overcome problems in sustained and targeted drug delivery. With this aim, liposomes from different phospholipids namely L-α-Phosphatidylcholine (PC), 1,2-Dipalmitoyl-sn-glycero-3-phosphocholine (DPPC) , 1,2-Distearoyl-sn-glycero-3-phosphocholine (DSPC), 1,2-Diacyl-sn-glycero-3-phospho-L-serine (PS) and L-α-Phosphatidylinositol (PI) were formulated in combination with surfactants Polysorbate 80 (TWEEN® 80) and dihexadecyl phosphate (DCP) under physiological conditions. Phosphatidylinositol and dicetyl phosphate were expected to enhance the negative zeta potential of the liposomes in order to mimic red blood cell zeta potential. The newly prepared liposomes were formulated for efficient anticancer drug delivery applications. Liposomes were prepared from thin film hydration technique followed by sonication. Under the optimal experimental conditions, liposomes were formulated to mimic red blood cell surface charge (-3 mV to -14 mV) with a particle size range of 70 nm to 80 nm. The stability of all formulations was investigated by their mean particle size and zeta potential at 4 °C, 28 °C, and 37 °C for 28 days. The presence of liposomes in unsonicated formulations was identified by an optical polarizing microscope which was followed by transmission electron microscopy

and field emission scanning electron microscopy for identification of sonicated liposomes. Encapsulation efficiency for all liposomes loaded with different anticancer drugs was more than 60 % using viva spin centrifugal units, however, anticancer drugs with intermediate log *P* were encapsulated more than 60 %. Less than 20 % of the anticancer drugs were released in first 12 hours showing a released property very useful for inhibiting the proliferation of cancer cells. MDA-MB-231 breast cancer cell line was selected to investigate the in vitro cytotoxic effects of selected liposomes with most commonly used anticancer drug DOX (F1-DOX, F2-DOX, F3-DOX as model formulations) and their response to free and encapsulated DOX concentrations. These liposomes were found to induce significant suppression in MDA-MB-231 breast cancer cell growth qualitatively, whereas no cytotoxicity was observed due to unloaded F3-Liposomes. An obvious cell uptake of DOX was observed by its fluorescence property. Cell uptake by flow cytometry though was quantitatively less than free drug, yet these newly formulated DOX-loaded targeted F3-liposomes suggest potential utility as anticancer agents and may be beneficial for manufacturing biomimetic systems for drug delivery applications.

Keywords: liposomes, phospholipids, anticancer drugs, biocompatibility, cell cytotoxicity

LIPOSOM MEMBRAN DWILAPISAN MENIRU SEL DARAH MERAH UNTUK KEGUNAAN PENGHANTARAN UBAT

ABSTRAK

Kemajuan penyelidikan dalam sistem koloid telah mengakibatkan peningkatan penggunaan teknologi ini dalam sasaran penghantaran ubat yang lebih berkesan. Lapisan sistem fosfolipid yang pertama, sistem liposom, telah membuat kemajuan yang mantap dalam mencapai banyak parameter yang diingini seperti pemuatan dadah, pengukuran kawalan saiz, kestabilan peredaran setengah hayat, pencetus pelepasan dan langkah-langkah dalam mengatasi halangan-halangan ke atas pengambilan ubat terhadap sel dan tisu dengan biodistribusi yang lebih baik secara *in vitro* dan *in vivo*. Kajian semasa memberi tumpuan kepada penyediaan liposom yang boleh meniru ciri-ciri tertentu lapisan membran sel darah merah untuk mengatasi masalah dalam sasaran penyampaian dadah yang berkekalan. Dengan tujuan ini, liposom dari fosfolipid yang berbeza iaitu L-α-fosfatidilkolin (PC), 1,2-Dipalmitoil-sn-glisero-3-fosfokolin (DPPC), 1,2-Distearoil-sn-glisero-3-fosfokolin (DSPC), 1,2-Diasil-sn-glisero-3-fosfo-L-serin (PS) dan L-α-fosfotidillinositol (PI) telah dirumusankan dengan gabungan surfaktan Polisorbat 80 (TWEEN® 80) dan fosfat dihexadesil (DCP) di bawah keadaan fisiologi. Phosphatidylinositol dan dicetil fosfat dijangka dapat meningkatkan keupayaan zeta negatif liposom untuk meniru keupayaan zeta sel darah merah. Liposom yang baru disediakan dirumuskan untuk aplikasi penghantaran ubat antikanser yang cekap. Liposom telah disediakan daripada teknik penghidratan filem nipis diikuti oleh sonikasi. Di bawah keadaan eksperimen yang optimum, liposom dirumuskan untuk meniru cas permukaan sel darah merah (-3 mV hingga -14 mV) dengan julat saiz zarah 70 nm hingga 80 nm. Kestabilan semua rumusan diselidiki oleh saiz zarah dan nilai keupayaan zeta mereka pada 4 ºC, 28 ºC, dan 37 ºC selama 28 hari. Kewujudan liposom dalam rumusan yang tidak disonikasi telah dikenalpasti oleh mikroskop polarisasi optik yang

mana diikuti oleh mikroskop elektron penghantaran dan mikroskopi pengimbasan pelepasan medan elektron untuk mengenal pasti liposom yang telah berjaya disonikasi. Kecekapan pengkapsulan untuk semua liposom yang dimuatkan dengan ubat antikanser (leucovorin kalsium (LVC), methotrexate (MTR), doksorubicin hidrokloride (DOX) dan irinotekan (IRT)) yang berbeza adalah lebih daripada 60 % dengan menggunakan unit emparan vivaspin, bagaimanapun, ubat antikanser dengan log perantaraan *P* diungkapkan lebih dari 60 %. Kurang daripada 20 % ubat antikanser dilepaskan dalam 12 jam yang pertama menunjukkan ciri-ciri yang sangat berguna untuk menghalang percambahan sel-sel kanser. Kadar ubat yang dimuatkan, dilepaskan dari liposom dalam PBS. Sel kanser payudara MDA-MB-231 telah dipilih untuk mengenal pasti kesan sitotoksik *in vitro* dari liposom terpilih dengan ubat antikanser yang paling biasa digunakan DOX (F1-DOX, F2-DOX, F3-DOX sebagai model rumusan) dan tindak balas mereka untuk bebas dan terkandung dalam kepekatan DOX. Liposom ini didapati menyebabkan penindasan ketara dalam pertumbuhan sel kanser payudara MDA-MB-231 secara kualitatif, manakala tiada sitotoksisiti dapat diperhatikan yang disebabkan oleh F3-Liposom yang tidak dimuatkan. Pengambilan DOX oleh sel jelas diperhatikan melalui ciri-ciri pendarfluor yang dimilikinya. Pengambilan sel oleh aliran sitometri walaupun secara kuantitatif kurang daripada dadah yang bebas, namun F3-DOX liposom yang baru dirumuskan dapat mencadangkan utiliti yang berpotensi sebagai agen antikanser dan mungkin bermanfaat untuk pembuatan sistem biomimetik untuk aplikasi penghantaran dadah.

Kata kunci: liposom, fosfolipid, ubat antikanser, biokompatibiliti, sitotoksisiti sel

ACKNOWLEDGEMENTS

In the name of Allah, the REHMAN, the RAHIM. I would like to pay humble gratitude to my respected supervisors Professor Dr. Misni Bin Misran, Associate Professor Dr. Kiew Lik Voon Professor Dr. Chung Lip Yong for nourishing me with innovative ideas and guidance throughout the project. They provided me with the right balance of freedom and direction to make the project well defined, yet flexible enough to allow for a free ranging, interdisciplinary body of work to evolve. I also wish to express my sincere thanks to Dr. Kiew Lik Voon and Professor Lip Yong Chung for providing me with all the necessary laboratory consumables and facilities for this research while at Faculty of Medicine, University of Malaya (UM). Besides, I wish to express my sincere thanks to Dr. Geetha Viswanathan who patiently assisted and encouraged me throughout this project in Faculty of Medicine, UM. I am truly thankful and indebted to her for sharing her expertise and providing valuable guidance to me.

My special thanks to Dr. Teo Yin Yin, Dr. Vicit, Dr. Shu xain, Dr. Prema, Dr. Anita, Dr. Siew Hui, Dr. Siaw Fui, Suk Fong, and all Pakistani fellows for the stimulating discussions, for the sleepless nights we were working together before deadlines. I gratefully acknowledge the funding sources Bright Sparks Scholarship Unit, UM and IPPP (PG094-2014A) that made Ph.D work possible. Last but not the least, I would like to thank my family, my parents (my mother Mrs. Naseem Begum and my late father Mr. M. B. Naeem), to my brothers and sisters, to my in laws especially my father in law, my beloved husband, Mr. Sheikh Muhammad Sheikh, my daughters Dua and Ayesha whose continuous motivation, love, support and encouragement made this dream come true.

Sumaira Naeem

September, 2019

TABLE OF CONTENTS

LIST OF FIGURES

LIST OF TABLES

LIST OF SYMBOLS AND ABBREVIATIONS

A		Absorbance
A	:	Particle radius
C	:	Concentration of analyte
C_{aq}	:	Concetration of drug in aqeous medium
C_{oct}	:	Concentration of drug in octanol medium
CVC	:	Critical vesiculation concentration
D	:	Translational diffusion constant
DCP	:	Dicetyl phosphate
d_H	:	Hydrodynamic diameter
DLS	:	Dynamic light scattering
DOX	:	Doxorubicin hydrochloride
DPPC	:	1,2-dipalmitol-sn-glycero-3-phosphocholine
DSPC	:	1,2-dipalmitol-sn-glycero-3-phosphocholine
EE	:	Encapsulation efficiency
$F\ (ka)$	:	Henry‘s function
FESEM	:	Field emission scanning electron microscopy
I	:	Exiting light
i.e.		Id est (it is)
I_o	:	Incident light
IRT	:	Irinotecan
K	:	Boltzmann constant
LVC	:	Leucovorin calcium
MTX	:	Methotrexate
MWCO	:	Molecular weight cut off

OPM	:	Optical polarizing microscope
P	:	Partition coefficient
PBS	:	Phosphate buffer saline
PC	:	L-a-phosphatidylcholine
PI	:	L-a-phosphatidylinositol
PMT	:	Photomultiplier tube
TEM	:	Transmission electron microscopy
U_E	:	Electrophoretic mobility
V	:	Volume
W	:	Weight
W_f	:	Weight of the unloaded free drug
W_t	:	Total weight of drug
Z	:	Zeta potential
E	:	Molar absorptivity coefficient
ε_r	:	Dielectric constant

CHAPTER 1: INTRODUCTION

1.1 Overview

The fate of drug loaded nanomaterials in complex biological networks has become one of the most challenging issues in drug delivery systems. The major considerations while designing are targeting efficiency of these nanoparticles and circulation half-life in the blood. Liposomes have emerged as effective anticancer drug delivery carriers with ultimately achieving drug dissolution in a biological medium followed by an appropriate targeted drug release and absorption rate with near-zero damage to the rest of the body (Barenholz, 2016; Daraee *et al.*, 2016; Shi *et al.*, 2017).

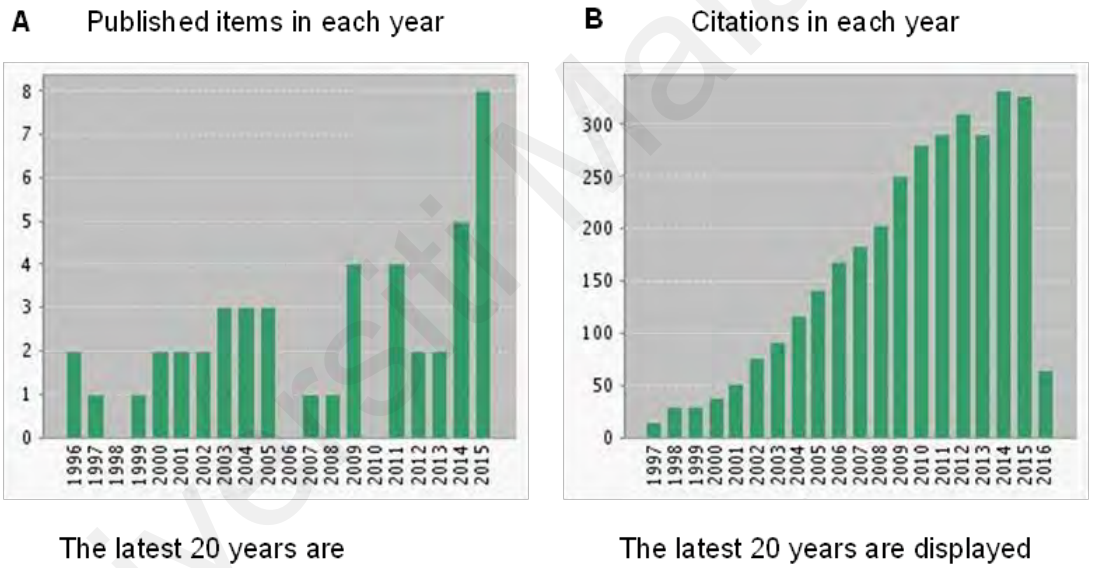

Figure 1.1: Total number of published (A) and cited (B) publications on liposomes as anticancer drug delivery carriers. Citation report graphic is derived from Thomson Reuters Web of Science, Copyright Thomson Reuters.

Being biocompatible and biodegradable with good possibility for size and surface manipulations, severa; liposome nanoformulations have been approved and commercialized against a multitude of human cancer diseases like HIV-related Kaposi sarcoma, ovarian cancer, and multiple myeloma, acute lymphoblastic leukaemia, metastatic breast cancer (Ahmad *et al.*, 2016; Allen *et al.*, 2013; Deng *et al.*, 2017;

Hsin-I *et al.*, 2012; Shamsi *et al.*, 2017). Figure 1.1 clearly reflects the increasing interest for liposomes for efficient anticancer drug delivery vehicles.

The term ‗cancer' actually refers to a class of diseases; therefore, it is unlikely to idealize a single cure for cancer. The attempts for cancer therapy have been revolutionized over decades as the underlying mechanisms are more explore and lead to more understanding the disease. Several experimental strategies are under development for a near complete cure of cancer (if detected at the early stage) with as minimum side effects of chemotherapeutic drugs as possible. Out of different choices of therapy like surgery, chemotherapy, radiation therapy, hormonal therapy, or targeted therapy; the selection criteria is specified with reference to the tumor location and grade, stage of disease and above all the general health condition of the patient. Current research offers new dosing routes via blood vessels to fuel tumor growth with more specific targeting actions. Whatever the route or treatment may be, the eventual expectation is the improved change in patient's quality of life and least damage to the normal healthy tissues.

Unfortunately, the treatments covering all oncological specifications are still not good enough to kill the cancer cells before the cancer kills the patient. Non-specific distribution of cytotoxic drugs may lead to variety of toxic effects by killing both normal and malignant cells (Ishida *et al.*, 2015). Controlled release, understanding target structure and function, achievement of the maximum therapeutic effect, minimized risk to benefit ratios have been the major factors in designing novel drug delivery systems in the past few decades (Daraee *et al.*, 2016; Sercombe *et al.*, 2015).

The advancement in nanotechnology had bridged the gap by offering different drug delivery carriers with a hope to move us away from near-toxic doses of non-specific agents (Bagalkot *et al.*, 2016; Brannon-Peppas *et al.*, 2012).

Colloidal systems, being at the epicenter of modern drug delivery systems in cancer management, have led the research to enter a new era of nanoengineering and nanotechnology. A variety of colloidal nanoparticles have been proposed as carriers like composite nano-shells, dendrimers, viral nanoparticles, magnetics nanoparticles, quantum dots, micells and liposomes (Bigdeli *et al.*, 2016). Among these, drug encapsulation into liposomes resulted in increased circulation times, increased drug deposition to tumor tissues by decreasing drug metabolic degradation, and their altered tissue distribution in the body. They provide a paradigm for the design of nanocarriers with a broad spectrum of functionality, applicability, and versatility of synthetic drug delivery particles.

Liposomes are amphiphilic carriers which possess both hydrophilic (polar) and lipophilic (non-polar) properties (Suzuki *et al.*, 2016; Xiao *et al.*, 2015). The amphiphilic compound tends to partition when placed in an immiscible biphasic system containing both aqueous and organic solvents. The extent of partitioning is evaluated by the extent of hydrophobic and hydrophilic portion of that compound. Liposomes prepared by phospholipids have gained tremendous attention as novel and efficient targeted drug delivery carriers. Phospholipids are very important amphiphiles and are found as main components of the biological membranes where they define the way of membrane formation (Li *et al.*, 2015). They position as bilayers whereby their polar groups are exposed towards the surrounding aqueous medium and lipophilic chains are sandwiched between polar head groups throughout the bilayer arrangement.

Drug delivery requires designing liposomes in such a way so as to optimize carriers with reference to drug loading, controlled drug release rate, rapid clearance by reticuloendothelial system, and above all the drug delivery across cell membranes to intracellular sites of action (Allen *et al.*, 2013). The nanoparticles are purposely engineered ranging from a few nm to several hundred nm so as to pass through the

fenestration of the leaky cancer endothelium. All the Nano-vehicles are constructed on the basis of their use and preferential accumulation at tumor sites with fewer accumulations in liver, lungs, spleen, and bone marrow (Haley *et al.*, 2008). It is very important to take a look at tumor environment for better understanding of its cure and problem solving aspects. It is important to understand the concepts of tumor vasculature, tumor interstitium, and cellular resistance abnormal cell growth phenomenon (Baban *et al.*, 1998; Eberhard *et al.*, 2000), resistance to the inward flux, EPR effect (Ishida *et al.*, 2003; Jain, 2001; Jang *et al.*, 2003) and cellular resistance mechanisms (Brown *et al.*, 1999; Vasir *et al.*, 2005).

Clinical trials have opened new era for the patients to choose the best option which may increase survival time and the quality of life by killing cancer before the cancer kills the patients (Halwani *et al.*, 2015). Some of the exemplary FDA approved liposomes like liposomal doxorubicin (Doxil), liposomal daunorubicin (DaunoXome), liposomal vincristine (Marqibo), liposomal irinotecan (Onivyde or MM-398), and liposomal doxorubicin (Myocet) have been used in clinical practice (Shi *et al.*, 2017).

Innovation in the field of synthetic drug delivery biomaterials has gained fundamental importance in terms of functionality and diversity. However, it cannot reach the complexity and sophistication levels exhibited by distinctive biological moieties. A huge scientific challenge in drug delivery has been to bring out ―adaptable" materials, inspired by nature, since they can mimic their structure and functionality dynamically on demand. The need to develop drug delivery systems to combat cancerous tissues has led researchers to craft new natural and synthetic formulations (Han *et al.*, 2015). Researchers have been investigating the use of natural moieties to design carriers with better biocompatibility and biodegradability; a classical example being mimicking of red blood cell (RBCs) bilayer membranes (Kirch *et al.*, 2012). Various anticancer drug carriers have been formulated to mimic different characteristics

of RBC membranes using diverse range of precursors. RBCs are one of the most investigated biological moieties for targeted drug delivery purposes. Being the only means to transfer oxygen to the whole body, RBCs also possess such unique membranes which serve to regulate surface deformability, flexibility, adhesion to other cells, and last but not the least, immune recognition. Bilayer membrane liposomes infusing phospholipids have long been synthesized to mimic bioconcave RBC carriers using the notion of stealth liposomes.

Three different types of RBC mimics have been utilized in drug delivery such as RBC membrane ghosts (Han *et al.*, 2012), engineered RBC as synthetic carriers (Doshi *et al.*, 2009), and RBC-membrane clocked vehicles (Fang *et al.*, 2013) as has been depicted in Figure 1.2.

Figure 1.2: Different strategies to prepare red blood cell mimics for drug delivery applications.

1.2 Problem Statement

In order to make a biocompatible and biodegradable carrier, a foremost scientific challenge has been an inspiration by natural cell membranes and to mimic some of their characteristics for drug delivery applications. This will lead to prepare liposomes which could mimic red blood cell bilayer membrane zeta potentials for efficient drug delivery applications.

1.3 Research Objectives

This work aims at the formulation of synthetic red blood cell bilayer membrane liposome for drug delivery applications. Keeping in mind, the aim and scope of this work, following specific objectives have been set:

1. To prepare liposomes mimicking RBC membrane zeta potential using thin film hydration method.
2. To characterize those liposomes for drug delivery application following measurement of mean particle size (including CVC measurement), mean zeta potential, stability studies, morphology via OPM, TEM, SEM, and DSC.
3. To evaluate % encapsulation efficiency for anticancer drugs, and to study in vitro drug release properties of anticancer drugs from RBC mimicking liposomes in PBS (pH 7.4).
4. To determine the hemocompatibility of the RBC mimicking liposomes via % hemolysis and cell aggregation tests.
5. To investigate application in biodistribution (cell cytotoxicity and cell uptake) of anticancer drug using breast cancer cell line.

1.4 Thesis Outlines

This thesis presents the scope of liposomes as hydrophilic and hydrophobic anticancer drug carriers. This work covers the formulation of liposomes based on mimicking red blood cell zeta potentials, characterization of these liposomes, properties and applications in *in vitro* drug delivery. Thesis outlines are presented below:

Chapter 1 emphasizes the basic introduction of the liposomes, an overview of the anticancer drug delivery with a special focus on red blood cell mimicking, its importance and applications in drug delivery.

Chapter 2 presents a detailed literature review on the need for drug delivery systems, its history and development; potential drug carriers developed so far, types of various red blood cell mimics. This chapter describes the method of preparing red blood cell mimicking liposomes, characterization with respect to average particle size, average zeta potentials, microscopic studies of the morphology, encapsulation of hydrophilic and hydrophobic anticancer drugs into the amphiphilic liposomes. It also describes the targeted drug release of anticancer drugs and biological challenges related to drug delivery applications.

Chapter 3 introduces the materials and methods adopted for the formulation of phospholipid liposomes using various liposomes, physicochemical characterization, biocompatibility assessment methods and *in vitro* cell uptake and cell cytotoxicity for drug delivery applications.

Chapter 4 presents the results obtained and covers the comprehensive discussion on the liposome formulation, characterization with reference to particle size, zeta potential, morphology, *in vitro* drug release of anticancer drugs, biocompatibility and application in biodistribution (cell cytotoxicity and cell uptake) of anticancer drug using breast cancer cell line.

The findings and results of this research work are summarized in chapter 5, followed by the list of recommendations for further studies.

CHAPTER 2: LITERATURE REVIEW

2.1 The Need for Nanocarrier Drug Delivery Systems (DDS)

One of the foremost scientific challenges in the field of drug delivery has been to design ‗adaptable' materials, taking inspiration from mother nature, since these could dynamically mimic their structure and functionality on demand (Chu *et al.*, 2013; Doshi *et al.*, 2010). Lipid bilayer vesicles, which are responsive to external stimuli, are gaining special attention in recent areas of development. The RBC membrane ghosts, RBC membrane cloaked polymeric nanoparticles and synthetic RBC mimics are a new class of nanocarriers as camouflaged by RBC membrane (Hu *et al.*, 2011). These nanocarriers have great potential to be used to deliver drug payloads with polymeric cores. Tremendous amount of work has been done on phospholipid bilayer microcapsules liposomes since their discovery by Bangham and his colleagues (Bangham *et al.*, 1965). Liposomes were later recognized as potential nanocontainers for targeted drug delivery due to their versatile nanosize (Han *et al.*, 2012).

The liposomes being biocompatible and biodegradable, do not invoke unwanted toxic and antigenic reactions hence have great advancement in research for pharmaceutical industry (Meyer, 1998). The phospholipids, in combination with some additional molecules, offer new horizons for obtaining desired size, surface charge and morphology when selected for varied compositions of liposome bilayers. Some of the key drug carrier properties have been narrated in Table 2.1 (Ahmed *et al.*, 2005; Allen *et al.*, 2013). Liposomal delivery systems have been developed to work well in life processes like transportation, distribution, controlled release, protection and localization of encapsulated constituents. They have subsequent applications such as entangled anticancer drugs, antimicrobial drugs, enzymes along with antigens and all these have been demonstrated by previous studies (Gomez-Hen *et al.,* 2006).

Table 2.1: Role of the key drug carrier properties in sustained drug delivery.

Key property	Applications	References
Size	Circulation times Renal clearance Target accumulation Endocytosis	(Bareford and Swaan, 2007; Geng *et al*., 2007; Karavas *et al.,* 2007; Petros and DeSimone, 2010)
Shape	Circulation times Vascular adherence Endocytosis Endosomal escape Toxicity	(Albanese *et al.,* 2012; Muro *et al.,* 2008; Vahidkhah and Bagchi, 2015; Xu *et al.,* 2006)
Surface Chemistry	Circulation time Target accumulation Endocytosis Endosomal escape Toxicity	(He *et al.,* 2011; Nel *et al.,* 2009; Vercauteren *et al.,* 2009; Verma and Stellacci, 2010; Xiao *et al.,* 2011)
Mechanical Properties	Circulation time Biodistribution Phagocytosis	(Amoozgar & Yeo, 2012; Boyer, Whittaker, Bulmus, Liu, & Davis, 2010; Mitragotri & Lahann, 2009; Polyak & Friedman, 2009; Simone, Dziubla, & Muzykantov, 2008)

2.2 Drug Carriers

Drug carriers have long been used to serve as mechanisms to prolong *in vivo* drug pharmacological activities. Various drug carriers are believed to be biodegradable and may include microspheres, albumin microspheres, synthetic polymers, nanofibers, Protein-DNA complexes, protein conjugates, red blood cell mimics, virosomes, and liposomes. A brief description of these drug carriers is as follows:

2.2.1 Microspheres

Micropsheres, sometimes referred to as microparticles, are spherical shells made up of polymers, waxy, or other protective materials such as starches, gums, proteins, fats and waxes. These exhibit a size typically between 1µm to 1000 µm (1mm). These are usually spherical in shape with no distinct outer membrane. These are used as drug carrier matrices for drug delivery applications. Biomedical applications include cell imaging (Gui *et al.,* 2014), controlled *in vitro* drug release (Metaxa *et al.,* 2014), to prevent microbial biofilms associated infections and to decrease the rates of microbial resistance to antibiotics (Grumezescu *et al.,* 2014).

2.2.2 Nanofibers

Nanofibers are unique structures making a new exciting class of materials which can be generated from different polymers. These nanofibers have different physical properties and potential application in medical, filtration, barriers, insulation and energy storage etc. Nanofibers, with diameters less than 100 nanometers, are efficient against infections caused by multitude resistant organisms (Ramalingam *et al.,* 2015), cell regeneration and proliferation for tissue engineering applications (Maleknia and Majdi, 2014), potential applications as wound dressing (Xu *et al.,* 2015), and may also be used to reduce toxicity levels to normal primary fibroblasts by killing HeLa (Henrietta Lacks) cancer cells (Chaudhary *et al.,* 2015; Wang *et al*., 2015).

2.2.3 Synthetic Polymers

These are man-made polymers and classified as thermosets, elastomers and synthetic fibers on the basis of their usage. Their functions include a contrast for different imaging modalities, targeted delivery of drugs/genes, and in thermal therapies (Bao *et al.,* 2013).

2.2.4 Dendrimers

Dendrimers, as a new class of polymeric materials, are repetitively branched molecules and have a typical spherically symmetrical three-dimensional morphology. These are nano-sized, homogenous, and monodieperse particles and can encapsulate hydrophobic compounds and have been reported to be used especially for the delivery of anticancer drugs (Lee *et al.,* 2005). These are preferred often for enhanced solubilization of drug.

2.2.5 Virosomes

Virosomes are like non-replicating artificial viruses and as a drug or vaccine delivery vesicle, can incorporate virus derived proteins and fuse with target cells (Hajizade *et al.,*

2015) with probably nasal route of administration (Scherließ, 2015). Virosome are platform for subunit vaccines with an excellent immunogenicity and tolerability profile for adjuvant non-influenza antigen systems has proven effective clinically (Moser *et al.,* 2003; Felnerova *et al.,* 2004).

2.2.6 Protein Conjugates

Peptides and proteins have drawn a special attention for their wide scope in the drug delivery. These are nano-sized, multi-component constructs already in clinics as anticancer compounds. These may also alter the pharmacokinetics profile of the loaded drugs after inhaled administration. Conjugates of polymers with proteins have long been investigated for potential renal drug targeting (Franssen *et al.,* 1992), increased stability without sacrificing binding affinity or bioactivity (Keefe & Jiang, 2012), and also in anticancer nanomedicine (Duncan, 2006).

2.2.7 Liposomes

One of the superior features of the liposomes are their amphiphilic nature, appreciable particle size distribution, exceptional surface properties, and pH-responsive release properties that make them ideal carriers for delivering anticancer therapeutics (Suzuki *et al*., 2016). A liposome is defined as a tiny spherical bubble that has a very similar composition as that of a cell membrane. They may also be prepared by disruption of biological membranes using sonication methods. Most of the animal cell membranes consist of approximately 50 % of lipids, which are all amphiphilic in nature, i.e. having a water-loving or polar end and a water-fearing or nonpolar end. An average animal cell contains approximately 109 lipid molecules in its plasma membrane. Extensive research has been going on globally to mimic natural cell membranes to formulate biocompatible and biodegradable drug carriers. Liposomes are most frequently prepared using phospholipids. Phosphatidylcholine has been found to be the

most commonly used one; however, other lipids such as egg phosphatidylethanolamine, phosphatidylserine (Hosseini *et al*., 2015, Bagalkot *et al*., 2016), and phosphatidylinositol (Van Den Bogaart *et al*., 2012, Dondelinger *et al*., 2014, Yoshida *et al*., 2016) have also been reported to be compatible with lipid bilayer structures (Szeto & Lavik, 2016). There are two types of liposomes, namely, unilamellar liposomes and multilamellar liposomes. The first type refers to spherical vesicles bounded by a single amphiphilic lipid layer or mixture of many lipids whereas the other type consists of several concentric lipid layers similar to an onion‘s layers. The size of the former may range from 100 nm up to a few micrometers whereas the latter may be up to several micrometers (Tsai & Rizvi, 2016). Both types are important for targeted drug delivery but multilamellar vesicles have a higher risk of being taken up by phagocytic cells in the body (Kume *et al*., 1991). Therefore, single lamellar vesicles are used preferably for overall drug delivery purposes (Schieren *et al.,* 1978, da Silva *et al.,* 2016). A simple layout of liposome formulation is shown in Figure 3. Our body is a complicated machine and is composed of four main classes of molecules, that is, carbohydrates, proteins, nucleic acids, and lipids (Prado *et al.,* 2014). The body cells are surrounded by some very important types of lipids called phospholipids (Matthews *et al.*, 2015). Their hydrophilic and hydrophobic ends align themselves in the form of a phospholipid bilayer as described earlier. These bilayers make up cell membranes that play a very critical role in cell functionality. As phospholipids consist of two long chains of fatty acids, which render them immiscible with water, this glycerol molecule is also attached to the phosphate molecule, thus granting water-loving properties to a phospholipid (Bozzuto & Molinari, 2015). Thus, overall, a phospholipid acts as an amphiphile. Once exposed to water, the adjacent water molecules are forced by phospholipids to acquire ice-like cages that surround the hydrophobic molecules. The free energy is increased owing to the more ordered cage formations compared with the

surrounding water molecules. When hydrophobic portions of the molecules cluster together, the free energy cost is minimized; facilitating the spontaneous aggregation of phospholipids by burying their hydrophobic tails in the interior and hydrophilic heads facing the surrounding water. As a result, thesecylindrically shaped molecules are assembled as bimolecular sheets or bilayers spontaneously in an aqueous environment giving bilayer membranes some fundamental characteristics of self-healing and fluidity (Lodish *et al.*, 2000). Membrane lipid molecules have been classified as phospholipids, cholesterols, and glycolipids. Phosphatidylcholine, phosphatidylethanolamine, phosphatidylserine, and sphingomyelin are the four major phospholipids in mammalian plasma membranes (Zhou *et al.*, 2015).

Among all, liposomes cover remarkably large area of applications in the pharmaceutical industry. Liposomes are amphipathic molecules possessing a hydrophobic and hydrophilic region (Figure 2.1). Their ability to aggregate spontaneously into a variety of structures makes them unavoidable in different areas. They can show self-assemblies or aggregate structures under certain conditions. Liposomes have their dual preference for solvents. The self-organization may also be attributed to spontaneous aggregation of amphiphiles above a certain level of their concentration, critical vesicular concentration (CVC) (Evans & Wennerström, 1999). Their behavior is a result of their attempt to minimize unfavorable hydrophobic interactions when dissolved in water which is accompanied by increased entropy of the system (Tanford, 1980). The entropy causes the water molecules to get arranged around the hydrophobic part when amphiphiles are suspended freely as monomers. The hydrophobic parts are derived out of aqueous medium as a result of release of ordered water molecules. Liposome-mediated drug delivery has been successful in overcoming obstacles to cellular and tissue uptake of drugs with improved biodistribution *in vitro* and *in vivo.*

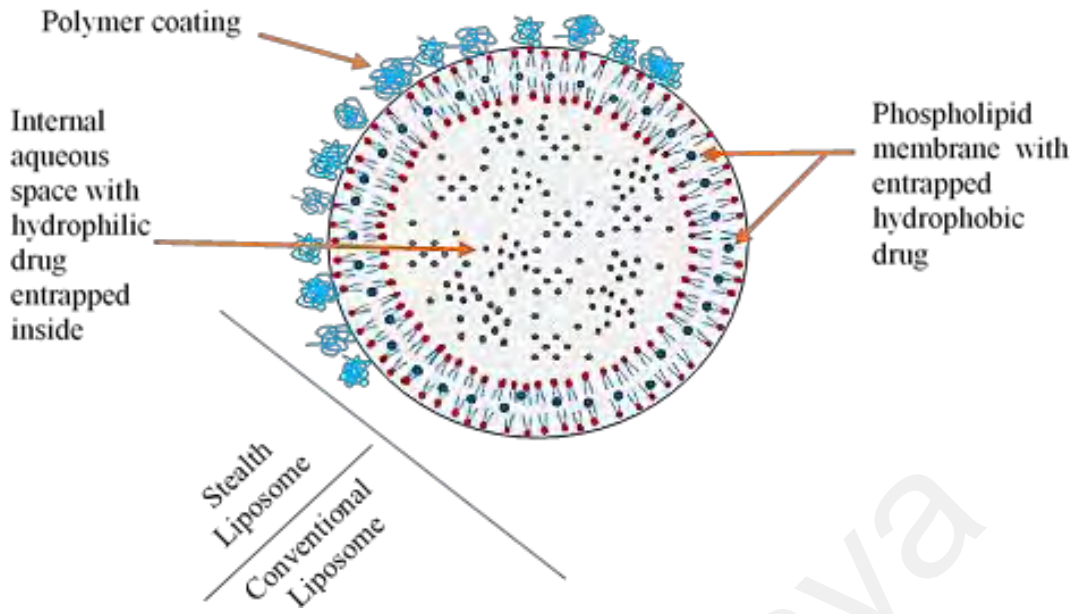

Figure 2.1: General representation of a synthetic drug carrier (red cell mimic) with ability to encapsulate both hydrophilic and hydrophobic drugs.

2.2.8 Red Blood Cell Mimics

Although synthetic drug delivery biomaterials are innovative in terms of functionality and diversity, yet they have failed to match the complexity and sophistication exhibited by distinct biological articles. Red blood cells represent a remarkably engineered biological entity designed for complex biological functionality in this regard. The RBC based drug delivery systems have been discussed many a times to analyze various conventional and novel engineering strategies (Bhateria *et al.,* 2014). In order to make drug carriers biocompatible and biodegradable in human blood stream, different types of drug carriers have been employed which are discussed below.

a. Membrane Ghosts as Potential Drug Carriers

Carrier RBCs (Sun *et al.,* 2015) have been studied as cellular vehicles for delivery of drugs and other bioactive agents for more than three decades (Kumar & Bhat, 2011). These vesicles stand closer to clinical use and commercialization due to their unique nature as proved by recently reported success stories in late-stage clinical trials (Garín *et al.,* 1996; Millan *et al.,* 2004; Zarrin *et al.,* 2014). The method follows physical

extrusion of RBC ghosts for passive targeting to the tissues with leaky vasculatures (Figure 2.2). Carrier RBC-based therapeutics have been resulted by the rapid development of cargo loading techniques (Bhattarai *et al.,* 2010; Muro *et al.,* 2008; Muzykantov, 2010; Simone *et al.,* 2008). The first reported RBC membrane –derived liposomes were named as nano-erythrosomes as the average size ranged from 100 to 200 nm (Lejeune *et al.,* 1993). Additional studies cover free drug molecular diffusion into the cells without discriminating cell categories and conjugation of drug molecules for targeting macrophages (Lejeune *et al.,* 1998).

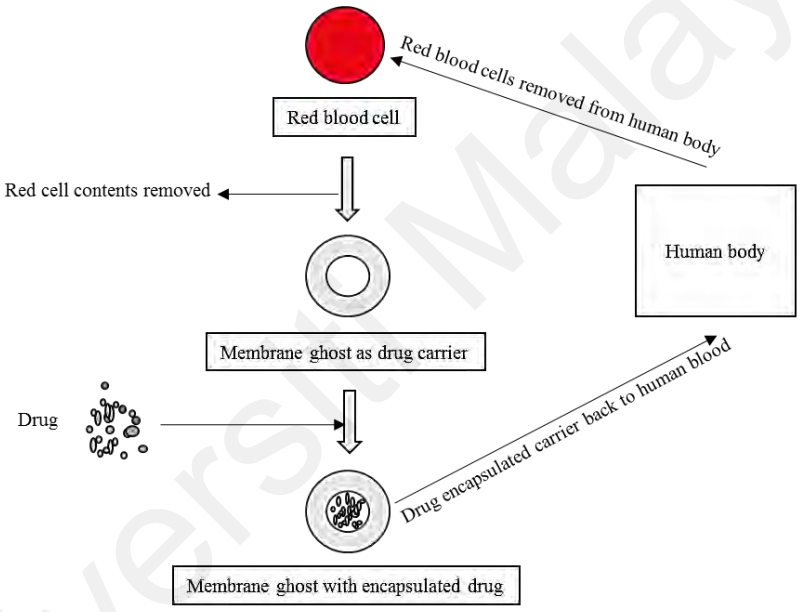

Figure 2.2: Schematic diagram showing preparation of membrane ghosts.

The use of RBC carriers also present some drawbacks that includes limited potential to non-phagocyte target tissue (Shah, 2011), possible clumping of cells and dose dumping (Millan *et al.,* 2004), storage problem upon re-entering the host body (Lynch *et al.,* 1980) and contamination risks owing to the blood origin, equipment used and loading environment (Valbonesi *et al.,* 2001). Further research can reveal the achievement of RBC surface charge to accord with the immune system as a game of hide and seek in a much promising way in the light of its pharmaceutical applications

b. Membrane Clocked Vehicles Mimicking Natural RBCs

Diversity of the drug delivery system follows two distinct _extremes' namely red blood cells and synthetic RBC mimics. The former is considered as conventional approach being natural, old and relatively simple while latter presents an attractive and modern aspect of novelty and sophistication. The blend of both has offered even better utility in terms of intracellular delivery, controlled release of multiple cargoes, and sustained delivery of biotherapeutics (Hu *et al.,* 2011; Muzykantov, 2013). Immune evasion by pathogens has redirected current therapeutic development from natural polymers to cloak drug carriers (Fu *et al.,* 2015; Parodi *et al.,* 2013; Sawdon & Peng, 2013). Carriers like membrane clocked vehicles mimicking natural RBCs (Figure 2.3) confer combined understanding from carrier formulations, drug loading to drug release kinetics for cancer like other blood diseases (Aryal *et al.,* 2013; Fang *et al.,* 2014; Gao & Zhang, 2015 2 ; Cole *et al.,* 2009).

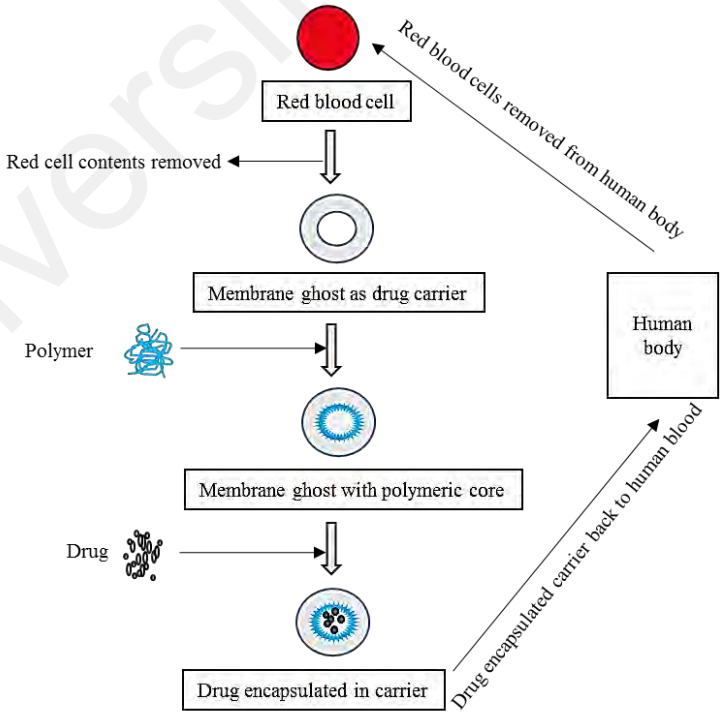

Figure 2.3: Schematic diagram showing preparation of membrane ghosts (empty red blood cell membrane) with enclosed polymeric core and entrapment of drug.

c. Engineered RBCs as Synthetic Carriers

The efficient transport and long circulation half-life of the natural red blood cells has motivated the continual pursuit of man-made carriers with comparable competences (Kirch *et al.,* 2012). The mechanobiological mimicking of red blood cells follows the pattern of physiological properties of natural moieties (Kaoui *et al.,* 2009; Mohandas & Gallagher, 2008; Wan *et al.,* 2011). On the basis of optimized unique size, shape, composition, and mechanical flexibility, red blood cell mimicking particles have been designed to carry out imaging agents and various encapsulated drugs (Discher *et al.,* 1994; Mohandas & Chasis, 1993). The most structural characteristics of red blood cells are their bioconcave discoidal shape and unmatched mechanical stability (Discher *et al.,* 1994).

2.3 Synthetic RBC Bilayer Membrane Liposome from Phospholipids

The organization of phospholipids in the human red blood cell membrane was discovered by Bretscher (Bretscher, 1972) with further confirmation by other groups (Gordesky *et al.,* 1975; Tardieu *et al.,* 1973). Virtually, all human red blood cells are composed of a typical lipid bilayer as shown in Table 2.2 (McNamara *et al.,* 2010; Yazdanbakhsh *et al.,* 2000). Bilayer-forming phospholipids consist of two hydrocarbon acyl chains linked to a head group by means of a glycerol backbone. The head group can either be neutral, zwitterion or charged (positively or negatively). The structural formula of a typical phospholipid has been shown in the Figure 2.4, where R1 and R2 are saturated or unsaturated acyl chains with R3 as the head group.

The key to successful preparation of an injectable liposome formulation is in the selection of some suitable combination of biomimetic phospholipids (Kanapathipillai *et al.,* 2014; Li *et al.,* 2016).

Table 2.2: The phospholipid composition of the human erythrocyte membrane (Virtanen *et al.*, 1998). Reproduced by the permission from Proceedings of National Academy of United States of America.

Phospholipid	Percentage of whole membrane, ±SD	Outer leaflet, %	Inner leaflet, %
PC	29.3 ± 1.5	44.8	14.0
SM	25.5 ± 1.4	42.1	9.1
LPC	1.0 ± 0.8	2.0	—
CPs	55.8 ± 2.2 (55.6)	88.9 (88.9)	23.1 (22.2)
PE	27.6 ± 1.5 (27.8)	11.1 (11.1)	43.9 (44.4)
PS	14.9 ± 1.7	—	29.6
PI	0.6 ± 0.5	—	1.2
PA	1.1 ± 0.5	—	2.2
Aps	16.6 ± 1.8 (16.7)	0.0 (0.0)	32.9 (33.3)

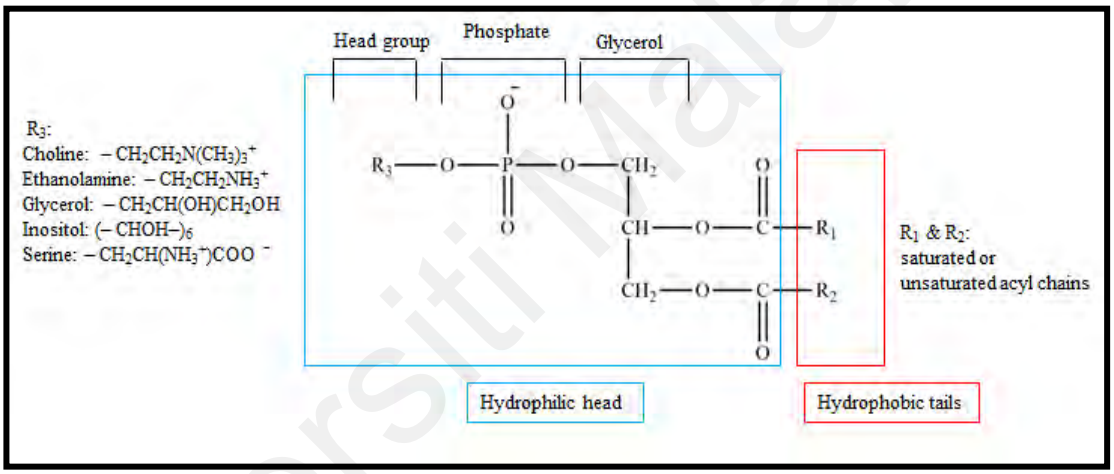

Figure 2.4: The general structure of a phospholipid where R1, R2 and R3 represent different acyl groups and head groups respectively.

Towards this end, phospholipid liposomes with specific size range and modified surface chemistry have extensively been studied as potential drug delivery vehicles (Allen & Cullis, 2013; Brannon-Peppas, 1995; Brigger, Dubernet & Couvreur, 2002; Moghimi *et al.,* 2001). Phosphatidylcholine (PC) (Chang & Yeh, 2012), phosphatidylethanolamine (PE) (Kraft *et al.,* 2014), phosphatidylinositol (PI) (Suzuki *et al.,* 2016), phosphatidylserine (PS) (van der Geest *et al.,* 2016) and phosphatidylglycerol (PG) (Kieler-Ferguson *et al.,* 2017) are among the most commonly used phospholipids. A brief classification of phospholipids has been given in Figure 2.5.

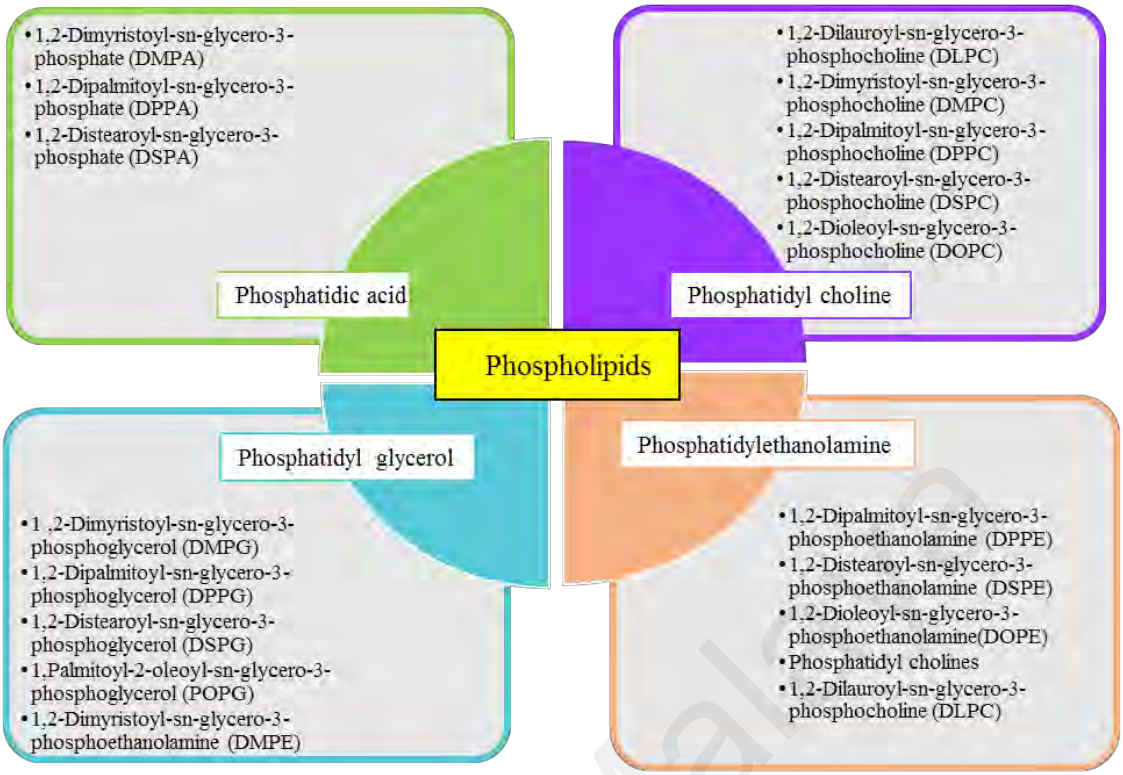

Figure 2.5: Classification of phospholipids.

Methods of liposome preparation among different liposome preparation techniques such as solvent injection techniques, reverse-phase evaporation techniques, detergent dialysis, heating methods, spray methods and supercritical thin film dispersion is the most commonly used preparation method (Akbarzadeh *et al.,* 2013). This method involves dehydration of the mixture of phospholipids and solvent leaving behind a thin layer of phospholipids inside the round bottom flask. These dried layers are the liquid crystalline bilayers which become fluid and swell upon hydration and result in the formation of liposomes (Lasic, 1988). The normal forces causing repulsion between lipid bilayers and tangential forces causing bending of these layers play a crucial role in early stage of liposome formulations (Bagatolli *et al.*, 2000). Large, self-closed, multilamellar vesicles are formed during agitation of lipid sheets which detach upon hydration. Once prepared sonic energy (sonication) or mechanical energy (extrusion) will be required for size reduction of these particles (Sala *et al.*, 2017). Sonication is considered perhaps the most widely used method for liposome size reduction with two

distinct types namely bath sonicator and probe sonicator (Akbarzadeh *et al.,* 2013). In bath sonicator, a test tube or vial containing liposome suspension is immersed in water bath, whereas the probe sonicator deliver high energy input while immersing probe tips directly inside lipid suspension. High-energy probe operation may also over heat the lipid suspensions causing oxidation and degradation of the lipids Therefore, it is recommended to keep sonicator vessel cold at all operation times. It is also important to note that temperature of the sonicator vessel must be maintained well above the lipid phase transition temperatures to ensure resealing of the broken vesicles. Homogenously distributed small liposomes can be prepared using this probe sonication method Lipid concentration and composition, temperature, suspension volume, sonication time and power play an important role in evaluating average particle size and particle size distribution of the vesicles formed. A simple lay out for general liposome preparation and characterization methods have been shown in Figure 2.6.

2.4 Preparaion of Liposomes

2.4.1 Particle Size of Liposomes

Particle size is very important in designating drug carriers with reference to reticuloendothelial system of the body. According to Li Tang *et al*., the overall therapeutic efficacy against cancer is affected by the optimum particle size which has a strong impact on its biodistribution, tumor penetration and internalization, clearance from blood plasma, tissues and excretion from the body as well (Tang *et al.*, 2014). One of the natural clearance mechanisms of human body involves rapid clearance of nanocarriers by phagocytosis. Phagocytosis is facilitated by surface deposition of opsonizing factors and activation of complement proteins which in turn are highly influenced by particle size and their surface properties (Moghimi *et al.*, 2001).

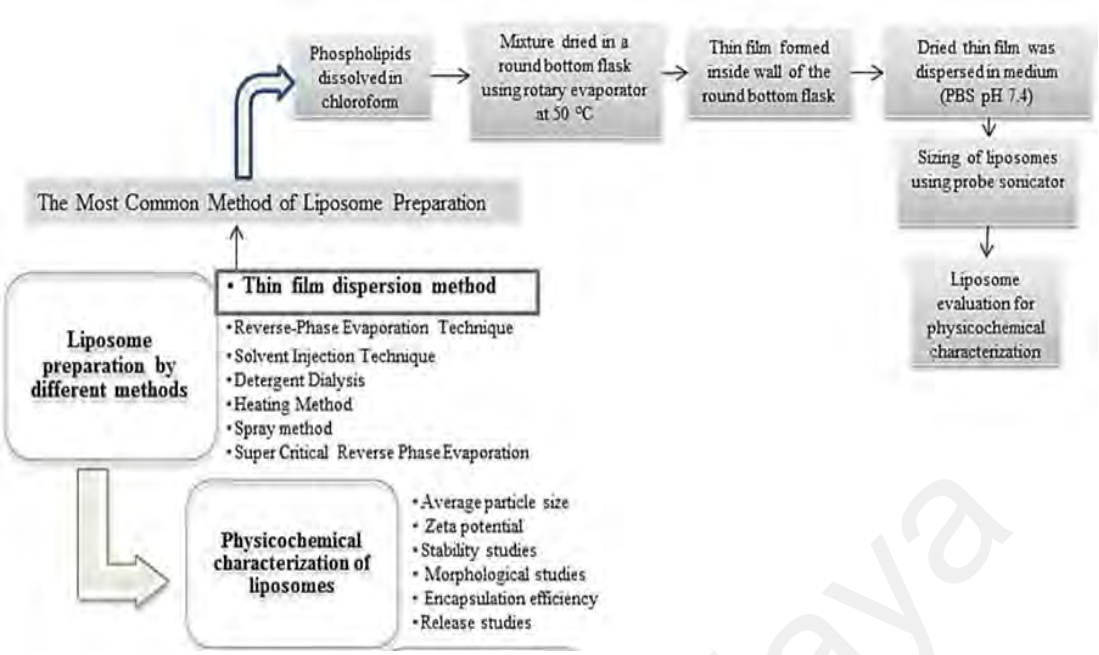

Figure 2.6: A simple layout showing general liposome preparation and characterization methods.

In general, particles over 200 nm diameter are considered to activate complement system more actively. They are at risk of being filtered out of blood or destroyed by liver, spleen or bone marrow, whereas particles with ≤ 10 nm diameter will tend to leave blood stream faster via kidney or extravasation from a tumor (Carboni *et al.*, 2014). However, according to Kraft et al., majority of the clinically approved liposome have diameters of about 50 to 300 nm (Kraft *et al.*, 2014) which may also be attributed to interdependency of some other physicochemical properties of nanocarriers such as composition, proper engineering of particle surface and morphology etc.

A number of techniques have been used to characterize particle size of liposomes such as static light scattering (Holthoff *et al*., 1996; Xu *et al*., 2015), Dynamic image analysis (Ulusoy *et al*., 2016), Sedimentation analysis (Bakker *et al*., 2016), Electrical sensing Zone (Ripple *et al*., 2015), Air permeability analysis (Arvaniti *et al*., 2015), and Dynamic light scattering (Stetefeld *et al*., 2016).

Table 2.3: A brief overview of some recent liposomal publications pointing at importance of particular particle size and zeta potential in anticancer drug delivery.

Liposomes Tested	**Size of Nanoparticle (nm), Surface charge (mV)**	**Cance Cell Line**	**Encapsulated payload**	**Endpoints Studied**	Ref.
Liposomal DHA and ghost (no DHA, control) liposomes	137 ± 12 nm with a slightly negative charge	Human breast cancer cell lines(MCF-7 cells,MDA-MB-231 cells)	Docosahexaenoic acid (DHA)	Cell viability assay, Cell death detection ELISA, Western blot analysis.	(Skibinski *et al.*, 2016)
Lipids and PEGylated lipids with single-tail peptide-Amphiphiles (Thermosensitive stealth liposomes)	122–131 nm for the Brij78 liposomes, 118–133 nm for the 0% C16-PR_b liposomes, 121–143 nm for the 3% C16-PR_b liposomes, 119-136 nm for the 3% C16-GCRGRRST liposomes, and 127–140 nm for the 3% C16-GRGDSP liposomes	Human breast cancer cells MDA-MB-231	Calcein	In vivo hyperthermia studies, Liposome binding assays, Live-cell confocal microscopy.	(Shroff *et al.,* 2016)
Dexamethasone (Dex)-associated liposome (DX)	DXE: 272.1±11.9 23.6±5.7(in DMEM), 198.6±12.8 18.6±3.4(in 10 % FBS with DMEM)); DXE+HSP90: 660.5±41.6 16.5±6.1(in DMEM), 270.5±23.6 10.8±2.5 (in 10 % FBS with DMEM)	Breast cancer stem-cell-like cells, ANV-1, Mice	ESC8	Cell Viability, Western Blot, Drug Sensitivity Assay, ESC8 Plasma Assay Development, Pharmacokinetic Analysis.	(Ahmad *et al.*, 2016)
ICAM-1 antibody labeled, Lcn2 siRNA encapsulating, pH-responsive liposomes (ICAM-Lcn2-LPs)	ICAM-Lcn2-LP: 114 ± 51 -14.8 ± 0.3 IgG-Lcn2-LP: 111 ± 60, -12.2 ± 2.6 Lcn2-LIPO: 703 ± 345, -3.4 ± 2.5, ICAM-SCR-LP: 118 ± 58 -11.4 ± 7.1 ICAM-RD-LP: 119 ± 60 -13.5 ± 9.9 IgG-RD-LP: 123 ± 67 -8.0 ± 3.0	Human TNBC MDA-MB-231 cells, non-neoplastic human MCF10A cells	Lcn2 siRNA	Measurement of Human VEGF Protein Levels in Conditioned Media (CM), Endothelial Cell Proliferation, Endothelial Cell Migration, Endothelial Tube Formation, Chicken Chorioallantoic Membrane (CAM) Assay.	(Guo *et al.*, 2016)
PEGylated liposome doxorubicin (PLD)	Z average (nm): 25 AHNP-PLD: 95.68 ± 0.90 50 AHNP-PLD: 97.53 ± 3.44 100 AHNP-PLD: 99.91 ± 4.96 200 AHNP-PLD: 95.3 ± 0.79 Doxil-mimic: 97.01 0.157	Murine breast tumor modelHER-2/neu-positive cell clone TUBO, MDAMB-231 cell line	AHNP, Anti-HER2/neu peptide, (FCDGFYACYADV)	In vitro cell uptake study, Cytotoxicity investigation, In vivo evaluation, Treatment, Biodistribution study.	(Zahmatkeshan *et al.*, 2016)

Continued…

Liposomes Tested	Size of Nanoparticle (nm), Surface charge (mV)	Cance Cell Line	Encapsulated payload	Endpoints Studied	Ref.
Nitrogen containing bisphosphonates (N-BPs)	150–500 nm	Breast cancer cell lines:MCF-7, T47D cell line,	Chlorpromazine	Encapsulated Drug Concentration Analysis, Preparation of Cell Lysates for IPP and AppI With ESI–HPLC–MS, Kinetics ofMetabolite Formation in Free, Ca2+-enriched and Liposomal Formulation, High Pressure Liquid Chromatography Electrospray Ionization Analysis, Uptake of [14C]-zoledronic Acid.	(Zlatev *et al.*, 2016)
Lipoplexes	DO-DNA: 503.8 ±5.3 nm 4.8±1.0 mV SP-DNA: 436.6±15.9 nm 4.8±1.0 mV	Cancer (MCF-7, A549, MDA-MB-231) and non-cancer (CHO, HEK293 and NIH-3T3) cells	pCMV-β-gal plasmid in SP lipoplex	Gene transfection study, Cytotoxicity studies, Apoptosis study, Western blot studies, Mineralocorticoid receptor down-regulation by siRNA delivery, Effect of siRNA down-regulation on transfection efficiency andCytotoxicity.	(Sharma *et al.*, 2016)
Pegylated liposomal doxorubicin (anti-HER2 affibody coupling to liposomal Doxorubicin)	94.05±1.01nm to 98.43±1.32, -13.3±6.5 to -17.6±3.8 mV	HER2+ and HER2_ human breast adenocarcinoma cells (SK-BR-3 and MDA-MB-231, respectively; ATCC HTB-30TM and CRM-HTB-26)	Doxorubicin	Dox cell uptake assay, Cytotoxicity study, Competition assay, In vivo studies: Tumor growth inhibition efficacy, Biodistribution study	(Akhtari *et al.*, 2016)
Phototriggerable liposomes	91.2±0.94 nm to 118.4±0.59 nm	MDAMB231LM2^{LUC+} Cells, MDAMB231cells (without luciferase gene), mice	Calcein, HPPH(2-[1-hexyloxyethyl]-2-devinyl pyropheophorbide-a)	Luciferase expression, Cellular viability, Tumor growth, Tumor histopathology.	(Sine *et al.*, 2015)
thermosensitive liposomes (TSL)	100.63 ± 3.69 nm and 103.2 ± 5.91 nm, _10 mV	Breast cancer cell line, MDA-MB-231, mice	Doxorubicin	Intracellular uptake of liposomes into tumor cells, Observation of CO2 generation in TSL-C by ultrasound imaging, Drug release from TSL-C, Cytotoxicity of TSL-C, Antitumor efficacy, Immunohistochemical staining.	(Han *et al.*, 2015; Sun *et al.*, 2015)

Continued…

Liposomes Tested	Size of Nanoparticle (nm), Surface charge (mV)	Cance Cell Line	Encapsulated payload	Endpoints Studied	Ref.
Paclitaxel/Epigallocatechin gallate coloaded liposome	131.6±2.5 nm to 126.7± 4.3 nm, -36.45 to −39.45	Human breast cancer cells (MDA-MB-231)	Paclitaxel, Epigallocatechin gallate (EGCG)	Cytotoxicity against human breast cancer cells, Hoechst 33342 staining and caspase-3 assay, MDA-MB-231 invasion assay, MMP-2 and MMP-9 ELISA assay, Gelatin zymography.	(Ramadass, Anantharaman, Subramanian, Sivasubramanian, & Madhan, 2015)
Multifunctional gold coated thermo-sensitive Liposomes	150–200 nm	MDA-MB-231 cells	Calcein	Cell uptake study, Biocompatibility and in vitro photothermal therapy, Photothermal mediated model drug (calcein) release, Optical imaging experiment, X-Ray CT imaging experiment.	(Rengan, Jagtap, De, Banerjee, & Srivastava, 2014)
Tamoxifen guided liposomes	188.8 ± 2.2 nm, +47 mV	MCF-7 and MDA MB 231 human breast cancer cell lines	Doxorubicin	MTT assay for in vitro cyto-toxicity studies on MCF-7 and MDAMB- 231 cell lines,Confocal microscopy studies,FACS (fluorescence assisted cell sorting) studies on MCF-7 cell Lines, In vivo studies in nude mice.	(AJain et al., 2014)
Combined mTOR inhibitor rapamycin and doxorubicin-loaded cyclic octapeptide modified liposomes	31.40 ± 1.31 nm to 96.24 ± 3.13, -2.43 ± 0.54	Triple-negative breast cancer MDA-MB-231, highly metastatic breast cancer MDA-MB-435S, mouse melanoma cell line B16 and non-metastatic breast cancer MCF-7	Doxorubicin, rapamycin (RAPA)	Flow cytometry analysis, Laser confocal microscopy analysis, In vitro cytotoxicity studies on the synergetic effect of RAPA with DOX Nanomedicines, Site-specific delivery of LXY-LS-DOX to model TNBC mice by living fluorescence, Imaging, Effect of co-administration on the bio-distribution of nanocarriers in model, TNBC mice, Combinational anti-tumor efficacy against model TNBC and toxicity studies in vivo, Immunohistochemistry of HIF-1a protein.	(Dai et al., 2014)

Continued…

Liposomes Tested	Size of Nanoparticle (nm), Surface charge (mV)	Cance Cell Line	Encapsulated payload	Endpoints Studied	Ref.
Hyaluronic acid derivative-coated nanohybrid liposomes	124.47 ± 4.00 nm to 130.07 ± 4.90 nm, 7.09 ± 0.28 mV to −27.92 ± 0.37 mV	MDA-MB-231 cells	Doxorubicin	In vitro cellular uptake, Phantom study, In vivo MRI study, In vivo pharmacokinetic study	(Prat *et al.*, 2010)
Indocyanine green loaded liposome Nanocarriers	51 to 85 nm,~ 71±10 nm	human triple negative breast cancercells, nontumorigenic mammary epithelial cell line MCF-10A.	Indocyanine green	Photodynamic therapy, MTT assay, Clonogenic assay, Gamma-H2AX immunofluorescence assay.	(Shemesh *et al.*, 2014)
Legumain proteaseactivated TATliposome Cargo	112.3 nm, 0 mV	4T1 murine breast cancer cells, A549 human lung cancer cells, MDA-MB-231human breast cancer cells, murine macrophage RAW 264.7	Doxorubicin	Flow cytometry assay, Cell viability assay, Western blot assay, Activity assay of legumain, Legumainspecific peptide Ala–Ala–Asn cleavage assay, Tumour growth and survival curves, Biodistribution assay.	(Liu *et al.,* 2014)
Lipid-based nanoparticles (liposomes)	----	Breast cancer model	Doxorubicin, Paclitaxel	----	(Markman *et al.*, 2013)
PEGylated liposomal doxorubicin (PLD)	----	MDA-MB-231-BR-luciferase-expressing cells (mice)	Doxorubicin	Cell viability assay, Single agent and combination treatments in cell lines, Animal use and intracranial tumor inoculation, Bioluminescence imaging, Pharmacokinetic study design. Efficacy study design.	(Anders et al., 2013)
Modified stealth liposomes (liposomes functionalized withpolyethylene glycol, PEG)	97nm, 131 nm	MDA-MB-231 cells	Doxorubicin	Flow Cytometry, Confocal Microscopy, Cytotoxicity Studies,	(Shroff *et al.*, 2012)
Unmodified stealth liposomes (LS)	~100 nm.	Highly metastatic ancer cells (MDA-MB-435S and MDA-MB-231), non-metastatic cancer cells (MCF-7)	Doxorubicin	Flow cytometry analysis, Laser confocal microscopy analysis, In vitro cytotoxicity assay, Animal models.	(Wang *et al.*, 2012)

Continued…

Liposomes Tested	Size of Nanoparticle (nm), Surface charge (mV)	Cance Cell Line	Encapsulated payload	Endpoints Studied	Ref.
A novel liposome formulation containing a synergistic combination of vincristine and quercetin	~130 nm	Trastuzumab-insensitive breast tumor xenograft model	Vincristine	In vitro cytoxicity assay, Median-effect analysis for drug combinations, Animal studies, Pharmacokinetic study, In vivo efficacy study, UPLC method development and drug extraction .	(Wong *et al.*, 2011)
Stealth liposomes	~80 nm	Human breast cancer MCF-7, MDA-MB-231 cells	All-trans retinoic acid, vinorelbine, coumarin	Uptake by breast cancer cells and the uptake inhibition, Sorting and identification of breast cancer stem cells, Breast cancer stem cell-cycle arrest, Proliferation inhibition to breast cancer and cancer stem cells, Differentiation of breast cancer stem cells, Effect on the relapse model of breast cancer.	(Li *et al.*, 2011)
Core-eshell nanoparticles properties	363.6 ± 4.5 nm, 435.9 ± 8.7, ~ 30.02 ± 0.78 mV	MDA-MB-231 cells	Co-delivery of Doxorubicin and pEGFP	In vitro drug uptake and gene transfections, Confocal microscopy, Flow cytometry	(Wang *et al.*, 2010)
Liposomes loaded with histone deacetylase inhibitors	100 ± 23.2 to 150 ± 38.3 nm, −22.2 ± 7.1 to −24.9 ± 7.6 mV	MCF-7, T47-D A 1-2, SKBr-3 and MDA-MB-231 cell lines	Histone deacetylase inhibitors	In vitro liposome uptake, Cell viability determination, Immunobloting.	(Urbinati *et al.*, 2010)

2.4.2 Zeta Potential of Liposomes

Zeta potential, a most commonly used term in colloidal chemistry, maintains the dispersion or discreteness of the particles in a suspension. Zeta potential is one of the key physicochemical properties of liposomes which have strong impact on circulation half-live and cellular uptake of liposomes in drug delivery applications. According to Nishit Dochi *et al.,* ―biomaterials form the basis of current and future biomedical technologies‘ and that some key challenges in drug delivery may also be addressed by

mimicking biological moieties like RBC. It has long been investigated that RBC membranes have negatively charged surfaces which contribute to their repulsive electrical zeta potentials between cells. Any negatively charged particle entering blood stream is expected to remain stable due to such repulsive interactions. Based on this strategy, liposomes have long being designed to attain long circulation half-life in blood stream. Following stability aspects, zeta potential values of either – 30mV or + 30mV are the most widely accepted values for various liposomal and other colloidal suspensions. However, RBC zeta potential values have also suggested another range of zeta potential values which may be followed to avoid protein adsorptions and RES of the body. For example, Fontes *et al.,* narrated the normal range of RBC zeta potential between -9.30 mV and -15.0 mV with an average value of -12.5 mV (Chevalier *et al.*, 2013; Fontes *et al.*, 2006). A brief overview of some recent publications pointing out the importance of particular particle size and zeta potential of liposomes in anticancer drug delivery has been given in the Table 2.3. The table reflects some brief information on interaction of liposomes with some exemplary breast cancer cell lines.

A number of techniques have been used to characterize zeta potential of liposomes such as electrophoretic light scattering (ELS) (Adelantando *et al*., 2016), Dynamic light scattering (Bhattacharjee *et al*., 2016), tunable resistive pulse sensing (TRPS) (Sikora *et al*., 2016), and zeta particle tracking analysis (z-PTA) (Sikora *et al*., 2015).

2.4.3 Microscopic Characterization of Liposomes

Different microscopic techniques have been used to examine objects for their topography, morphology, composition and crystallographic information. Microscopic techniques are used to view objects which are not in the range of normal eye. Optical, electron and scanning microscopic techniques are the well-known branches of microscopy and have found tremendous applications in the field of drug delivery.

Liposomes have also been characterized using these microscopic techniques as for instance optical polarizing microscopy (Bagatolli *et al.*, 2014; Bunjes *et al.*, 2016) transmission electron microscopy (Garg *et al.*, 2014) and field emission scanning electron microscopy etc. Optical polarizing microscopy (OPM) is considered an ideal choice for liposome like birefringent specimens which offer quantifiable refracting difference measurements with increased quality of the image contrast. Optical microscopy is important in determining crystal morphology and symmetry; crystal defects; phase identification, morphology and homogeneity; and refractive index measurements. Transmission electron microscopy (TEM) operates with a principle similar to OPM but uses electrons of very short wavelength as _light source‘ which help in getting resolutions thousand times better than normal light microscopes. As a major analytical tool in physical, chemical and biological sciences, TEM has found tremendous applications in the field of cancer research, material science, virology and nanotechnology. Field emission scanning electron microscopy (FESEM) involves interaction of a scanning probe with the object of interest. The principle involves generation of narrower probing beams from a field-emission cathode in the electron gun of a scanning electron microscope which produces images with improved spatial resolution and minimized sample charging and damage. It helps in determining advanced coating thickness, elemental composition measurements, cross sectional studies of semiconductors, and structural uniformity etc. The specialty of the microscopic techniques is that they help to obtain improved specimen contrast and to highlight certain structures with increased resolution and less sample damage.

2.4.4 Differential Scanning Calorimetry

DSC is a suitable thermoanalytical technique in which the difference in the amount of heat required to increase the temperature of a sample (whereby the sample undergoes a physical transformation such as phase transitions) and reference is measured as a

function of temperature is called differential scanning calorimetry (Knopp *et al*., 2016). This technique helps determining purity, the polymorphic forms and the melting point of a sample in the pharmaceutical industry and also considered a tool to study the thermal behavior of lipid bilayers and of lipidic drug delivery systems . So, thermal behavior of liposomes can be measurined by thermodynamic parameters (i.e. DeltaH and Tm), which affect the stability of the liposomal suspension under given storage conditions (Wei et al., 2017; Casadó *et al*., 2016).

2.4.5 Encapsulation of Drug

As liposome preparations are mixtures of trapped and untrapped drug fractions, therefore, the first step is the separation between the encapsulated drug and free drug before proceeding to the determination of encapsulation efficiency. Several separation techniques have been used in literature such as mini-column centrifugation (Padamwar *et al*., 2006), using dialysis membrane (Berger *et al*., 2001), and ultracentrifugation technique (Sun et al., 2008; Wang *et al.,* 2011). Encapsulation Efficacy can be determined by two methods i.e direct and indirect. After applying the separation methods, methanol or Triton X-100 has been used to disrupt the lipid bilayer of the liposomes obtained in the form of a pellet and the drug entrapped within the liposomes is measured. Whereas in indirect method, the unencapsulated drug molecules in supernatant may be measured and its result are reduced from the drug concentration in formulation (Khoshneviszadeh *et al*., 2016). The quantification techniques depends on the nature of encapsulant and include spectrophotometry, fluorescent spectroscopy, enzyme-based methods, HPLC, FFF, and electrochemical techniques (Laouini *et al*., 2012).

Lipophilicity, a physicochemical property of encapsulated drugs, is of principal importance in determining its pharmaceutical and pharmacokinetic actions on targeted

sites. This is an equilibrium property which is measured most commonly by its distribution behavior in a biphasic system i.e. partition coefficient in octanol/water system. The quantitative description of lipophilicity, the partition coefficient, is expressed as below:

$$\boldsymbol{p} = \frac{\boldsymbol{C_{oct}}}{\boldsymbol{C_{aq}}} \quad (2.1)$$

Where, C_{oct} and C_{aq} is partition coefficient in octanol and aqueous medium respectively. The term ‗*p*' is usually expressed in logarithmic scale, log *p*, which represents partitioning of unionized species (Rutkowska *et al.*, 2013). The majority of liposome applications as therapeutic DDS are based on their unique amphiphilic nature. Drug that are highly lipophilic tend to encapsulate within the lipophilic liposome bilayer whereas hydrophilic drugs are trapped inside the aqueous core. Owing to this property, about 600 clinical trials involve lipid particle drug delivery systems at present (Kraft *et al.*, 2014). Some of the representative anticancer drugs with their log *p* values have been shown in Table 2.4.

Table 2.4: Some commonly used anticancer drugs with their log *p* values.

Anticancer drug	Molecular weight	log *p*	Reference
Paclitaxel	854	3.96	(Pattni *et al.*, 2015)
Irinotecan	586.7	2.78	(Parhi *et al.*, 2012)
Etoposide	588.6	1.16	(Brown *et al.*, 2014)
Ifosfamide	261.1	0.86	(Wang *et al.*, 2016)
Doxorubicin hydrochloride	579.9	-0.53	(Yuan *et al.*, 2017)
5-fluorouracil	130	-0.89	(Al Sabbagh *et al.*, 2015)
Topotecan hydrochloride	457.9	-0.36	(Xing *et al.*, 2015)
Methotrexate	454.4	-1.8	(Fathi *et al.*, 2016)
Cisplatin	300	-2.2	(Kieler-Ferguson *et al.*, 2017)
Leucovorin calcium	511.5	-2.7	(Kozovska *et al.*, 2014)

Insulin therapy has utilized liposomes as a means to selectively target insulin to liver, its enhanced oral absorption, and to prolong its action (Spangler *et al*., 1990). To enhance encapsulation efficiency and sustained-release delivery for parenteral

administration of a protein drugs have long been a challenge. In order to develop a sustained delivery system it has been focused to reduce the administration frequency of such drugs. Short biological half lives, extreme instability due to proteolytic inactivation and degradation are well known issues of insulin like protein drugs and their frequent injections, local tissue necrosis, microbial contamination and other problems like nerve damage have prompted researches to look for some alternative routes (Al-Remawi *et al*., 2017). So, the current study also has utilized to investigate encapsulation of insulin as a small case history in this regard (Naeem *et al*., 2016).

2.4.6 Targeted Drug Release

Liposomes, as bioactive delivery cargoes, have been experiencing a challenge to control effective release of payloads to the site of interest. The encapsulated drugs are idealized to become bioavailable prior to any cytotoxic actions. Different methods to destabilize liposomes at tumor sites have therefore been developed to improve drug bioavailability with substantial therapeutic outcomes as for example enzymatic, hyperthermia, ultrasound, and pH mediated strategies (Chen *et al.*, 2014; Kieler-Ferguson *et al.*, 2017; Lu *et al.*, 2012; Yoshida *et al.*, 2016). Design of liposome formulations, route of administration, and interaction of liposomes with fluid and tissues of the body (once injected) are among key factors for kinetic studies of the drug release rates.

The dialysis tube diffusion technique can be used to perform *in vitro* release studies (Kaushik *et al*., 2018). Another technique called Franz diffusion cell has also been used successfully to investigate the in vitro release profiles for different anticancer drugs (Balzus *et al*., 2016) and low pressure chromatography (Alves *et al*., 2016). Then the samples obtained from dialysate at various time intervals are assayed for the drugs by HPLC and spectrophotometer.

Liposomal formulations are important for drug release rates with respect to specific composition, average particle size and its distribution, nature of the loaded drugs (hydrophilic or hydrophobic), and release mechanisms (Cipolla *et al.*, 2014; Dawidczyk *et al.*, 2014). Release mechanisms such as Higuchi, Weibull, Pappas, zero order, First order, Gompertz and others have continuously been exploited to analyze whether drug remains in circulation or reaches at targeted sites (Jain *et al.*, 2016). Such mathematical *in vitro* drug release model fittings have been considered as a promising approach to deduce the delivery processes and their underlying physicochemical release phenomenon. They not only help in designing effective and improved liposomal formulations from the knowledge of diffusion equations (based on liposomal compositions and release conditions), but also help to predict *in vivo* behavior (Nounou *et al.*, 2006).

2.5 Intravenous Route of Administration

In pharmacology and toxicology, the path by which the fluid, drug or any other relevant substance is taken into the body is termed as the route of administration, and is generally classified based on their applied locality. These may be classified according to the targeted action such as topical (on the skin surface or mucous membrane), transdermal (absorbed through the skin or mucous membrane), enteral (delivered through the gut) or parenteral (delivered by routes other than the gut). Liposomes are designed and used for different modes of applications such as transportation of oral (Nguyen *et al.*, 2016), transdermal (Agarwal *et al.*, 2016) and intravenous drug payloads. The most critical of all is their use in intravenous drug delivery. The intravenous route is believed to be the fastest way of delivering fluids (Gref *et al.*, 2012) and other medications throughout the body with a medication bioavailability of ideally, although not practically, 100 % (Allen *et al.*, 2013; Durymanov *et al.*, 2016). The infusion is made directly into a vein to ensure its maximum bioavailability.

2.6 Biocompatibility

Anything administered through the intravenous route must not be harmful to the blood, especially red blood cells, which are the only means of delivering oxygen to the body tissues via circulatory system (Biagiotti *et al.*, 2011; Muzykantov, 2010). The phenomenon of rupturing the red blood cells by any means is called hemolysis (Ji *et al.*, 2014). As a result of hemolysis, the contents of the red blood cells are released into the surrounding fluid and accelerated hemolysis rates lead to anemia, jaundice and reticulocytosis (Han *et al.*, 2012; Shalel *et al.*, 2002). Hence, carriers administered via the blood route must be evaluated according to their hemolytic potentials using pharmacology and toxicity assays (Elmowafy *et al.*, 2013; Feng *et al.*, 2016; Roggers *et al.*, 2014). Hemolysis may be studied both by *in vitro* or *in vivo* methods. A simple lay out for the hemolysis process has been shown in Figure 2.7. Circulation half-life has become one of the major design considerations in nanoparticle drug delivery systems. By taking cues for designing long circulating carriers from natural entities such as red blood cells (RBCs) has been explored for many years. Among all the cellular carriers including leukocytes, broblasts, islets, and hepatocytes, RBCs offer several distinctive features. RBC mimics can evade the body‘s reticuloendothelial system overcoming many barriers such as size, shape, accelerated blood clearance, mechanical properties, control over particle characteristics, and surface chemistry.

The intravenous delivery of drugs has long been practiced for the treatment of a number of diseases. The drug delivery of anticancer drugs has become a big challenge due to the side effects of these drugs (Holliday *et al.*, 2011; Lee *et al.*, 2016; Suzuki *et al.*, 2016). The focus is more towards intravenous drug delivery than any other route of administration based on its immediate bioavailability. The direct injection of anticancer drugs is quite risky due to various risky side effects. Therefore, drug carriers are now receiving attention for drug delivery application these days (Chen *et al.*, 2013).

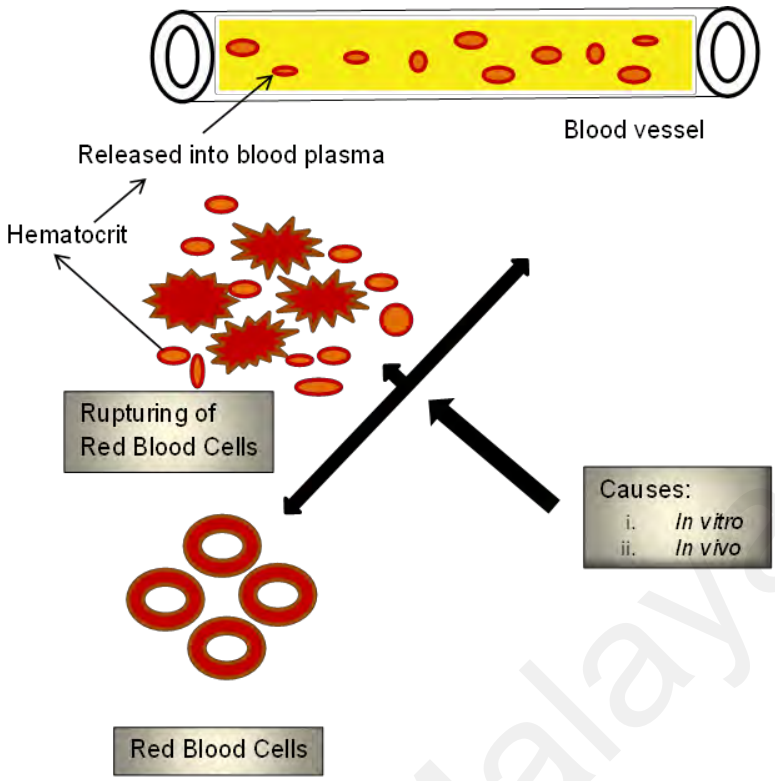

Figure 2.7: A simple illustration of the hemolysis process when the payloads are injected intravenously.

Among them, liposomes are being used most commonly owing to their amphiphilic nature. Liposomes are spherical bodies with lipid bilayers. Both hydrophilic and hydrophobic drugs have encapsulated and administered for biomedical applications. Liposomes formulated with different precursors have different properties such as size, morphology, surface charges, circulation half times as well as blood compatibility tests such as hemolysis, aggregations, cytotoxicity, and others. (Akhtari *et al.*, 2016; Fröhlich, 2012).

Both qualitative and quantitative compositions of the liposomes have been long been considered important aspect for intravenous anticancer drug delivery applications (Edwards *et al.*, 2006). Liposomes targeting intravenous injection of drugs must have to be formulated under physiological conditions such as using 0.01 M phosphate buffer saline with pH 7.4.

Knowledge of the interfacial energy of liposomes with blood is very important in establishing liposome blood compatibility as red blood cells are believed to be the very first site of interaction in intravenous drug delivery (Ruan *et al.*, 2015). Biocompatibility is often referred to the extent of a foreign substance being accepted by the biological subsystem of the body once it has been introduced and it has interacted with cells and tissues. In the field of liposome-drug conjugate therapeutics, potential evaluation of carrier biocompatibility is important for longer plasma half-life and gradual degradation in the body. Such degradations are prone to severe complications such as red blood cell lysis, cell aggregation and tissue toxicity including immune system stimulation. For a carrier to be biocompatible, the foremost investigation is that it should not induce hemolysis and red cell aggregation (Psarros *et al.*, 2016). Secondly, the carrier is expected to provoke negligible toxicity to the body tissues at a specific working concentration (Fröhlich, 2012; Tacar *et al.*, 2013). Thirdly, the carrier together with its payload should not induce any cellular or hormonal responses from the body and the neoplastic changes as far as the long term affects are concerned (Fox *et al.*, 2013; Hanke, 2013). An array of experiments have been performed to evaluate biocompatibility with reference to biocompatible assays, such as percent occlusion, flow reduction, pressure drop across devices, antibody binding to thrombus components, thrombus mass, light microscopy and scanning electron microscopy of adhered platelets, leukocytes, aggregates, erythrocytes, fibrin, and others. Being a versatile drug carrier, liposomes have a vast range of applications including research regarding cosmetics (Filipović *et al.*, 2016), cosmeceutical viral infections (Jordheim *et al.*, 2013), imaging (Yue *et al.*, 2016), and intracellular delivery such as mitochondrial targeting and lysosomal targeting.

2.7 Cell Cytotoxicity

Contemporary cancer therapy, particularly with respect to drug delivery, has evolved from traditional methodologies. Part of this change is based on the need to increase the therapeutic index of chemotherapy drugs (Yoo *et al.*, 2011). Although cancer cells are inherently more vulnerable to the effect of chemotherapy agents, the drugs are nonselective and can cause injury to normal tissues (Wan *et al.*, 2013). Indeed, it is this toxicity of normal cells that constrains dose and frequency in persistence of cancer cells after completion of chemotherapy treatment. Before proceeding to specific applications, it is important to know that what the tumor cells are and their relationship with the surrounding environment (Jain, 2001; Kieler-Ferguson *et al.*, 2017).

The cells which have lost their ability to divide in a controlled way, thereby generating progressive mutations, are called cancer cells. The rapid growth of these cells needs a dedicated blood oxygen supply and other nutrients to grow beyond a certain general size range of 1 to 2 mm^3 (McDougall *et al.*, 2006; Spill *et al.*, 2015). An overview of the tumor microenvironment and the tumor cell helps to elucidate the problems of drug delivery in cancer. The environment in which the tumor grows and exists, including immune cells, inflammatory cells derived from bone marrow, fibroblasts, lymphocytes, signaling molecules, and extracellular matrix, is called tumor environment (including of course all the surrounding blood vessels) (Joyce *et al.*, 2015). This bidirectional communication can eventually become quite critical for both normal tissue homeostasis and for tumor growth (Quail *et al.*, 2013). Attempts are now dedicated on efforts to kill cancer cells by more specific targeting while sparing normal cells. To achieve these goals, the focus is the development of novel carriers for both existing and new drugs and defining better therapeutic targets relative to the molecular changes in the cancer cells, their vasculature, and the related stroma. The studies are now focusing on the expanding field of nanoparticle development as the carrier for

therapeutic drug delivery in oncology and how this methodology may break some of the physiologic and pharmacologic barriers to effective breast cancer drug treatment.

The commonest cause of cancer death among women worldwide has been investigated to be the breast cancer (Key *et al.*, 2001). Breast cancer, a malignant tumor in the cells of breast, grows in surrounding tissues and may even spread to distant areas of the body. The disease occurs almost entirely in women and very rarely in men. There are different types of breast cancer cells. These tumors are characterized on the basis of their size, cell types, and the features that fuel its growth. A tumor is a mass of abnormal tissue. Noncancerous tumors are called benign while cancerous tumors are termed as malignant. Being a very complex and heterogeneous disease, the first breast cancer cell line was modeled over about 60 years ago by George Gey (Gey *et al.*, 1952). MDA-MB-231 is a very commonly used cancer cell line to investigate cancer biology and to test cancer treatments. It is a breast cancer cell line. This cell line was derived at M.D. Anderson in 1976 from a pleural effusion from a 31 years old woman. She had a history of breast cancer. MB stands for the metastatic breast cancer (Ramadass *et al.*, 2015). A brief overview of interactions between liposomes and breast cancer cells has been illustrated in Table 2.3.

2.8 Biological Challenges Faced by Liposomal Drug Delivery Systems

Any foreign particle that enters body has to encounter multiple defense systems aiming at recognition, neutralization, and elimination from the body. Liposomes, being the foreign particles, experience such responses when administered into the blood steam. These defense systems comprised of reticuloendothelial system (RES), opsonization, and immunogenity including some other enhanced permeability retention (EPR) like factors have extensively been exploited to enhance drug delivery and optimal liposomal functions (Sercombe *et al.*, 2015). RES is the main site of liposome accumulation which is associated with some primary organs like liver, spleen, kidney, lungs, lymph nodes and bone marrow. Opsonization and vesicular destabilization by

serum proteins depends upon liposome stability. Stability of liposomes in aqueous dispersion medium may be addressed in two different expects. Chemical stability is mainly caused by oxidation and/or hydrolysis. Different factors such as pH, temperature, buffer concentration and ionic strength play a vital role in hydrolysis kinetics of phospholipids. Physical instability due to vesicle aggregation and fusion may lead to changes in average particle size, size distribution and loss of entrapped drug due to leakage. This eventually leads to larger particle size of liposomes that promote drug leakage (Crommelin, 1984; Grit *et al.*, 1993). Consequently, this leakage affects therapeutic index of loaded drug as larger particles are rapidly cleared by phagocytic cells once they evade RES and opsonization. This refers to the increased permeability of the vasculature that supplies pathological tissues. Depending on the exposure to inflammatory mediators and microenvironment of the pathological sites, the width of tight junctional regions in endothelial cells (*in vivo*) increases from a normal reported range of 2 – 12 nm to 0.2 – 1.2 μm pore size range. Importantly, interaction of all types of liposomes with immune system has being investigated to improve efficacy, circulation times, reduce cytotoxicity and RES clearance from the body.

So far, it has been found from literature that RBC membranes have negatively charged surfaces which contribute to their repulsive electrical zeta potentials between cells. Any negatively charged particle entering blood stream is expected to remain stable due to such repulsive interactions. Based on this strategy, liposome in the current study will be designed to attain long circulation half-life in blood stream. Following stability aspects, zeta potential values of either – 30 mV or + 30 mV are the most widely accepted values for various liposomal and other colloidal suspensions. However, RBC zeta potential values have also suggested another range of zeta potential values which may be followed to avoid protein adsorptions and RES of the body. Thin film hydration method was used to prepare liposomes because of the simplicity and practicability of

this method. Moreover, it has the ability to produce small and uniform liposomes. Nano technology measurements for colloids includes a range of models which enables analysts to select the best system for their applications out of which the Malvern Zetasizer Nano ZS makes the sizing of nano particles extremely simple, rapid,repeatable and non-destructive. It is a compact and versatile instrument which enables high sensitivity nanoparticle characterization. It combines the measurement techniques of Dynamic Light Scattering (DLS: determines size by measuring the Brownian movement of particles or molecules in a solvent or buffer whereby this diffusion speed is converted into a size distribution using the Stokes-Einstein relationship), Static Light Scattering (SLS: used to determine the molecular weight and the second virial coefficient which provides a measure of protein solubility) and Electrophoresis (micro-electrophoresis used to measure the Zeta potential of dispersions and surfaces). Four anticancer drug namely leucovorin calcium, methotrexate, doxorubicin hydrochloride and irinotecan will be entrapped into the formulated liposomes which are chosen on the basis of their lipophilicity. The Franz diffusion cell was used to assess the skin permeability, providing key insights into the relationships between skin, drug and formulation. Human blood will used to investigate hemocompatibility (hemolysis and cell aggregation) of the liposomes under study. Human bread cancer cell line i.e MDA-MB-231 will be used to carry out cell cytotoxicity and cell uptake studies for doxorubicin encapsulated liposomes only as doxorubicin will be taken as model drug which has most commonly been used to investigate such studies so far.

CHAPTER 3: MATERIALS AND METHODS

3.1 Materials

L-a-phosphatidylcholine (PC) from Soybean (97.7 %) was purchased from CALBIOCHEM. The solvent chloroform was purchased from Merck whereas dipalmitoylphosphatidylcholine (DPPC ≥ 99 %, sigma), distearylphosphatidylcholine (DSPC, ≥ 98 %,), phosphatidylserine (PS, ≥ 97 %, TLC), L-a-phosphatidylinositol (PI, ~ 50 %, TLC) from Glycine max® (soybean), Polyethylene glycol sorbitan monooleate (Tween® 80, viscous liquid), insulin from bovine pancease (≥25 USP units/mg (HPLC), powder) and dicetyl phosphate (DCP,) were obtained from Sigma-Aldrich. Leucovorin calcium was purchased from Sigma-Aldrich, USA. Methotrexate, Doxorubicin (hydrochloride), and irinotecan were purchased from CAYMAN Chemical Company, USA and Sellechem company, USA respectively. Phosphate buffer saline (PBS) tablets were also obtained from Sigma. Phosphate Buffered Saline tablets have been used to prepare 0.01 M phosphate buffer throughout in this project. Each tablet contained 0.0027 M potassium chloride and 0.137 M sodium chloride (pH 7.4) at 25 °C when dissolved in 200 mL of deionized water. All the solutions and samples used in this study were prepared with deionized (DI) water having resistivity of 18.2 Ω/cm (Barnstead Diamond^{TM} RO unit, Barnstead International, USA). Dulbecco‘s modified minimal essential medium (DMEM), foetal bovine serum (FBS), trypsin EDTA, and 10X phosphate buffer saline solution were purchased from Invitrogen (Carlsbad, CA, USA). Disposable microtitre plates (6, 24 and 96 wells), cell culture flasks, sterile disposable filter units and disposable serological pipettes (2, 5, 10, 25 ml) were purchased from Nunc (Rochester, NY, USA). Sterile 15 and 50 ml centrifuge tubes were bought from Falcon (Becton Dickson, Franklin Lakes, USA).

3.2 Methodology

3.2.1 Liposome Preparation

The phosphatidylcholine stock solution for critical vesicle concentration (CVC) determination was carried out via thin film hydration method previously described by Bangham (Bangham *et al.*, 1965). The turbid solution obtained after thin film dispersion in PBS was subjected to CVC determination using UV/Vis spectrophotometer (Cary 50, Agilent technologies, USA). Briefly, a definite amount of phospholipids (2 %) was dissolved in 8 mL of the solvent chloroform. Chloroform was purged with nitrogen gas (3-5 bar) prior to use in order to avoid any oxidation of phospholipids. The phospholipid-chloroform solution was transferred to a 100 mL round bottom flask. The contents of the flask were subjected to a rotary evaporator (Buchi R-114 rotary evaporator, Buchi-B-480 water bath, Eyela Aspirator A-1000 S, vacuum system, New Castle, DE) to get a well-mixed thin film. The lipid residual film was then reconstituted in PBS buffer of pH 7.4 leaving behind a turbid suspension of large multilamellar vesicles in flask.

Spectrophotometry is a technique that uses absorbance of light in UV and visible part of the electromagnetic spectrum to determine the analyze concentrations. The atoms and molecules of every analyte are excited to higher energy levels by the absorbance of a particular wavelength of light. The working principles involve the passage of a beam of light through the sample solutions. A part of that incident light (I_o) light is absorbed by the sample solution whereas the remainder part of that light (I) is transmitted through the sample. The ratio of the intensity of the incident light (I_o) to the exiting light (I) at a particular wavelength is termed as transmittance (T) and a negative logarithm of this transmittance is referred to as absorbance (A).

$$A = -\log (\%T/100\%) \quad (3.1)$$

This technique is based on the Beer-Lambert law which states that the absorbance of a sample is proportional to the absorbtivity of the substance and path length and concentration of the absorbing analyte. The absorbitivity for any sample is constant at constant wavelength. The path length is the distance travelled by the light through a sample during its analysis. Mathematically, this law can be shown as:

$$A = \log_{10} (I/I_o) = \varepsilon cL \qquad (3.2)$$

Where, ‗ε' is termed as wavelength-dependent molar absorptivity coefficient which has units of M^{-1} cm^{-1}. *A* is the measured absorbance, *L* is the path lenth, c is concentration of the analyte. Important parts of the instruments consist of a source of light, monochromator, sample holder, photomultiplier tube and a detector. Briefly, 0.2 % (w/v) of PC solution was prepared by dispersing thin film of 10 mg of phosphatidylcholine into 5 mL of PBS (pH 7.4). The subsequent steps involved preparation of series of diluted solutions of phosphatidylcholine with PBS at pH 7.4. Absorbance of each diluted solution of PC was observed at 25 °C using UV/Vis spectrophotometer at a wavelength of 350 nm. A plot of absorbance versus natural log (*ln*) concentration of each diluted solution was constructed to determine the CVC.

Liposomes were prepared as previously described by Bangham in 1965. Composition of each liposome formulation has been described in Table 3.1. Briefly, each combination of phospholipids was dissolved in 8 mL of the solvent chloroform. Chloroform was purged with nitrogen gas (3-5 bar) prior to use in order to avoid any oxidation of phospholipids. The phospholipid-chloroform solution was transferred to a 100 mL round bottom flask. The contents of the flask were subjected to a rotary evaporator (Buchi R-114 rotary evaporator, Buchi-B-480 water bath, Eyela Aspirator A-1000 S, vacuum system, New Castle, DE) to flask get a well-mixed thin film. The lipid residual film was then reconstituted in PBS buffer of pH 7.4 leaving behind a turbid suspension of large multilamellar vesicles.

Table 3.1: Composition of formulated phospholipid liposomes.

	Liposome Formulation	Formulation Composition (% w/v)
F1	PC: Tween® 80: DPPC: DSCP: PS	2 : 0.5 : 0.01 : 0.01 : 0.01
F2	PC: Tween® 80: DPPC: DSCP: PS: DCP	2 : 0.5 : 0.01 : 0.01 : 0.01 : 0.72
F3	PC: Tween® 80: DPPC: DSCP: PS: PI	2 : 0.5 : 0.01 : 0.01 : 0.01 : 0.72
F4	PC: Tween® 80: DPPC: DSCP	0.5 : 0.125 : 0.02 : 0.06
F5	PC: Tween® 80: DPPC: DSCP: DCP	0.5 : 0.125 : 0.02 : 0.06 : 0.26
F6	PC: Tween® 80: DPPC: DSCP: PI	0.5 : 0.125 : 0.02 : 0.06 : 0.5

The temperature of the buffer was maintained at 65 ºC well above phase- transition temperature of lipids under study. Sizing of liposomes was done by subjecting the liposomes suspension to sonication with a total process time of 2 min (8 s pulse on, 10 s puls off). Sonication was done in a probe ultrasonicator (Sonic Dismembrator FB 505 (Ultrasonic Processor), Fisher scientific). Probe sonicator is used for processing nanomaterials in terms of dispersing, deagglumerating, reduction in particle size, particle synthesis and particle preparations, and surface functionalization. These are highly effective sonicators which make use of a probe-type ultrasonic homogenizer by introducing high power ultrasound into the sample medium. Alternating high-pressure (compression) and low-pressure (rarefaction) cycles are created when these ultrasound waves are transmitted in the sample medium. Small vacuum bubbles or voids are created in the liquid during low-pressure cycles. At a volume where these bubbles can no more absorb energy, they violently collapse during the cycles of high-pressures and the phenomenon is termed as cavitation. Very high pressures and temperatures are seen locally during these implosions. The energy input and the sonotrode surface area affect the intensity of the ultrasonication. The larger the surface area of sonotrode, the smaller is the intensity of ultrasound for a given energy input. The small nanosized liposomes were analyzed for particle size and zeta potential measurements after sonication. DOX was encapsulated into the liposomes using the same thin film dispersion method. DOX

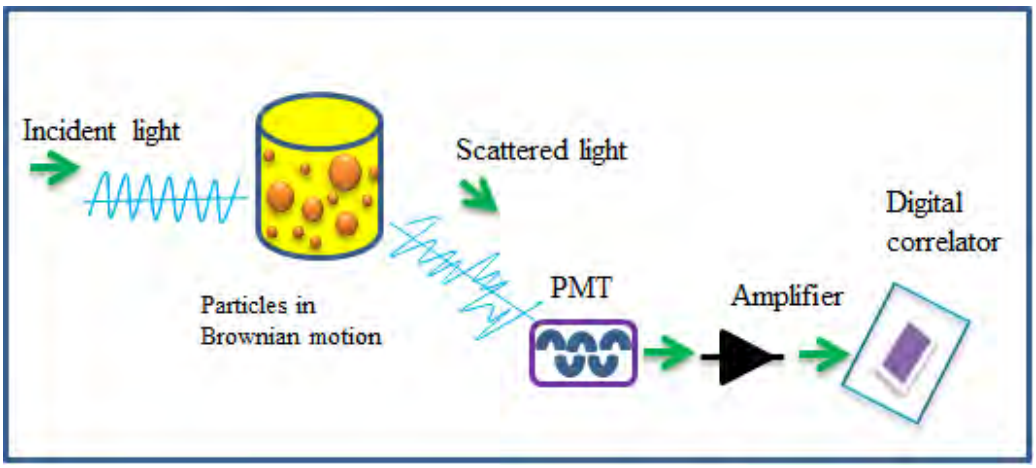

Figure 3.1: A simple illustration showing general working principle of dynamic light scattering.

was dissolved in PBS (pH 7.4) to disperse resultant thin film along the wall of round bottom flask. Multilamelllar vesicles with trapped active ingredients like insulin, LVC, DOX, MTX, and IRT were subjected to sonication to get nano-sized liposomes as mentioned above.

3.2.2 Particle Size Measurement

The average diameter and particle size distribution of liposomes were measured sing the well-known dynamic light scattering technique (DLS). The techniques employed a Malvern Zetasizer ZS via a DTS Nano software (version 6.12, Malvern Instruments LTd. UK). It is equipped with a 4 mW He-Ne laser at 633 nm using a scattering angle of 17 and 173º from the scattering axes respectively. Particles, suspended in a suspension or solution, undergo Brownian motion. Size and distribution of these particles can be determined by measuring random changes in the intensity of light scattered by these particles. DLS is a non-invasive, well-established technique that allows particle sizing down to 1 nm diameter with typical applications in the field emulsions and micelles. This technique is sometimes referred to as Quasi-Elastic Light Scattering . The basic principle involves the sample illumination by a laser beam. The speed at which the particles are diffusing due to Brownian motion is measured by recording the rate at

which the intensity of the scattered light fluctuates. These fluctuations of the scattered light are detected at a known scattering angle by a fast photon detector (Figure 3.3). Given below is the Stokes-Einstein equation which shows that diffusion speed of this motion is inversely proportional to the hydrodynamic diameter of the particles which is defined as the size of a hypothetical hard sphere that diffuses in the same fashion as that of the particle being measured.

$$\boldsymbol{D = \frac{kT}{3\pi\eta d_{\mathrm{p}}}} \qquad (3.3)$$

Where, D is translational diffusion constant, k is Boltzmann constant, T is temperature, η is viscosity, and d_p is hydrodynamic diameter. Precise values of parameter T and η must be known in order to determine particle size of the sample accurately. Interference, either constructive (intensification) or destructive (cancellation), occurs within the light which is scattered by the different particles. Due to the free motion of particles in liquid, this interference may change over time leading to disparity of the scattered light intensity which is recorded by a highly sensitive Photomultiplier (Figure 3.4). This time reliance of the scattered light intensity is directly affected by the speed of the particles which in turn relies on particle size and usually analyzed via autocorrelation.

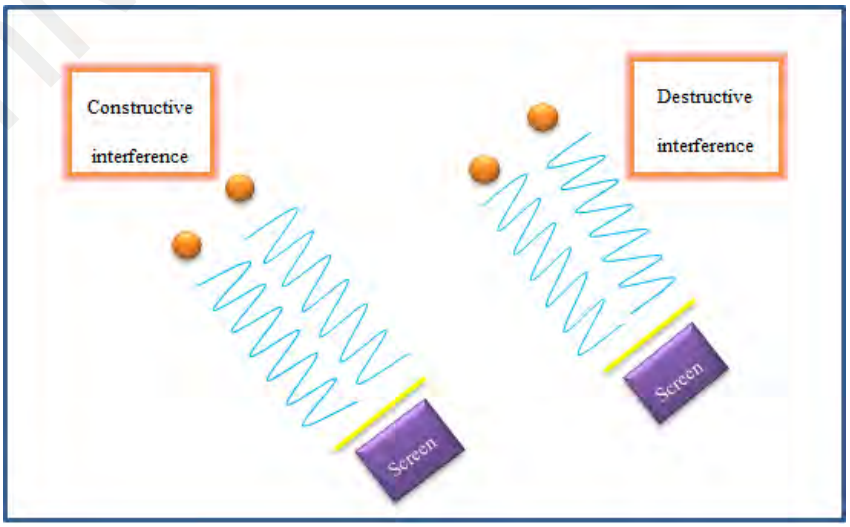

Figure 3.2: Phase addition of scattered light.

Hence, the name photon correlation spectroscopy is also given to this technique. In routine analysis, the scattered light is recorded either at 90° angle to the incident laser light or else the back scattering (173°-177°) is record depending upon the scattering intensity and concentration of the sample.

Particle size measurements involved a U-shaped polycarbonate sample cuvette equipped with gold plated electrodes. All the samples were measured at 25 °C. The results obtained were measured in triplicates and were presented as an average values for particle size for all liposomes.

3.2.3 Zeta Potential Measurement

The liposomes were analyzed for their average zeta potential measurement using a Malvern Zetasizer ZS (version 6.12, Malvern Instruments, UK). It is equipped with a 4 mW He-Ne laser at 633 nm and works on dynamic light scattering method employing a scattering angle of 17° and 173° from the scattering axes respectively. The term zeta potential refers to the potential difference between the surface of particles and dispersing medium. Stability of the suspended particles is accessed by the magnitude of the zeta potential. The higher the magnitude of zeta potential, the greater will be the repulsive interactions between colloidal particles. Knowledge of the surface charge helps in understanding accumulation of high ionic concentrations of opposite charges on the particle surface as compared to the bulk of the solution. This surface charge is developed due to the formation of electrical double layer around each particle with an inner region of stern layer and outer being the diffuse region. The former corresponds to the strongly bound ionic layer whereas the later refers to the less firmly attached ions. This diffuse layer contains a notional boundary within which ions and particles form a stable entity. Ions within the boundary move along with the movement of any particle. This boundary is termed as the surface of hydrodynamic shear or slipping plane and the potential at this boundary is known as the Zeta potential (Figure 3.5).

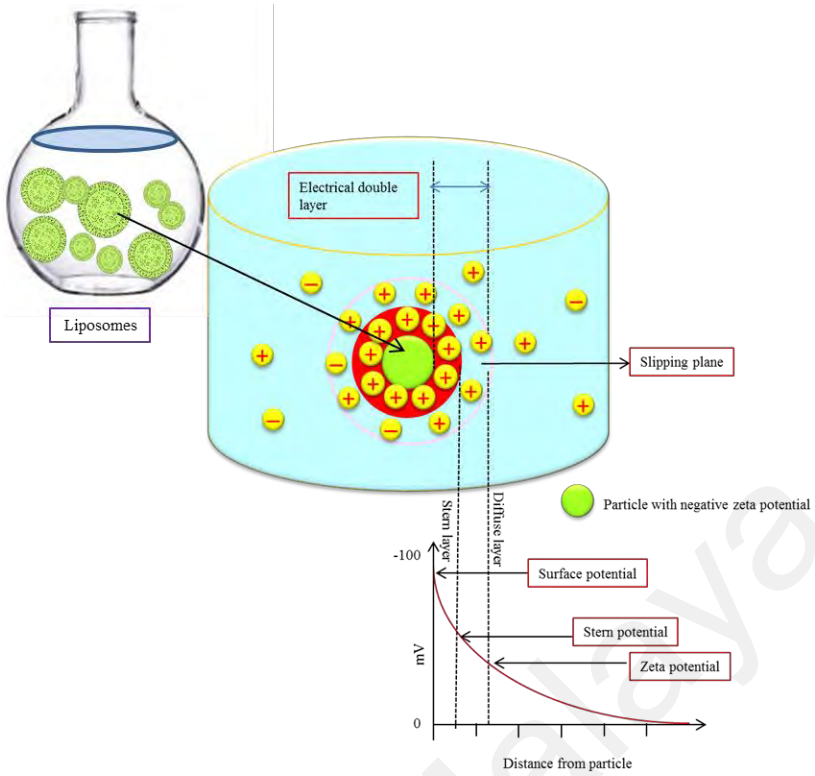

Figure 3.3: Schematic representation of zeta potential measurements of liposomes.

Electrophoresis is the movement of a charged particle relative to its surrounding liquid under the influence of an applied electric field. The particles move with a velocity which is dependent on Zeta potential, field strength, dielectric constant of medium and viscosity of the medium. Velocity of a particle in a unit of applied electric field is defined as electrophoretic mobility which is related to the zeta potential by the Henry equation:

$$\boldsymbol{U_E = \frac{2\,\varepsilon\, z\, F(k\,a)}{3\eta}} \qquad (3.4)$$

Where, U_E is Electrophoretic mobility, z is zeta potential, ε is Dielectric constant, η is viscosity of the solution, and F is *(ka)* Henry's function. Henry's Function gives information about the electrical double layer thickness (Debye length) with the dimensions of inverse length ($1/k$), and particle radius (a). Therefore, the term ka is equal to the ratio of particle thickness to the Debye length (a/k). Particles present in the polar medium are described by Smoluchowski approximation with 1.5 F (ka) value

whereas Huckle‘s approximation has been applied to the non-polar solvents with a (9 *ka*) value of 1.5. The samples were measured at 25 °C. The results obtained were measured in triplicates and were presented as an average values for particle size for all liposomes.

3.2.4 Stability of Formulations

After obtaining optimum sonication time, all formulations were subjected to stability tests. Stability tests were performed by storing the small unilamellar vesicles (SUV) in a dark oven at 37 °C for a period of 28 days. The liposomes were also analyzed for storage stability at room temperature and 4 °C for 28 days. The samples were analyzed for particle size, zeta potential and polydispersity index and the results were recorded in the form of graphs.

3.2.5 Optical Polarizing Microscopy

A Leica Optical polarizing microscope (equipped with Leica QWin software, Leical Mycrosystems, Germany) was used to evaluate size, polydispersity and morphology of the F1, F2, F3, F4, F5 and F6 liposome formulations at 25 °C.

Polarizing microscope is a contrast enhancing technique which is used for identification or imaging of birefringent structures of optically anisotropic specimens on the basis of characteristic refraction properties and colors. It uses polarizing filters to make use of polarized light, configuring the movement of light waves and forcing their vibration in a single direction. A single light ray is divided into two sister rays by refraction using a birefringent object. Refraction of these sister rays can result in color effects like rings and lighting up of structures using combination of birefringence and linearly polarized light in microscopy. A simple layout showing main components and working of an optical microscope has been given in Figure 3.6.

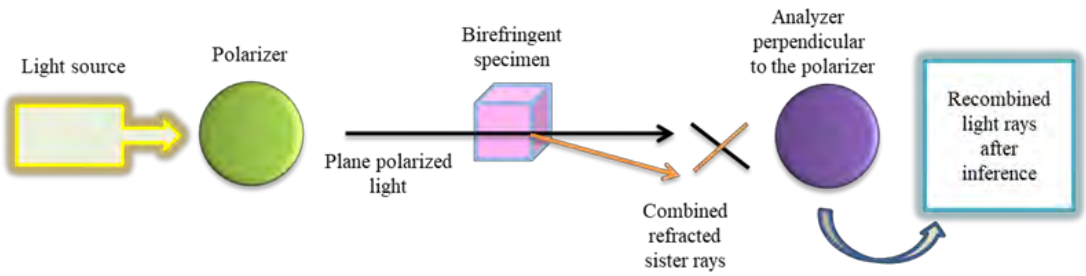

Figure 3.4: A simple working principle of an optical polarizing microscope.

The procedure involved application of a drop of each liposome sample suspension onto a glass slide which was later covered with a cover slip. The micrographs were taken after placing a drop of immersion oil on the glass cover slip. The presence of liposomes was observed with the help of an objective lens of 50x at 500 magnification times using a light and a dark phase.

3.2.6 Transmission Electron Microscopy (TEM)

The prepared formulation was subjected to an energy Filtered TEM model LIBRA 120 (quipped with an Olympus SIS-iTEM, version 5, Germany) to study morphology of nanosized liposomes. Transmission electron microscope works on many of optical principles similar to light microscope. TEM is provided with an additional advantage of greater resolution which allows the study of ultrastructure of organelles, viruses and many other macromolecules. The working principle involves a beam of highly energetic electrons despite of a simple light as in light microscope. When this electron beam falls on the material sample, the electrons may be stopped or deflected by different parts of the samples. A phosphorescent screen or a camera collects these electrons from beneath the sample. The image obtained may be dark, light or grey depending upon the electron interactions with the different sample sites. The dark image appears when no passage of electrons takes place through the sample, whereas the unscattered electrons generate a brighter image. The grey images are observed due to the different interactions of the

electrons with the different sample areas. A simple layout of scattering of electron beam from the specimen sample is shown in the figure 3.7. The resolution of the instrument is as good as below 1 nm with magnifications of up to 1,000,000x achieved in route analysis. This high magnification has made TEM such a valuable tool in various fields of medical, biological and material research for analyzing two dimensional image quality, shape, size, quantum wells, wires and dots. The procedure followed the placement of one drop of each formulation onto an individual carbon-coated copper grid. A filter paper was used to remove the excessive amount of formulation after one minute. As a negative staining agent, 1 % phosphotungstic acid, was applied on the grid for only one minute. The excessive stain was also removed with the help of a filter paper. The grid was air dried initially and then was put in desiccator for two days before being examined under transmission electron microscope.

3.2.7 Field Emission Scanning Electron Microscopy (FESEM)

The morphology of the liposomes was also studied by using a Field emission scanning electron microscope (JEOL JSM-7600)**.** Field emission scanning electron microscopy is a technique that works with electron liberated by a field emission source whereby the object can be scanned by electron to visualize very small topographic details on its surface. This is employed to observe topographical and elemental information with a magnification of 10x to 300, 000x providing much clearer and less electrostatically distorted images. The spatial resolution of as low as 1 nm (three to six times better than conventional scanning electron microscopy) can be obtained to examine smaller-area contamination spots, high quality & low-voltage images with negligible charging of samples and analysis of insulating materials without placement of conducting coatings. The working of this microscope involves emission of electrons liberated from emission source. These electrons are then accelerated in a high electrical field gradient and are called primary electrons. Secondary electrons are generated when

these primary electrons are focused and deflected by electron lenses which are bombarded on the objects. The surface structure of these objects is related to the angle and velocity of these high energy secondary electrons. Electrical signals are generated when these secondary electrons are collected by the detectors which are amplified and transformed to three dimensional video scan-images. Its applications cover a wide range of research areas to characterize cell size, size distribution, shape, thickness measurement of thin coatings and films, measurements of dimensions of nano-sized objects, fracture and defect analysis.

The samples for F1 to F6 formulations were prepared using freeze drying method. The dried samples were observed under FESEM to analyze particle size, morphology and particle distribution.

3.2.8 Differential Scanning Calorimetry (DSC)

Thermal behavior of unloaded (empty) liposomes after freeze drying was characterized by using Pyris 6 DSC (PerkinElmer, USA). A thermoanalytical technique in which the difference in the amount of heat required to increase the temperature of a sample and reference is measured as a function of temperature is called differential scanning calorimetry (DSC). In this technique, both the sample and reference are maintained at nearly the same temperature throughout the experiment. Generally, the temperature program for a DSC analysis follows a designed in which the sample holder temperature increases linearly as a function of time. The reference sample used in such studies must have a well-defined heat capacity over the range of temperatures to be scanned.

Approximately 5 mg of sample was weighed into an aluminum sample pan and an empty sample was used as a reference. The heating was performed from 15 °C to 110 °C with a heating rate of 2 °C /min.

3.2.9 Encapsulation Efficiency

Encapsulation efficiency of the prepared liposomes for different active ingredients was measured using centrifuge method. Insuline was entrapped to F1 liposomes in one study to analyse its % EE for one active ingredient only. Later, LVCMTX, DOX, and IRT were encpasultaed in all F1-F6 liposomes. Briefly I mL suspension of each anticancer drug loaded liposome sample was transferred to an individual viva spin centrifugal unit (Vivaspin 6, 10 kDa MWCO, Sartorius Stedim Biotech, Germany). The viva spin units were then subjected to a centrifugation speed of 1500 rpm for 15 minutes at 25 ± 1 ºC using a Velocity 18R refrigerated centrifuge (Dynamica Scientific Ltd., UK). The aliquot in the viva spin collection tube was analyzed for unencapsulated anticancer drug using a UV/Vis Spectrophotometer (Varian Cary 50 UV/Vis Spectrophotometer, Agilent Technologies, USA). The percent encapsulation efficiency (%EE) was calculated using the following equation:

$$\% \mathbf{EE} = \frac{\mathbf{WT} - \mathbf{WF}}{\mathbf{WT}} \boldsymbol{X}\ \mathbf{100}\ \% \qquad (3.5)$$

Where WT is the total amount of anticancer added during liposome preparation, and WF is the amount unloaded free drug.

3.2.10 In Vitro Anticancer Drug Release in Phosphate Buffer Saline (PBS)

In vitro release of anticancer drugs from prepared liposomes was carried out via an automated Franz Diffusion Cell System (Hanson Research Co., USA). For this purpose, the drug loaded liposomes were separated from the unbound drug using dialysis membrane, 3500 MWCO. The washing of DOX-loaded liposomes was done using PBS with pH 7.4. The dialysis membrane was soaked in DI water overnight and was washed gently before use. The sample aliquot was taken in the dialysis tube which was sealed from both ends with the help of a thread. The sample tube was suspended in PBS (washing medium). The washing medium was analyzed after every 15 minutes to observe release of unbound drugs from dialysis tube using UV/Vis spectrophotometer.

The washing was continued until no more DOX was observed in the washing medium. The same procedure was repeated for LVC, MTR and IRT anticancer drugs. For the purpose of release studies, receptor chambers of Franz Diffusion Cell System were filled with PBS media. Cellulose dialysis membranes of 3500 MWCO were placed between donor and receptor chambers. Both chambers were later clamped together with the help of pinch clamps. 1mL aliquot of the liposomal suspension (drug equivalents of 30 µg/mL) was introduced into the donor chamber with a stirring speed of 100 rpm and a controlled temperature of 37 ± 1 °C. Samples collected from the receptor chamber for LVC, MTR, DOX and IRT loaded liposome samples were analyzed by UV/Vis spectrophotometer at 288 nm, 303 nm, 485 nm and 255 nm respectively.

Log *p* values can well explain the partitioning behaviour of the drugs between liposomes and bulk. As the drugs with more negative log *p* values (more hydrophilic) are encalpulated within the core of liposomes, the drugs with intermediate log *p* values were encapsulated both in hydrophilic bilayer and core of liposomes whereas the drugs with more positive log *p* values (more hydrophobic) were encapsulated only in the lipid bilayers. The encapsulation efficiency has quantitativley expalined the higher entrapment percentage of drugs (doxorubicin hydrochloride and methotrexate) with intermediate partitioning properties i.e upt 80 %, however, this percentage is arount 60 while talking about either highly hydrophilic (leucovorin calcium) or highly hydrophobic (irinotecan) drugs used in this study. Therefore, comparison of *in vitro* release profiles in PBS (pH 7.4) and kinetcs) has demonstrated that most of the drug release profiles have followed Gompertz model. The exponential model known as Gompertz model describes in-vitro dissolution profile. This model explains well the release profiles of drugs having good solubility and intermediate release rates.

3.2.11 Release kinetics

Drug release data was fitted to Zero order, First order, Higuchi and Gompertz models to investigate the release kinetics in DD solver software (Zhang *et al.*, 2010).

3.2.12 Hemolysis Assay

Hemocompatibility of the prepared formulations was investigated using EDTA (Ethylene Diamine Tetra Acetic acid) stabilized human whole blood. This *in vitro* hemolysis assay is a test used to evaluate the potential of liposomes in biomedical application. In order to isolate red blood cells (RBC) from serum, 10 mL of the EDTA stabilized human blood sample was centrifuged at 500 × g for 10 min at a temperature of 4 ºC. The RBC were washed three times with chilled PBS (4 ºC and then diluted to 2 % (v/v) in PBS (20 µL RBC pellet + 980 µL PBS at 4 ºC). Each liposome formulation was diluted using serial dilution method as follows: 20 mg/ml, 10 mg/ml, 5 mg/ml, 2.5 mg/ml, and 1.25 mg/ml. Different concentrations of the samples were analyzed for hemolytic activity by incubating 100 µL of phospholipid suspension with 100 µL of diluted RBC suspension at 37 °C in a water bath (with mild shaking). A 96 well plate was used to for sampling purpose. The plate was taken out of the water bath after 5 hrs of incubation. It was centrifuged at 500 × g for 10 minutes at 4 °C. 100 µL of the supernatant from each well was transferred to another 96 well plate. The plate was analyzed for determining absorbance using a microplate reader (Tecan Infinite M200) at 550 nm. The negative control comprised of the RBC in PBS (0% lysis) whereas the positive control was prepared by mixing Triton® X 100 solution with RBC (100 % lysis.) The negative control was PBS (pH 7.4). The formula used for calculating per cent hemolysis is as under:

$$\% \text{ Hemolysis} = \frac{\text{sample absorption} - \text{negative control absorbance}}{\text{positive control absorbance} - \text{negative control absorbance}} \times 100\ \% \qquad (3.6)$$

3.2.13 Liposome Aggregation Analysis

100 µl aliquot of 2 % RBC suspension in Ringer solution was mixed with 100 µl of liposome suspension at concentrations of 1 mg/ml and 10 mg/ml in a 96 well microtitre plate. For positive control, 100 µl of PBS was mixed with 100 µl 2 % RBC suspension (in modified Ringer‘s solution that contains no sodium citrate). All the test and control samples were incubated for 2 hours at 37 °C. After incubation, the samples were examined using an inverted microscope (Shinjuku- Ku, Tokyo, Japan) at 100 × magnification.

3.2.14 *In vitro* Cytotoxicity Study

a. Media Preparation

In the current study, MDA-MB-231human breast cancer cells were used. The cells were grown to confluence in Dulbecco‘s modified minimal essential medium (DMEM) containing 10 % foetal bovine serum (DMEM-growth medium, DMEM-GM). To maintain the confluent cells, DMEM containing 2 % foetal bovine serum (DMEM-maintenance media, DMEM-MM) were used. Periodically, cryopreservation was performed onto the populated cells so as to maintain the cell stock.

b. Cell Line Preparation

The cell line (MDA-MB-231) was revived from cryopreservation and populated for at least three rounds prior to use. To perform the cell growth inhibition study, the confluent monolayer of cells in the cell culture flask was trypsinized and resuspended in DMEM-GM.

c. Effect of DOX-Loaded Nanoparticles on Suppression of Cellular Growth

A diluted cell sample of 10 µl was estimated using a haemocytometer. Following that, a working cell suspension with a concentration of 50,000 cells per ml was prepared. 100 µl of the suspension was added into each of the 96-well cell culture

microplate. The microplate was incubated for 24 hours at 37 ºC in a 97 % humidified atmosphere of 5 % CO_2 before it was used for further study. After that, the culture medium was replaced with 100 µl fresh medium in each well containing DOX-F1, DOX-F2 and DOX-F3 liposomes, with 1 µg/ml and 10 µg/ml DOX concentrations for each formulation. A positive control containing 1 µg/ml and 10 µg/ml of free DOX was run along in the same plate. A negative control comprising of the freshly replaced medium without treatment was also included. A control carrier group congaing unloaded liposomes was also included. All tests were performed in triplicates. Thereafter, cells in the microplates were incubated for 48 hours or for 24 hours respectively at 37 ºC in a 97 % humidified atmosphere of 5 % CO_2. At the end of incubation, the microplate was subjected to an inverted microscope to get images.

d. Cell uptake of DOX-loaded liposomes by Flow Cytometry and Confocal Microscopy

A cell suspension of 1 X 10^5 cells per ml for flow cytometry and 2.5 X 10^5 for confocal microscopy was prepared as given in section 3.7.3. For flow cytometric analysis, 1 ml from the prepared cell suspension was added to 24-well cell culture plate. The cells were incubated for 24 hours at 37 °C in a 97 % humidified atmosphere of 5 % CO_2. After 24 hours incubation, the wells were treated with DOX-loaded liposomes as mentioned above in section 3.7.3. The plate was incubated for 3 hours at 37 °C in a 97 % humidified atmosphere of 5 % CO_2. After three hours incubation, the medium was discarded and each well was washed with 500 µl PBS. 200 µl of trypsin was added to each well and the plate was again incubated for 3 minutes under the above mentioned conditions. After incubation, 600 µl of DMEM-growth medium was transferred to each well. After mixing, the contents from each well were transferred to eppendorf tubes. The tubes were centrifuged at 2500 rpm for 5 minutes. Each pellet was resuspended in 400 µl flow buffer medium (1 % FBS) and contents from individual tubes were transferred

to flow vials. The vials were kept at 4 ºC before use. For microscopic analysis, 1 ml from the prepared cell suspension was added to 6-well cell culture plate. Before adding the cell suspension, a glass cover slip was added to each well after washing with 70 % ethanol. The cells were incubated for 24 hours at 37 °C in a 97 % humidified atmosphere of 5 % CO_2. After 24 hours incubation, the wells were treated with DOX-loaded liposomes as mentioned above in section 3.7.3. The plate was incubated for 3 hours at 37 °C in a 97 % humidified atmosphere of 5 % CO_2. After three hours incubation, the medium was discarded and each well was washed with 1 ml PBS twice. 1 ml of 4 % paraformaldehyde solution was added to each well after that and kept at room temperature for 10 minutes. Paraformaldehyde was removed after 10 minutes and 1 ml PBS was added to individual wells. Glass slides were labeled and one drop of DAPI was put on each glass slide. Cover slip from each well was taken out very gently and was inverted carefully onto the DAPI stain placed on respective glass slides. The slides were preserved at 4 °C until used for analysis.

CHAPTER 4: RESULTS AND DISCUSSION

4.1 Preparation of Liposomes

The key to successful preparation of an injectable liposome formulation is in the selection of some suitable combination of biomimetic phospholipids (Kanapathipillai *et al.*, 2014; Li *et al.*, 2016). Therefore, phospholipids namely lecithin, DPPC, DSPC, (Chang & Yeh, 2012), phosphatidylinositol (PI) (Suzuki *et al.*, 2016), and phosphatidylserine (PS) (van der Geest *et al.*, 2016) were mixed together into F1, F2, F3, F4, F5 and F6 formulations (Table 3.1) with the aim to develop and optimize them for average particle size and RBC zeta potentials and their evaluation for anticancer drug delivery applications. Tween® 80, an emulsifier, is used in the current study to optimize particle size as it has been approved by various pharmacopoeias for parental administration and has been included in various reported parenteral formulations (Nielsen *et al.*, 2016; Shabnama *et al., 2014*; Tsai *et al.*, 2015). DCP, also used as surfactant, is a negatively charged lipid that has been used to induce a negative charge to the model membranes (Deamer *et al.*, 1976; Zylberberg *et al.*, 2017). In our current project, combination of PC, Tween® 80, DPPC and DSPC were used to optimize and establish stable liposomal suspensions, whereas PS, DCP and PI were used to optimize average zeta potentials of the final formulations.

4.1.1 Particle Size of Liposomes

Among Pharmacokinetic Parameters, the first aspect of a liposome that affects its disposition is its size. It is very important in designating drug carriers with reference to reticuloendothelial system (RES) of the body. According to Li Tang *et al.,* the overall therapeutic efficacy against cancer is affected by the optimum particle size which has a strong impact on its biodistribution, tumor penetration and internalization, clearance from blood plasma, tissues and excretion from the body as well (Tang *et al.*, 2014).

In this study, size optimization for final mix of phospholipids was initiated by considering lecithin as base material. In the first step, therefore, critical vesicle concentration (CVC) of lecithin was investigated using UV/Vis spectrophotometry (Figure 4.1). CVC, an important quantitative parameter, refers to the minimum concentration of lipids required in forming liposomes which also implies the tendency to self-assemble. CVC was determined via the inflection point through the plot of absorbance versus lecithin concentration. Below CVC, no significant changes in the absorbance were observed in the presence of lecithin monomers. However, a remarkable enhancement of lecithin absorption was noticed just above the CVC of the lecithin (Domínguez *et al.*, 1997). The result show that absorbance of all liposome solutions was increased with increasing concentration of lecithin indicating the self-assembly of large vesicles (Apel *et al.*, 2002).

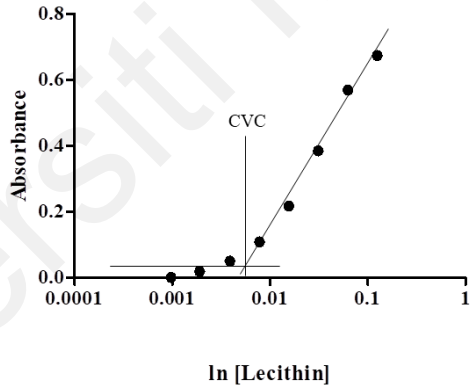

Figure 4.1: Determination of CVC for phosphatidylcholine using UV/Vis spectrophotometer.

The increased absorbance may also be attributed to the presence of more number of vesicles with similar particle size as the lecithin concentration increases. Once introduced into the system, the lipids initially partition into the interface, reducing the system‘s free energy by either lowering the energy of interface or by removing the hydrophobic parts of the lipids from contact with water. Upon dissolution in water, the lipids adsorb and orient themselves in water in such a way that the hydrophobic regions are removed from the aqueous environment. The replacement of water molecules at

surface causes the reduction in surface tension which arises from the reduction in concentration at the air/water surface. This happens due to lower intermolecular forces between lipids and water molecules compared to those between water molecules. Subsequently, the lipids start aggregating in bilayers by decreasing contact areas of hydrophobic parts of the lipids with water (Attwood *et al*., 2013). Lower values of CVC suggest that the self-assembly of phospholipids into bilayers is more favorable. The CVC value of lecithin was obtained at 0.01 mg/ml. This study implies that lecithin at a concentration above 0.01 mg/ml tend to self-assemble into vesicles. Besides, it also suggests avoiding the use of either too high or too low concentration of liposome solution for physicochemical studies (Evans *et al.*, 1983; Ninham *et al.*, 1983).

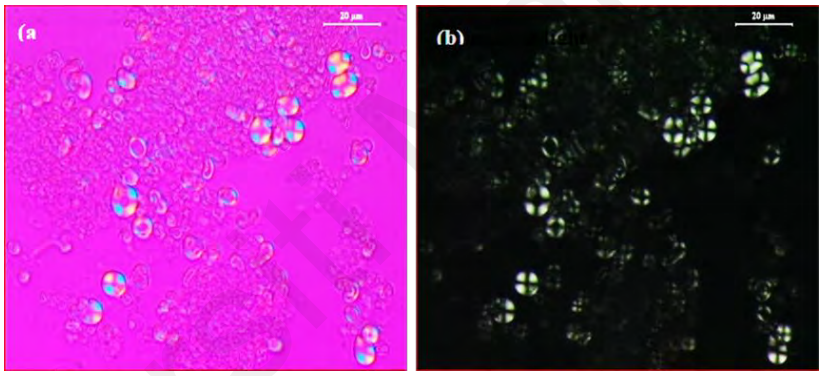

Figure 4.2: The optical polarizing micrograph of lecithin liposomes which showed birefringence effect under light field (a) and maltese cross under dark field.

The presence of liposomes was confirmed by optical polarizing microscope as shown in Figure 4.2. Liposomes formulated for drug delivery purpose were prepared by mixing lecithin with Tween® 80 , DPPC, DSPC, PS, PI and DCP under the formulation codes F1, F2, F3, F4, F5 and F6 (Table 4.1). The concentration of these added lipids and tween 80 were optimized according to the required particle size and stability in PBS medium with pH 7.4. According to the DLS and as observed under polarizing microscope, the particle size for all six liposomal suspensions was quite big and could not be used for anticancer drug delivery purpose. Therefore, all the suspensions were

subjected to the probe ultrasonicator (Sonic Dismembrator FB 505 (Ultrasonic Processor), Fisher scientific).

Table 4.1: Effect of sonication on average particle size, polydispersity index and zeta potential of formulated liposomes.

Liposome Formulation	Average Particle Size (nm)		Polydispersity Index		Zeta Potential (mV)	
	Before sonication	After sonication	Before sonication	After sonication	Before sonication	After sonication
F1	1233 ± 47.00	76.49± 0.91	0.56 ± 0.04	0.33 ± 0.5	- 2.1 ± 0.82	-4.52± 0.22
F2	1555 ± 153.1	70.61 ± 1.92	0.70 ± 0.13	0.31 ± 0.04	-6.46 ± 1.52	-9.68 ± 0.97
F3	1031 ± 24.21	80.67 ± 0.16	0.43 ± 0.07	0.34 ± 0.05	-8.30 ± 0.77	-12.3 ± 1.31
F4	1040 ± 21.22	69.92 ± 0.48	0.61 ± 0.15	0.23 ± 0.00	-4.26 ± 0.23	-3.39 ± 1.06
F5	996.5 ± 157.4	74.98 ± 1.12	0.71 ± 0.01	0.17 ± 0.01	-11.7 ± 1.35	-13.3 ± 0.70
F6	726.2 ± 19.14	76.36 ± 2.18	0.41 ± 0.8	0.27 ± 0.01	-10.9 ± 1.24	-13.7 ± 1.04

*F1= PC: Tween® 80: DPPC: DSCP: PS, F2 = PC: Tween® 80: DPPC: DSCP: PS: DCP, F3= PC: Tween® 80: DPPC: DSCP: PS: PI, F4= PC: Tween® 80: DPPC: DSCP, F5= PC: Tween® 80: DPPC: DSCP: DCP, F6= PC: Tween® 80: DPPC: DSCP: PI.

Probe sonicators are used for processing nanomaterials in terms of dispersing, deagglumerating, reduction in particle size, particle synthesis and particle preparations, and surface functionalization. These are highly effective sonicators which make use of a probe-type ultrasonic homogenizer by introducing high power ultrasound into the sample medium. The optimized liposomal particle size obtained after sonication has been shown in the Table 4.1. The particle size and distribution of the prepared liposomes was determined using Malvern Nanoseries ZetaSizer based on the phenomenon of dynamic light scattering. This technique is the most popular and established technique to measure the hydrodynamic size of the particles up to submicron level (Varenne *et al.*, 2017). The control over liposome size plays a significant role since it determines the circulation time in blood. Particles with a size smaller than 10 nm are more likely to be removed by the renal clearanc (Dhand *et al.*, 2014; Longmire *et al.*,

2008) whereas particles bigger than 200 nm may be recognized and engulfed by phagocytes in the body (Wahajuddin, 2012). Thus, the optimum particle size for unloaded liposomes from F1 to F6 was found to be in the range of 70 - 80 nm which is in accordance with the reported particle size suitable for drug delivery application with a good polydispersity index (Mousa *et al.*, 2017). The term polydispersity and % polydispersity have been derived from the Polydispersity Index (PdI). It is a parameter calculated from a Cumulants analysis of the DLS-measured intensity autocorrelation function. This term ―polydispesity" describes the degree of non-uniformity of a size distribution of particles in liposomal suspension whereby the larger PdI values reflect the larger size distribution in the principle sample. It has been found that PdI values smaller than 0.4 are considered acceptable for drug delivery applications because they indicate a homogenous and monodispersed population (Manconi *et al*., 2009). In current study F1 to F6 formulations showed a good PdI in the range of 0.17 ± 0.01 to 0.34 ± 0.05. The method of preparation of liposomes, pH of the bulk of solution, molecular structure and the composition of the substances in formation of liposomes may affect the particle size of the liposomes. The present study was carried out to optimize drug carrier formulation parameters for intravenous drug delivery using response surface methodologies (RSM). In one of the study, the optimized F1 liposomes were encapsulated with insulin as active ingredients to analyse F1 formulation's % EE for insulin before treating all formulations for other active ingredienrs as well (Naeem et al, 2016). Later, anticancer drugs namely leucovorin calcium, methotrexate, doxorubicin and irinotecan loaded liposomes (F1-F6) were subjected to sonication process as well. Table 4.2 shows a comparison of the various anticancer drug loaded liposomes with respect to their particle size, PdI and zeta potentials. Loading the liposomes with different anticancer drugs did not show significant changes in the mean particle size, polydispersity index and zeta potentials of all liposome formulation except for DOX in

and methotrexate in some formulations. The increased mean particle size of DOX loaded liposomes is owing to the nature of doxorubicin molecules. Doxorubicin is an anticancer drug which has though a hydrophilic functional group (amine and phenol) and is water soluble. But it is fundamentally amphiphilic because of its aromatic backbone and many DOX molecules may be encapsulated in the liposome core whereas some are assumed to be closed to the core/shell border and may increase the particle size of the liposomes (Viswanathan *et al.*, 2016). Methotrexate also has the intermediate log *p* value similar to DOX, and hence shows similar effects on the liposome particle size (Wang *et al.*, 2003).

4.1.2 Zeta Potential

Zeta potential indicates the surface charge of the nanoparticles. Its magnitude plays a significant role in explaining the properties of colloidal suspensions. Flotation, flocculation, and stability of the suspended particles is accessed by the magnitude of the zeta potential. The higher the magnitude of zeta potential, the greater will be the repulsive interactions between colloidal particles.

Solids, liquids and gases are three fundamental states of matter and if any of these is finally dispersed in another we obtain a ‗colloidal system'. Colloidal system mostly carries an electrical potential which may arise from many origins depending upon the nature of the particles and its surrounding medium. These possible mechanisms may include either ionization of surface groups of the building materials which gives negative charge upon dissociation of acidic groups on surface of a particle or a basic surface giving a positive charge. The other mechanism may involve adsorption of charged species whereby cationic surfactants contributing to a positively charged surface and anionic surfactants to a negative value. This surface charge is quantified as zeta potential which is exhibited by a particular particle in a particular medium. It is a

well-recognized concept that zeta potentials give good index of the interaction between various colloidal particles (Laouini *et al.*, 2012).

Knowledge of the surface charge helps in understanding accumulation of high ionic concentrations of opposite charges on the particle surface as compared to the bulk of the solution. This surface charge is developed due to the formation of electrical double layer around each particle with an inner region of stern layer and outer being the diffuse region. The former corresponds to the strongly bound ionic layer whereas the later refers to the less firmly attached ions. This diffuse layer contains a notional boundary within which ions and particles form a stable entity. Ions within the boundary move along with the movement of any particle. This boundary is termed as the surface of hydrodynamic shear or slipping plane and the potential at this boundary is known as the Zeta potential (Honary *et al.*, 2013).

The current study involves the preparation of numerous synthetic red blood cell bilayer membrane liposomes (RBC mimics) for drug delivery applications. It has been investigated that RBC membranes have negatively charged surfaces which contribute to their repulsive electrical zeta potentials between cells (Chevalier *et al.*, 2013; Fontes *et al.*, 2006). Any negatively charged particle entering blood stream is, therefore, expected to remain stable due to such repulsive interactions. Based on this strategy, current liposome formulations have been designed to attain long circulation half-life in blood stream. Though, large repulsive forces help to avoid aggregation of the particles, zeta potential values of either > +30mV or < -30mV are the most widely accepted values for most stable liposomal and other colloidal suspensions (Laouini *et al.*, 2012). RBC zeta potential values (-9 mV to -15 mV) have also suggest another range of zeta potential values which may be followed to avoid protein adsorptions and RES of the body (Chevalier *et al.*, 2013).

Table 4.2: Mean particle size, polydispersity index and zeta potential of formulated liposomes.

Sample	Drug	Average Particle Size (nm)	Polydispersity Index	Zeta Potential (mV)
F1	Unloaded	076.49 ± 00.91	0.33 ± 0.50	-04.52 ± 0.02
F1-LVC	LVC	080.83 ± 01.62	0.35 ± 0.05	-03.33 ± 0.86
F1-MTX	MTX	074.27 ± 01.03	0.25 ± 0.01	-03.18 ± 0.84
F1-DOX	DOX	123.00 ± 41.24	0.47 ± 0.13	08.92 ± 2.08
F1-IRT	IRT	081.16 ± 01.00	0.29 ± 0.16	-02.40 ± 1.07
F2	Unloaded	070.61 ± 01.92	0.33 ± 0.04	-09.68 ± 0.97
F2-LVC	LVC	081.97 ± 01.40	0.43 ± 0.02	-10.90 ± 1.80
F2-MTR	MTX	152.60 ± 12.17	0.80 ± 0.12	-12.60 ± 2.22
F2-DOX	DOX	096.39 ± 01.24	0.27 ± 0.03	-09.55 ± 0.87
F2-IRT	IRT	076.13 ± 01.46	0.35 ± 0.05	-09.83 ± 0.18
F3	Unloaded	080.67 ± 00.16	0.34 ± 0.05	-12.30 ± 1.31
F3-LVC	LVC	083.05 ± 01.03	0.41 ± 0.01	-10.40 ± 1.11
F3-MTR	MTX	084.69 ± 02.16	0.33 ± 0.03	-10.60 ± 1.07
F3-DOX	DOX	084.69 ± 02.16	0.57 ± 0.09	-10.60 ±1.07
F3-IRT	IRT	088.56 ± 01.27	0.40 ± 0.08	-07.99 ± 1.42
F4	Unloaded	069.92 ± 00.48	0.23 ± 0.00	-03.39 ± 1.06
F4-LVC	LVC	084.00 ± 10.02	0.21 ± 0.04	-03.16 ± 0.61
F4-MTX	MTX	076.95 ± 00.74	0.27 ± 0.01	-02.10 ± 1.26
F4-DOX	DOX	233.50 ± 46.11	0.61 ± 0.06	-01.65 ± 1.60
F4-IRT	IRT	069.38 ± 00.88	0.23 ± 0.02	-02.55 ± 0.59
F5	Unloaded	074.98 ± 01.12	0.17 ± 0.01	-13.03 ± 0.70
F5-LVC	LVC	083.88 ± 00.11	0.21 ± 0.02	-08.14 ± 1.55
F5-MTX	MTX	144.70 ± 09.33	0.52 ± 0.05	-15.07 ± 0.51
F5-DOX	DOX	137.70± 03.66	0.57 ± 0.02	-10.04 ± 0.30
F5-IRT	IRT	078.15 ± 00.29	0.20 ± 0.00	-10.07 ± 0.26
F6	Unloaded	076.36 ± 02.18	0.27 ± 0.01	-13.07 ± 1.04
F6-LVC	LVC	078.21 ± 01.42	0.34 ± 0.02	-07.79 ± 0.78
F6-MTX	MTX	080.78 ± 01.02	0.28 ± 0.03	-18.00 ± 1.19
F6-DOX	DOX	095.75 ± 01.22	0.52 ± 0.03	-11.06 ± 0.72
F6-IRT	IRT	077.89 ± 00.16	0.32 ± 0.05	-15.04 ± 0.21

*F1= PC: Tween® 80: DPPC: DSCP: PS, F2 = PC: Tween® 80: DPPC: DSCP: PS: DCP, F3= PC: Tween® 80: DPPC: DSCP: PS: PI, *F4= PC:Tween®80:DPPC:DSCP, F5= PC:Tween® 80:DPPC: DSCP:DCP, F6=PC:Tween® 80:DPPC:DSCP:PI.

The nanoparticles in the formulations F2, F3, F5 and F6 were negatively charged with a zeta potential range of -9 to -14 mV. The zeta potential of liposomes in the formulations F1 and F4 was approximately -4 mV, which is close to neutral to prevent premature clearance by the RES. Most colloidal dispersions in aqueous media carry an electric charge and this charge is affected by the nature of particles and its surrounding medium. As the larger value of zeta potential generally indicates the formation of a more stable liposome suspension, hence, it is expected to get a stable liposome formulation with an ionic head group compared with a neutral charge (Feng *et al.*, 2001). The formation of phospholipid liposomes has been attributed to the structure of phospholipid with amphiphilic nature of a surfactant. The solubility of surfactants in an aqueous medium may be evaluated by determining interaction between the hydrophilic head group and water molecules through hydrogen bonding. Therefore, based on the type of head group, phospholipids have been classified as cationic, anionic, zwitterionic and nonionic. Cationic phospholipids dissociate into positively charged molecules, anionic into negatively charged molecules, zwitterionic possess both positive and negative charges at the head groups whereas non-ionic remain neutral in charge when dissolved in an aqueous solution. Therefore, PS, DCP and PI were added to the formulations to induce more negative charge to the liposomes.

Among the formulations F1 and F4, presence of small amount of PS in F1 liposomes induced slightly more negative zeta potential as compared with the F4 liposomes. Small amount of PS added to the formulations F1, F2 and F3 is based on the cell signaling behavior of the PS molecules in the cell membranes (Leventis *et al.*, 2010). High concentration of DCP in F2 & F5 and PI in F3 & F6 was to optimize zeta potential of liposomes for mimicking surface potential of red blood cells. The preparation of liposomes was improved by addition of negative charges in the form of dicetyl phosphate (F2 and F5). It helps in hydration of the lamellae as well as inhibiting

aggregation of the liposomes after they are formed. Two more liposome formulations were prepared in this manner from pure phospholipids carrying net negative charge such as phosphatidylinositol (F3 and F6) as shown in Table 4.2. The slight variation in of zeta potential value in DOX loaded and MTX loaded liposomes from negative to a positive value may be attributed to the amphiphilic nature and intermediate log p values of these drugs molecules (Viswanathan *et al.*, 2016). With the obtained negative values of zeta potentials in case of DCP and PI, liposomes are expected to be compatible with the cell membranes and fall within the reported range of zeta potential of the red blood cells (Fontes *et al.*, 2006).

4.1.3 Stability of Phospholipid Liposomes

Stability of liposomes during storage period is also one of the key requirements for successful drug carriers. More useful and accurate stability data relies on the parameters like proper design, implementation, monitoring and evaluation of the drug nanocarriers. Liposomes, as most effective model lipid bilayer membrane drug carriers, play an important in biological, pharmaceutical and medical research. Their efficacy may be altered due to instability in the biological media especially blood; aggregation and fusion among the main sources of their physical instability. This stability can be improved by preventing oxidation, aggregation and fusion and some other degradation processes such as hydrolysis. Such type of problems may lead to an increased particle size, enhanced permeability of liposome bilayers and various other related effects (Lasic, 1990). In the current study, all the liposomal formulations were evaluated for their storage stability at three different temperature conditions i.e., 37 °C, 28 °C (room temperature) and 4 °C. There are several approaches recommended to get enhanced stability of liposomes such as by mixing surfactants, identification of appropriate temperature, pH and ionic strength for preparation and storage of liposomes. It is important to maintain the temperature whereby liposome suspension is stable upon the

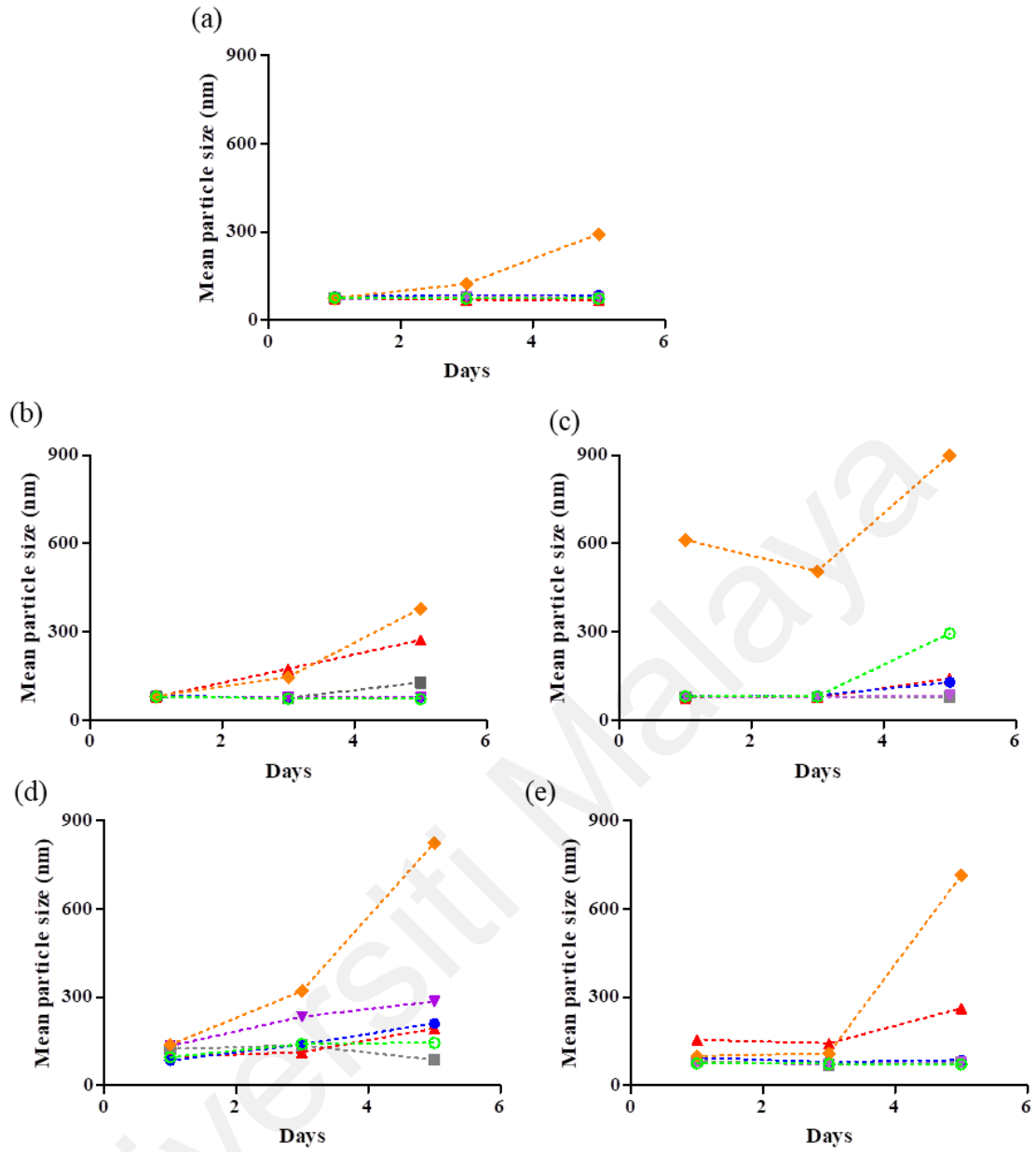

Figure 4.3: Mean particle size of empty liposomes (a), LVC-loaded liposomes (b), MTX-loaded liposomes (c), DOX-loaded liposomes (d), and IRT-loaded liposomes for 5 days at 37 °C. All the liposomes were washed with PBS (pH 7.4, 0.01 M, 25 °C) to separate free anticancer drugs using dialysis membrane (MCOW 3500) method, where ■ = F1 (PC:Tween®80:DPPC:DSPC:PS), ▲= F2 (PC:Tween®80:DPPC:DSPC:PS:DCP), ● = F3 (PC:Tween®80:DPPC:DSPC:PS:PI), ▼= F4 (PC:Tween®80:DPPC:DSPC), ♦ = F5 (PC:Tween®80:DPPC:DSPC:DCP), ●= F6 (PC:Tween®80:DPPC:DSPC:PI).

period of storage and during preparation of liposomes. Variation in the temperature may affect the stiffness of hydrocarbon chain and hence solubility phospholipid molecules. Thus, an inappropriate temperature may lead to dissolution of phospholipid molecules in liposomes. The current study, liposomes were composed of mixtures of neutral and acidic phospholipids. The neutral phospholipids, in addition to lecithin (PC) were DPPC

and DSPC whereas the acidic phospholipids examined were PS, DCP, and PI. The amount of PS has been fixed in formulations F1, F2 and F3, however, formulations F4, F5 and F6 contain no PS. The zeta potential of F1 and F4 formulations were close to neutral. Therefore, to induce and to investigate the effect of negatively charged lipid on zeta potential of F1 and F4 formulations, DCP was introduced into the formulation mixture of F1 to obtain F2 liposomes whereas F5 formulation was obtained by adding DCP to lipid mixture of F4 formulations. Introduction of PI to lipid mixture of F1 and F4 gave rise to two new formulations F3 and F6 respectively. The structural difference between the DCP and PI may attribute to the overall stability of these formulations. DCP contains a head group of hydrogen phosphate with a negative charge (Liang *et al.*, 2015). DCP contains two palmitic fatty chains. Phosphatidylinositol belongs to a family of phosphatidylglycerols and the phosphate group gives the molecule a negative charge at physiological pH. It consists of a glycerol backbone which is attached with two non-polar fatty acid tails (mostly stearic acid in the in SN1 position and arachidonic acid at SN2 position) and a phosphate group substituted with an inositol polar head group. This makes PI an amphiphile.

The blank (unloaded) and drug loaded liposomes under the formulation codes F1-F6 were incubated at 37 °C and the changes in particle size were monitored for the period of 5 days as shown in Figure 4.3. In the Figure 4.7, it can be clearly seen that liposomes in formulation F5 showed same trend of growth of mean particle size both in blank and drug loaded formulations. Similarly, F2 formulations with drug loaded also showed increase in particle size. An increased particle size of F2 and F5 liposomes especially after three days was due to the aggregation of liposomes. The stability of the liposomes at this particular temperature was monitored due to the fact that this is human body‘s temperature and the carriers must be stable at this specific temperature unless it reaches the targeted site.

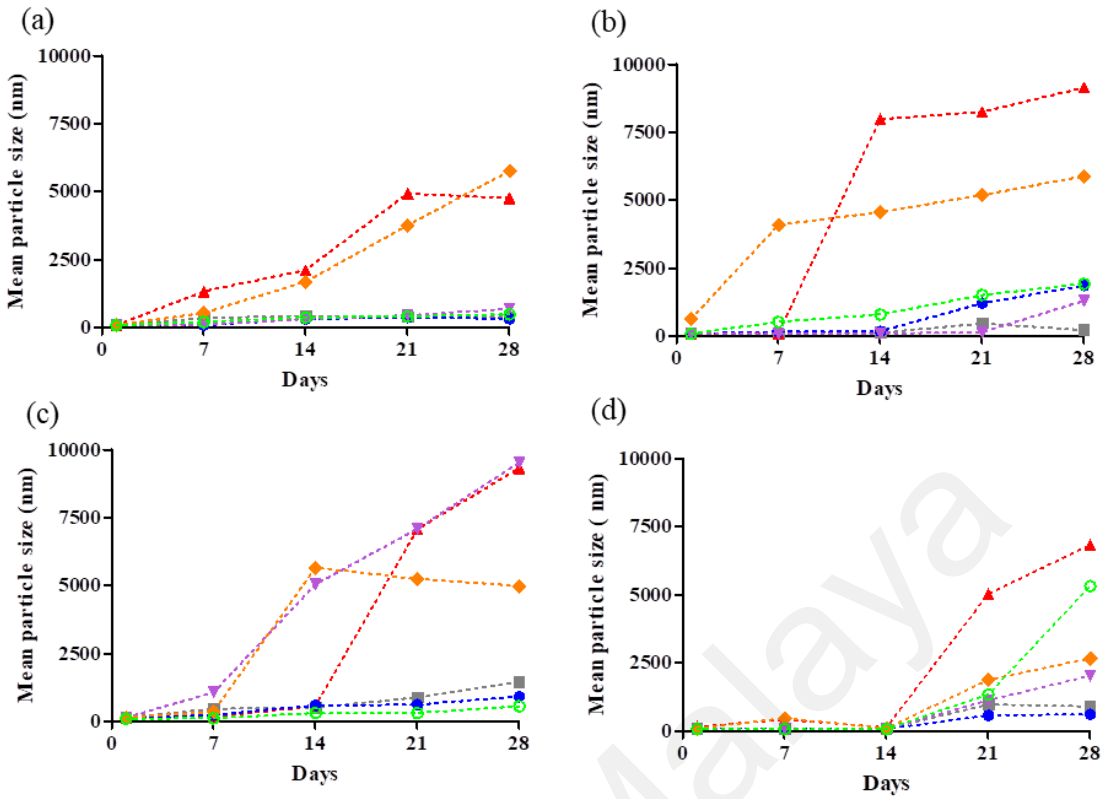

Figure 4.4: Mean particle size of drug loaded liposomes; LVC-loaded liposomes (a), MTX-loaded liposomes (b), DOX-loaded liposomes (c), and IRT-loaded liposomes (d) for 28 days at 28 °C. All the liposomes were washed with PBS (pH 7.4, 0.01 M, 25 °C) to separate free anticancer drugs using dialysis membrane (MCOW 3500) method, where ■ = F1 (PC:Tween®80:DPPC:DSPC:PS), ▲= F2 (PC:Tween®80:DPPC:DSPC:PS:DCP), ● = F3 (PC:Tween®80:DPPC:DSPC:PS:PI), ▼= F4 (PC:Tween®80:DPPC:DSPC), ♦ = F5 (PC:Tween®80:DPPC:DSPC:DCP), ● = F6 (PC:Tween®80:DPPC:DSPC:PI).

The stability of liposomes for five days was investigated due to the fact that whatever is introduced into the blood is excreted out of the body after three days. Therefore, it was required to analyze efficacy of all liposome formulations in this regard.

Figure 4.4 shows variation in mean particle size of drug loaded liposome monitored over a period of 28 days for their storage stability at 28 °C (room temperature). All of the data for mean particle size of the liposomes in this study is based on scattering intensity distribution. Method of preparation of liposomes, pH of the bulk solution, molecular structure and composition of the substances in liposome formulations may influence the particle size of the liposomes; however, the following discussion will be

focused on the effect of molecular structure and composition of liposomes. Figure 4.4 (a) , 4.4 (b), 4.4 (c) and 4.4 (d) demonstrate the changes of mean particle size for LVC, MTR, DOX and IRT loaded liposomes respectively. A same trend of increase in liposome particle size can be observed for formulations under the name F2 and F5 in all four figures. However, F4 formulation loaded with DOX also show an increase in the particle size. In Figure 4.4 (d) all the formulations were stable until day 14 and then an increase in particle size can be observed in almost all formulations. However, a less significant variation in the particle size of formulations F1, F3, F6 and F4 (except for F4-DOX) was observed until day 14.

Figure 4.5 demonstrates the changes in mean particle size of liposme formulation loaded with LVC (a), MTR (b), DOX (c), and IRT (d) at 4 °C over a period of 28 days. At 4 °C temperature, LVC loaded liposomes were stable until 28 days except for F2 (a). MTR loaded liposomes also showed stability over 28 days except for F5 liposomes (b). In case of DOX loaded liposomes, F2 and F4 formulations showed instability right from day one whereas, F1, F3, F5, and F6 were stable only until day 14 and their particle size started increasing after that. In case of IRT-loaded liposomes, an insignificant change in the particle size of liposomes was observed in all formulations.

A possible explanation for such variations in mean particle size is as follows. A primary tool to asses expiration date and storage conditions for pharmaceutical products is the stability testing. Liposomes, developed to be used as drug carriers in therapy, have to be sufficiently stable on storage. Their shelf life can be disturbed for a number of reasons and mainly determined by subdividing its shelf-life stability into physical and chemical stability. The formulations can be considered stable by optimizing the uniformity of size distribution, pH, ionic strength, addition of antioxidants and some chelating agents. Chemical stability of the liposomes is also very important since phospholipids usually form the backbone of the bilayers and the chemical degradation

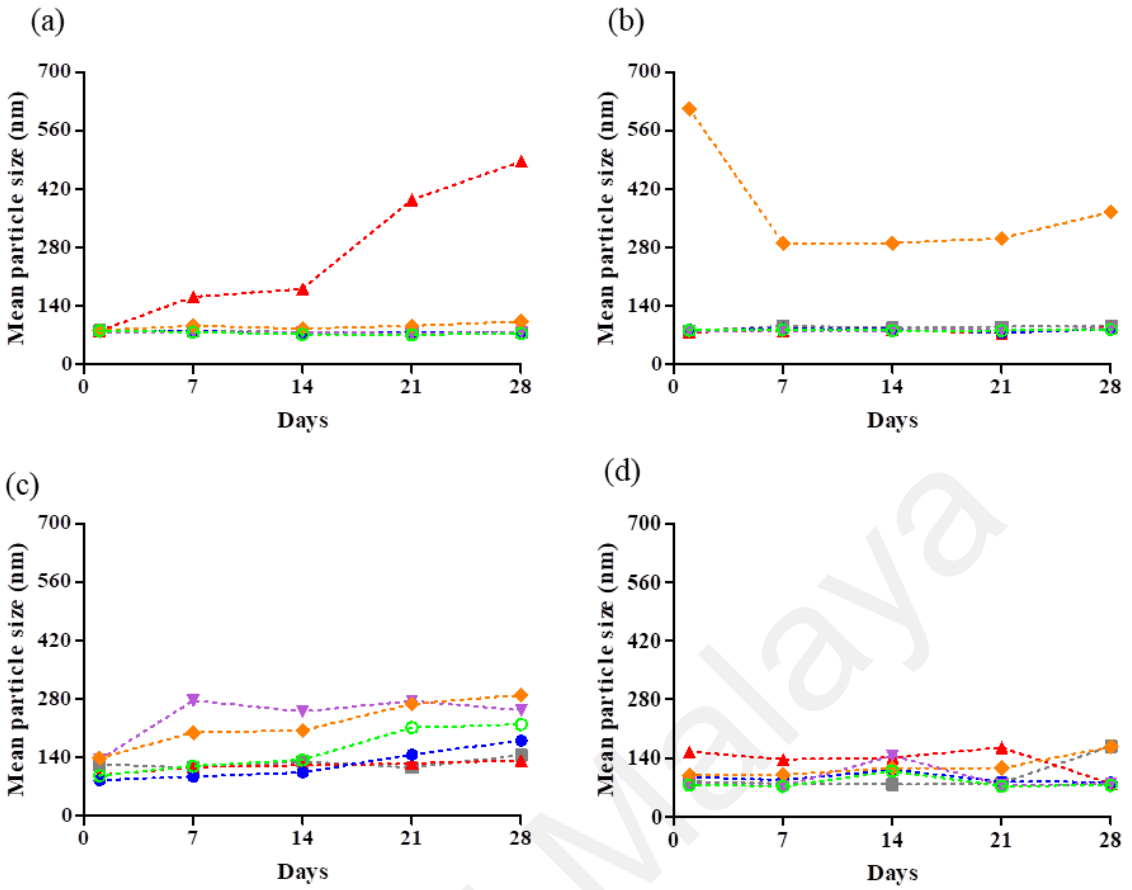

Figure 4.5: Mean particle size of drug loaded liposomes; LVC-loaded liposomes (a), MTX-loaded liposomes (b), DOX-loaded liposomes (c), and IRT-loaded liposomes (d) for 28 days at 4 °C. All the liposomes were washed with PBS (pH 7.4, 0.01 M, 25 °C) to separate free anticancer drugs using dialysis membrane (MCOW 3500) method, where ■ = F1 (PC:Tween®80:DPPC:DSPC:PS), ▲= F2 (PC:Tween®80:DPPC:DSPC:PS:DCP), ● = F3 (PC:Tween®80:DPPC:DSPC:PS:PI), ▼= F4 (PC:Tween®80:DPPC:DSPC), ♦ = F5 (PC:Tween®80:DPPC:DSPC:DCP), ●/= F6 (PC:Tween®80:DPPC:DSPC:PI).

reactions may affect the performance of phospholipid bilayers due to hydrolysis or oxidation processes. Hydrolysis of ester bonds linking the fatty acids to the glycerol backbone and peroxidation of unsaturated acyl chains may lead to the appearance of short-chain lipids and then produce soluble derivatives in the membranes, thus contributing to decrease in the quality of liposome products. In addition to such chemical instability, physical processes such as aggregation/flocculation and fusion/coalescence result in loss of liposome-associated drugs and changes in particle size.

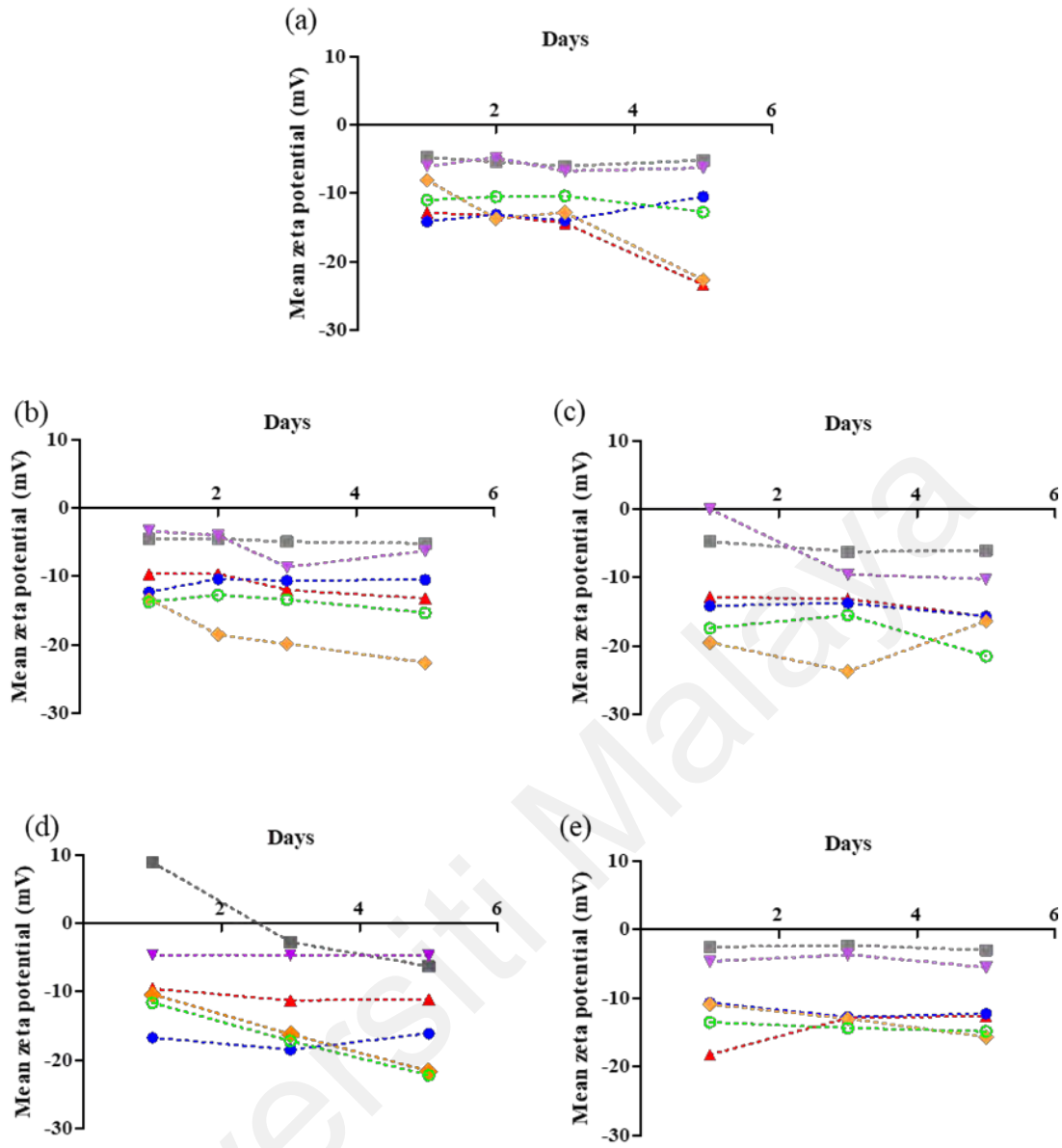

Figure 4.6: Mean zeta potential of empty liposomes (a), LVC-loaded liposomes (b), MTX-loaded liposomes (c), DOX-loaded liposomes (d), and IRT-loaded liposomes for 5 days at 37 °C. All the liposomes were washed with PBS (pH 7.4, 0.01 M, 25 °C) to separate free anticancer drugs using dialysis membrane (MCOW 3500) method, where ■ = F1 (PC:Tween®80:DPPC:DSPC:PS), ▲ = F2 (PC:Tween®80:DPPC:DSPC:PS:DCP), ● = F3 (PC:Tween®80:DPPC:DSPC:PS:PI), ▼= F4 (PC:Tween®80:DPPC:DSPC), ♦ = F5 (PC:Tween®80:DPPC:DSPC:DCP), ● = F6 (PC:Tween®80:DPPC:DSPC:PI).

Formation of larger units of liposomes as a result of aggregation may still be containing individual liposomes. Aggregation may also accelerate the process of coalescence of liposomes indicating the formation of new liposomal structures. Aggregation is a reversible process and may be reversed by applying mild shear forces whereas coalescence is an irreversible process (Yadav *et al.*, 2011).

Zeta potential is also one of the parameter to monitor the stability of colloidal suspensions over a period of time. The value of zeta potential of the liposomes may be affected by either the bilayer composition of the liposomes. In this study, negative values of zeta potentials have been obtained by varying the type of the molecules used for bilayer preparation. Figure 4.6, 4.7 and 4.8 show the variation of zeta potential with respect to the storage time at 37 °C, 28 °C and 4 °C respectively.

Figure 4.6 (a) shows stability of zeta potential values of unloaded (empty) liposomes at 37 °C. In this figure, formulations F1, F3, F4 and F6 displayed a small variation of zeta potential as compared with F2 and F5. The less stability of F2 and F5 formulation due to increase in zeta potential values after day 3 may be attributed to the surfactant nature of DCP. The zeta potential stability for LVC, MTR, DOX and IRT loaded liposomes has been shown in Figure 4.6 (b), 4.6 (c), 4.6 (d) and 4.6 (f) respectively. All the drug loaded liposomes depicted almost the same trend of stability as was observed in empty liposomes at 37 °C. Over the incubation period, the zeta potential of some liposomes was reduced to less negative value which may be due to the oxidation of ionized species at the bilayer of the liposomes. Though, liposomes containing DCP had high zeta potential values and may give good electrostatic stability in some reported literature, however, it does not always provide the best stabilization because it may produce aggregates (Chaw *et al.*, 2013) which may disturb the ionic concentration around the particles.

The storage stability is generally determined by some inter-particle and intra-particle interactions (Amani *et al.*, 2010). Therefore, if the size of the liposomes is bigger, that may be related to poor intra-particle interactions which may lead to poor storage stability (Liang *et al.*, 2015). Moreover, the stability of liposomes was also determined as a function of storage time at two different temperatures i.e., 28 °C and 4 °C as shown in Figure 4.7 and 4.8 respectively.

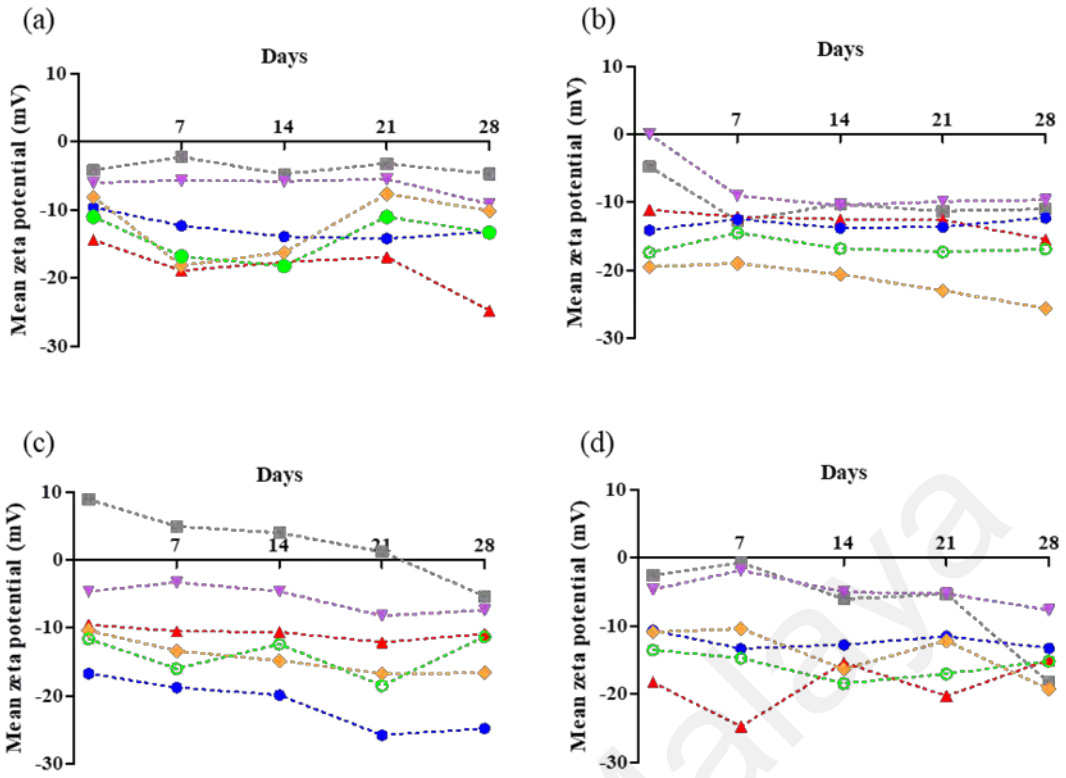

Figure 4.7: Mean zeta potential of drug loaded liposomes; LVC-loaded liposomes (a), MTX-loaded liposomes (b), DOX-loaded liposomes (c), and IRT-loaded liposomes (d) for 28 days at 28 °C. All the liposomes were washed with PBS (pH 7.4, 0.01 M, 25 °C) to separate unencapsulated anticancer drugs using dialysis membrane (MCOW 3500) method, where ■ = F1 (PC:Tween®80:DPPC:DSPC:PS), ▲= F2 (PC:Tween®80:DPPC:DSPC:PS:DCP), ● = F3 (PC:Tween®80:DPPC:DSPC:PS:PI), ▼= F4 (PC:Tween®80:DPPC:DSPC), ♦ = F5 (PC:Tween®80:DPPC:DSPC:DCP), ● = F6 (PC:Tween®80:DPPC:DSPC:PI).

Drug loaded liposomes showed less variation in zeta potential values at 4 °C as compared with 28 °C. These variations were notable in case of F2 and F5 formulations. stability of liposome formulations can be explained as a kind of colloidal stability which is predicted on the notion of two independent types of forces. One of them is named as attractive van der Waals forces and the other as repulsive forces. Two most important aspects of physical changes, particle size and size distribution, occur mainly via two mechanisms. The mechanism can be asymmetric molecular exchange at molecular level whereas it is mostly aggregation, fusion, flocculation or precipitation at particle level. It has been reported that the instability of the liposomes faced due to aggregation and fusion.

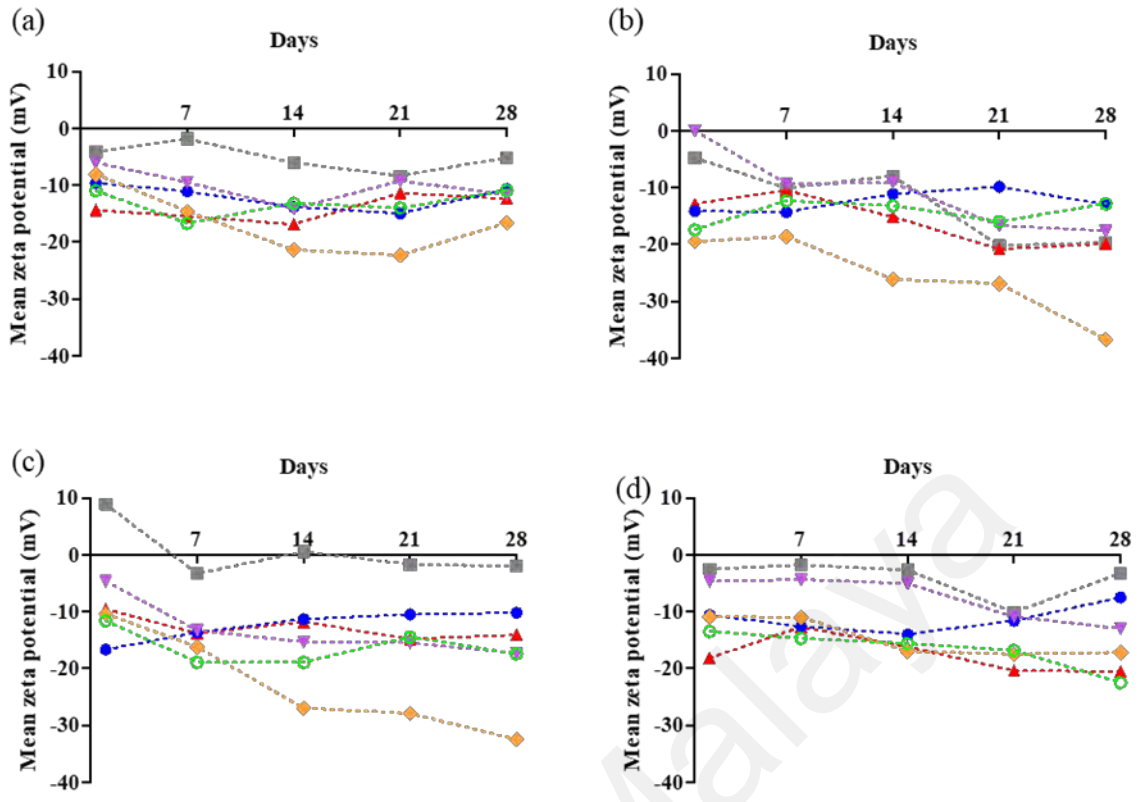

Figure 4.8: Mean zeta potential of drug loaded liposomes; LVC-loaded liposomes (a), MTX-loaded liposomes (b), DOX-loaded liposomes (c), and IRT-loaded liposomes (d) for 28 days at 4 °C. All the liposomes were washed with PBS (pH 7.4, 0.01 M, 25 °C) to separate unencapsulated anticancer drugs using dialysis membrane (MCOW 3500) method, where ■ = F1 (PC:Tween®80:DPPC:DSPC:PS), ▲= F2 (PC:Tween®80:DPPC:DSPC:PS:DCP), ● = F3 (PC:Tween®80:DPPC:DSPC:PS:PI), ▼= F4 (PC:Tween®80:DPPC:DSPC), ♦ = F5 (PC:Tween®80:DPPC:DSPC:DCP), ● = F6 (PC:Tween®80:DPPC:DSPC:PI).

That can be overcome by introducing charges into the lipid mixtures as neutral liposomes face such problems due to Van der Waals interaction which brings unavoidable phenomenon for uncharged membranes (Woodle *et al.*, 1998).

4.2 Optical Polarizing Microscope (OPM)

Unsonicated liposomes were evaluated for vesicle confirmation and size using optical polarizing microscopy prior to any additional physical characterizations. The optical micrographs of empty (unloaded) liposomes F1, F2, and F3 are shown in Figure 4 whereas F4, F5 and F6 are shown in Figure 4.4.

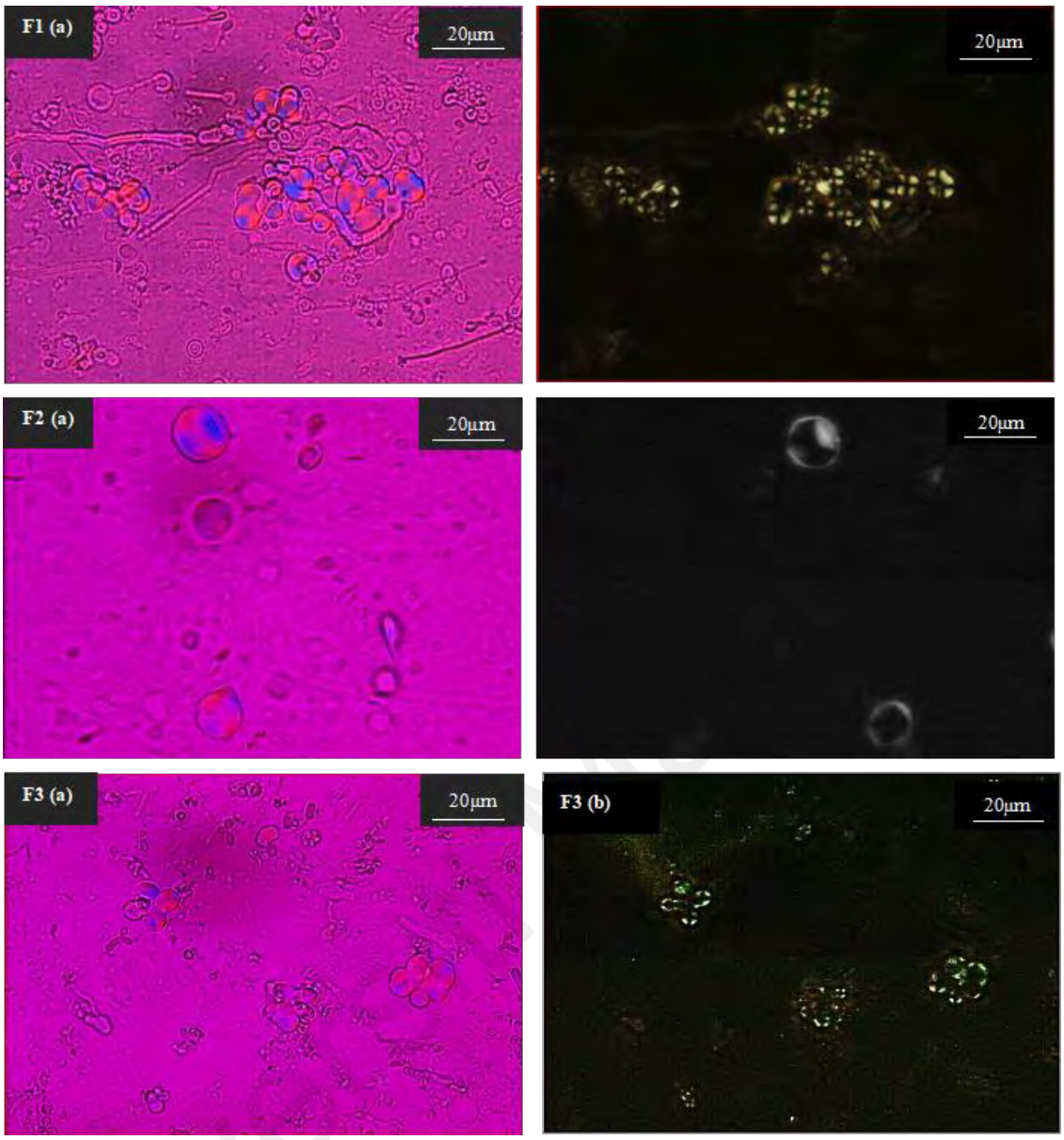

Figure 4.9: The optical polarizing micrograph of F1, F2 and F3 liposomes which showed birefringence effect under light field (a) and maltese cross under dark field (b) where F1 = (PC:Tween®80: DPPC:DSPC:PS), F2 = (PC:Tween®80: DPPC:DSPC:PS:DCP), F3 = (PC:Tween®80: DPPC:DSPC:PS:PI).

Lipsomes were constructed from various phospholipids, which are biomimetic lipids similar to those present in the membranes of mammalian cells. Phospholipid bilayers have been reported to show optical birefringence due to their anisotropic behavior. Polarizing microscopy is employed in the analysis of liposomal dispersion systems to confirm their presence in the studies formulations. Birefringence is the property of anisotropic molecules is directionally dependent. These materials have refractive index that depends on the polarization and propagation direction of light. The maximum

difference between refractive indices exhibited by these anisotropic molecules is mostly quantified by the term birefringence. This birefringence is responsible for the double refraction phenomenon.

The incident ray of light is split by polarization into two rays taking slightly different path. The micrographs obtained from the interaction of plane-polarized light against specimen from diffraction, interference and existence of ordered molecular arrangements in the liposome bilayers (Bibi *et al.*, 2011).

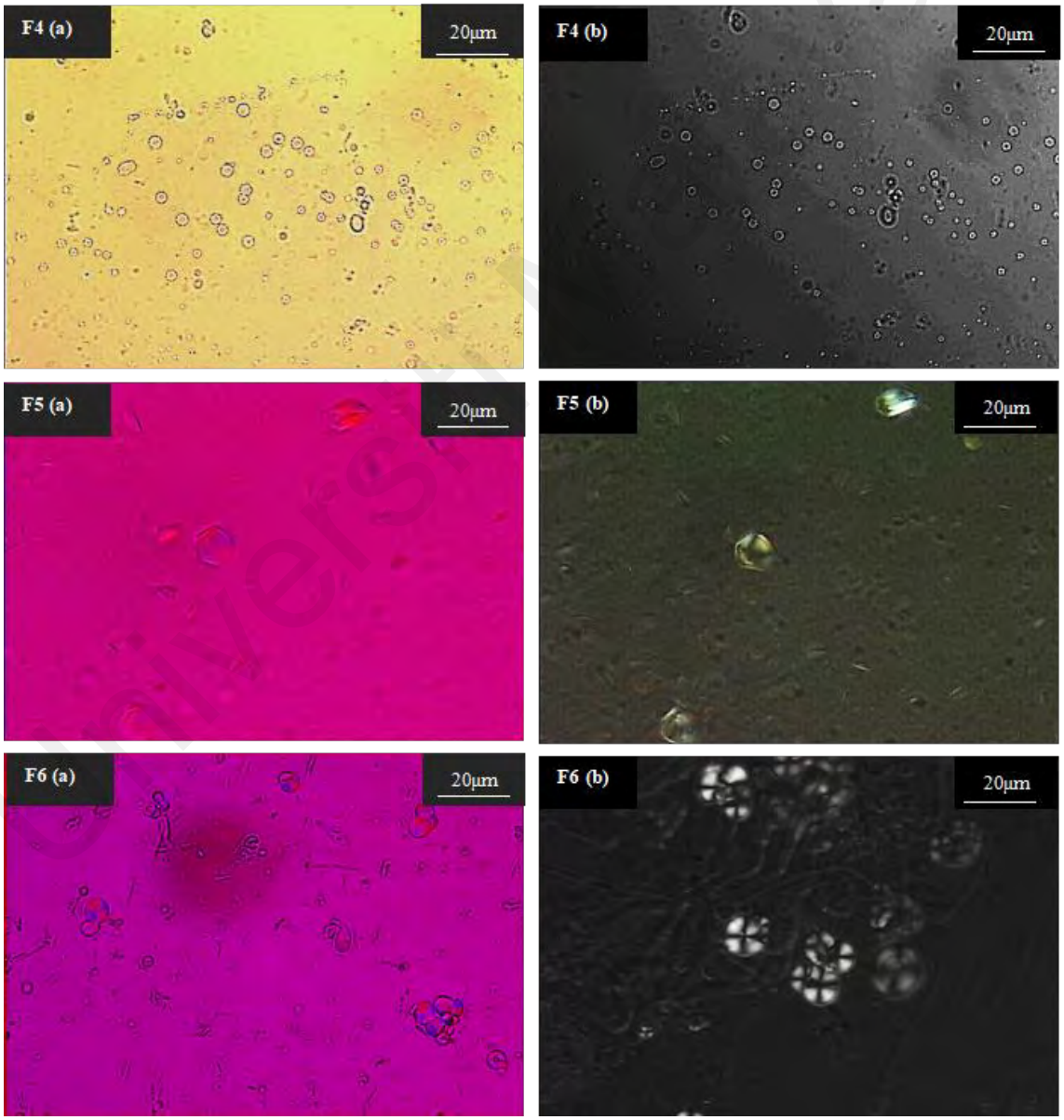

Figure 4.10: The optical polarizing micrograph of F4, F5 and F6 liposomes which showed birefringence effect under light field (a) and maltese cross under dark field (b) where F4 = (PC:Tween®80: DPPC:DSPC), F5 = (PC:Tween®80: DPPC:DSPC:DCP), and F6 = (PC:Tween®80: DPPC:DSPC:PI).

Figure 4.3 shows the presence of liposomes under light (a) and dark field (b). During the light field mode, the polarized light was interfered by the white polarized light through the rotational lambda plate, resulting from the formation of vivid first-order blue, yellow and red known as birefringent effect as shown in micrographs F1/a, F2/a and F3/a. Under the dark field mode, the presence of liposomes could be detected through the formation of Maltese cross as the perpendicularly polarized rays pass through the bilayers of liposomes (Figure 4.3 (b)). Presence of high amount of lecithin into F1 and F3 liposomes (2 %) promoted the formation of aggregates as displayed in micrographs in Figure 4.3. However, the effect of the same amount of lecithin was not observed I micrograph due to the presence of DCP which is a surfactant and promotes emulsification by reducing surface tension.

Micrographs of F4, F5, F6 liposomes are displayed in Figure 4.4. Under the light field mode, the blue and yellow birefringence revealed the liposome formation in the formulation (a). The presence of liposomes was obviously seen through the formation of Maltese cross during the dark field mode. The relatively small vesicles in case of F4 formulation can be seen due to the presence of high amount of DPPC and DSPC in the formulation. However, the liposomes were dispersed and not agglomerated due to the presence of only 0.5 % lecithin in the formulation. The presence of DCP in F5 liposomes did not allow the fusion of the liposomes. This problem was also not significant in the liposome formulation F6 due to the presence of comparatively small amount of lecithin in the suspension.

The liposome structures may tend to fuse, elongate or break down under mechanical stress using a cover slip on glass slides using a figure. However, the micrographs obtained from all unsonicated liposomes were all spherical in shape.

4.3 Transmission Electron Microscopy

Transmission electron microscopy (TEM) operates with a principle similar to OPM but uses electrons of very short wavelength as 'light source' which help in getting resolutions thousand times better than normal light microscopes. It is considered one of the best available options to observe liposomes in the solutions with ultrahigh resolution optics for atom to atom characterization. Transmission electron microscopic graphs of unencapsulated liposomes F1, F2, F3, F4, F5 and F6 liposomes have been shown in Figure 4.5. This technique helps in collecting vital information such as size, stability, and bilayer organization of the formulations. For examining liposome structures at electron microscopic level, negative staining using phosphotungstic acid (PTA) solution has been considered an easily used method. This method involves the deposition of heavy atom stains and hence flattering of spherical or cylindrical structures of liposomes has been observed very commonly. Liposome bilayer membranes show strong affinity with PTA and become very much electron dense when analyzed under TEM.

In the vacuum chamber, when electron beam from a tungsten filament travels through the liposomes, the electrons may either be stopped or deflected by different parts of sample grid. A phosphorescent screen or a camera collects these electrons from beneath the sample grid. The image obtained may be dark, light or grey depending upon the electron interactions with the different sample sites. The dark image appears compared to the background when lower electron density reaches the collector fluorescent screen, whereas the unscattered electrons generate a brighter image (representing the areas of the sample through which the electrons were transmitted). The grey images are observed due to the different interactions of the electrons with the different sample areas. The contrast generated between the sample and background is the result of the variable electron phase density around the liposomes.

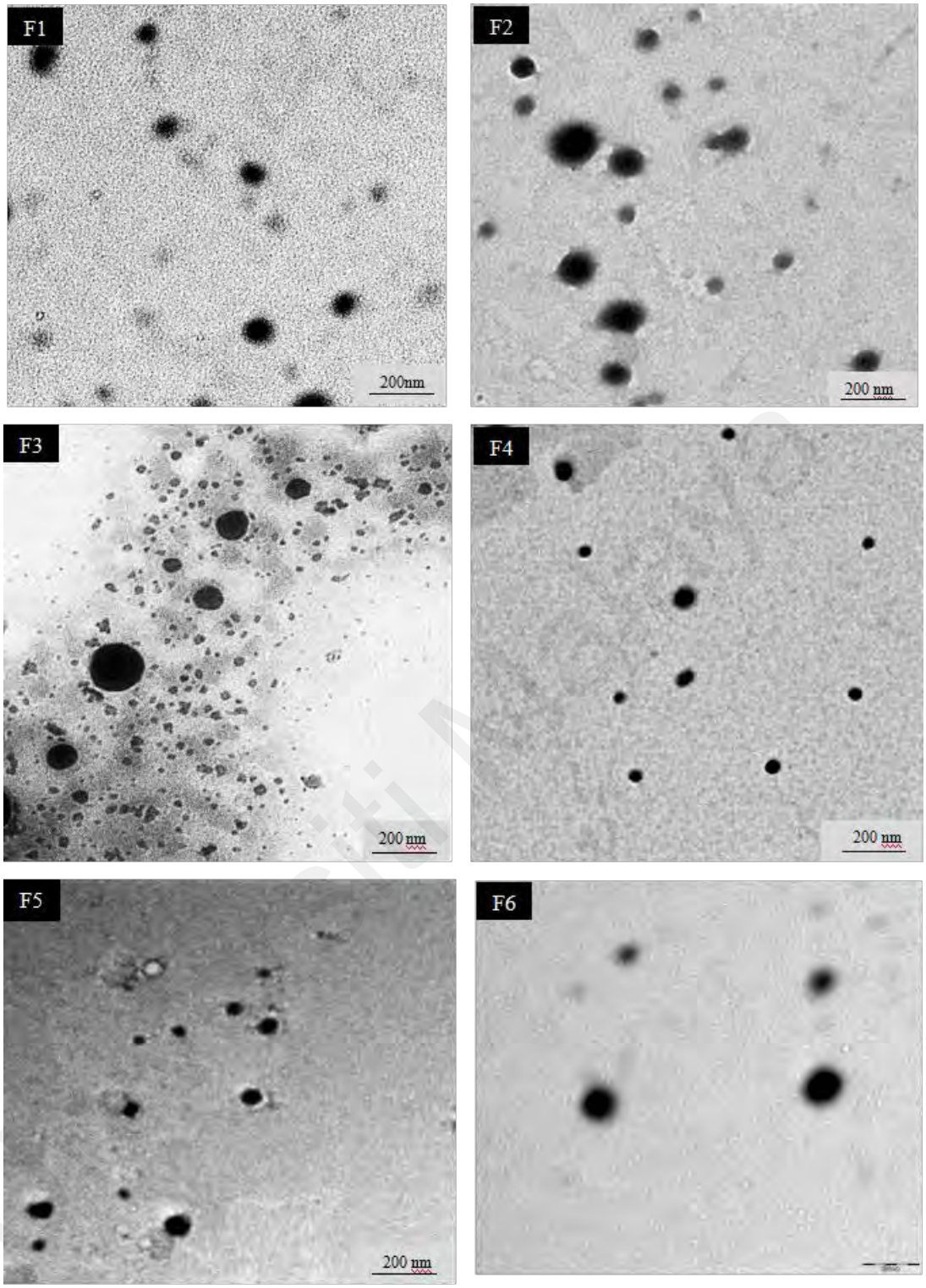

Figure 4.11: TEM micrographs of sonicated liposomes; F1, F2, F3, F4, F5 and F6 formulation. F1 (PC:Tween®80: DPPC:DSPC:PS), F2 (PC:Tween®80: DPPC:DSPC:PS:DCP), F3 (PC:Tween®80: DPPC:DSPC:PS:PI), F4 (PC:Tween®80: DPPC:DSPC), F5 (PC:Tween®80: DPPC:DSPC:DCP), F6 (PC:Tween®80: DPPC:DSPC:PI).

The particle size of the liposomes observed under TEM i-e 80 nm to 150 nm is consistent with the size distribution obtained using Malvern Zeitasizer NanoZS at pH 7.4. and are polydispersed. A slight variation in the particle size observed under TEM (80 nm - 200 nm) for a few particles may be attributed to the techniques used to prepare sample method. The flattening of the particles during drying process of the copper grid or particle collapse under the vacuum in TEM chamber are assumed to contribute in such particle size variations. There is also no evidence of the particle aggregation in any of the formulation system as well. However, many precautions need tpo be taken into consideration such as staining agent which may affect the structure of liposomes, drying of liposomes and the high vacuum as well as high energy of TEM may also contribute to alter the morphology of liposomes (Płaczek *et al.*, 2016).

4.4 Field Emission Scanning Electron Microscopy

In order to further investigate the surface morphology of the formulated liposomes, the freeze dried liposome samples were subjected to the Field emission scanning electron microscopy (FESEM) as shown in Figure 4.6. It is as practically useful technique to analyze three dimensional structures of the liposomes and involves interaction of a scanning probe with the object of interest. The specialty of the microscopic techniques is that they help to obtain improved specimen contrast and to highlight certain structures with increased resolution and less sample damage. FESEM is a technique that works with electron liberated by a field emission source whereby the freeze dried liposomes are scanned by electron to visualize very small topographic details on its surfaces. Its applications cover a wide range of research areas to characterize cell size, size distribution, shape, thickness measurement of thin coatings and films, measurements of dimensions of nano-sized objects, fracture and defect analysis. The working of this microscope involves emission of electrons liberated from emission source.

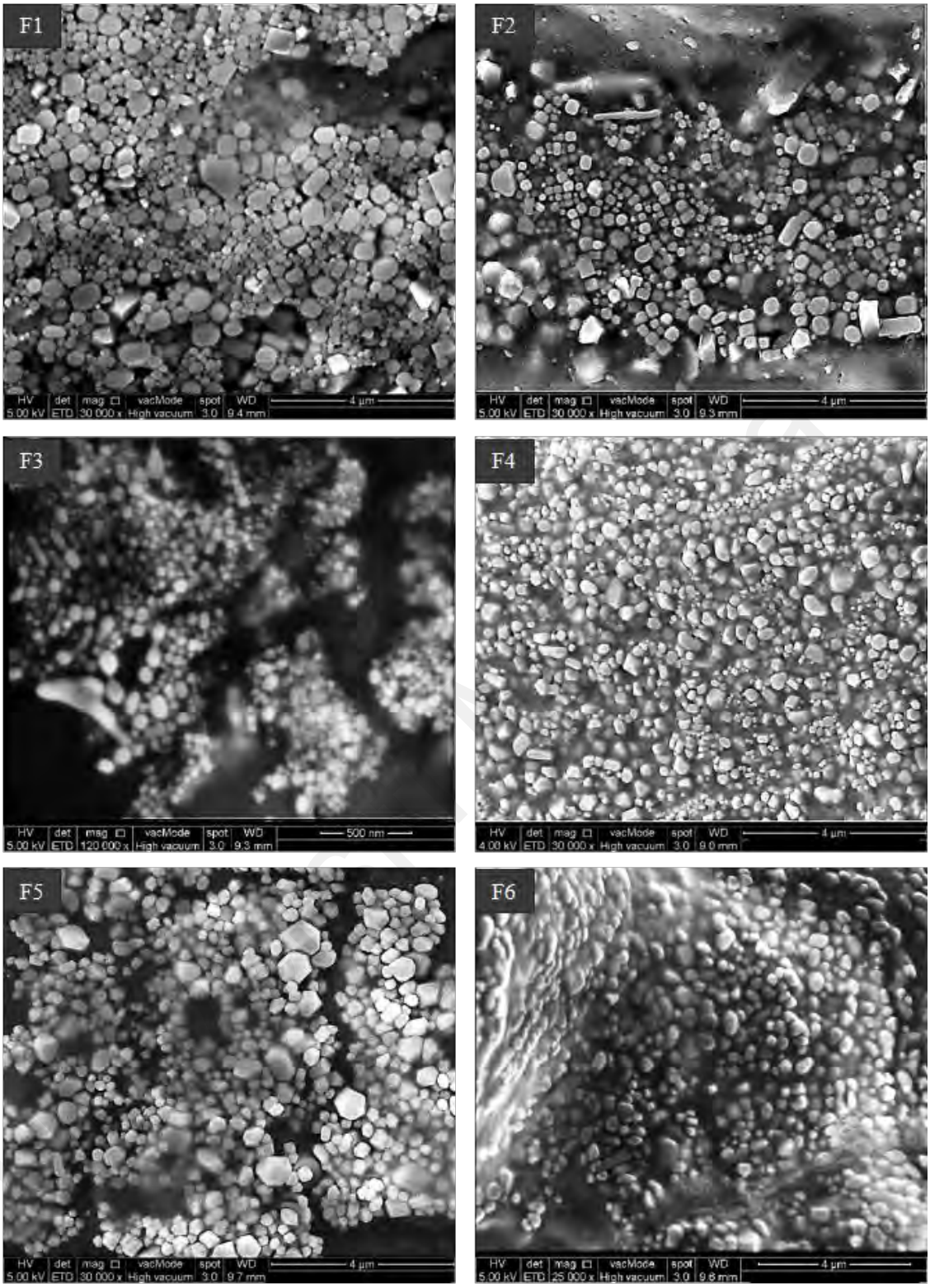

Figure 4.12: TEM micrographs of freeze dried sonicated liposomes; F1, F2, F3, F4, F5 and F6 formulation. F1 (PC:Tween®80: DPPC:DSPC:PS), F2 (PC:Tween®80: DPPC:DSPC:PS:DCP), F3 (PC:Tween®80: DPPC:DSPC:PS:PI), F4 (PC:Tween®80: DPPC:DSPC), F5 (PC:Tween®80: DPPC:DSPC:DCP), F6 (PC:Tween®80: DPPC:DSPC:PI).

These electrons are then accelerated in a high electrical field gradient and are called primary electrons. Secondary electrons are generated when these primary electrons are focused and deflected by electron lenses which are bombarded on the liposome samples. The surface structure of these samples is related to the angle and velocity of these high energy secondary electrons. Electrical signals are generated when these secondary electrons are collected by the detectors which are amplified and transformed to three dimensional video scan-images. Its applications cover a wide range of research areas to characterize cell size, size distribution, shape, and measurements of dimensions of nano-sized objects. The liposomes appeared as discrete spheres with smooth surfaces when observed under FESEM. However, a slight difference in the morphology and particle sizes was attributed to the method of drying the liposome samples.

4.5 Differential Scanning Calorimetry

Thermal behavior of the liposomes was analysed using differential scanning calorimetry (DSC). The results have been shown in Figure 4.13. Among F1, F2 and F3 liposomes, F1 (50 ºC) and F2 (25 ºC) showed a lower transition temperature compared with F3 liposomes (60 ºC). However, F1 liposomes showed a higher transition temperature compared with F2. This might be due to the presence of DCP in F2 formulation which disrupts the packing of phospholipids. DCP contains two C-16 fatty chains as compared with PI which consists of one stearic acid fatty chain and the other arachidonic acid making F3 liposomes more rigid. F1 liposomes do not contain DCP which could affect its thermal behavior. In case of liposome formulations F4, F5 and F6, a phase transition temperature of 23 ºC, 40 ºC and 50 ºC was recorded respectively. The trend of phase transition temperature of F5 and F6 due to the presence of DCP and PI was similar to those in F2 and F3. For the results obtained, a plausible explanation is as follows. Synthetic long-chain phospholipids, in their pure form, undergo a number of transitions at precisely defined temperatures depending on their structures.

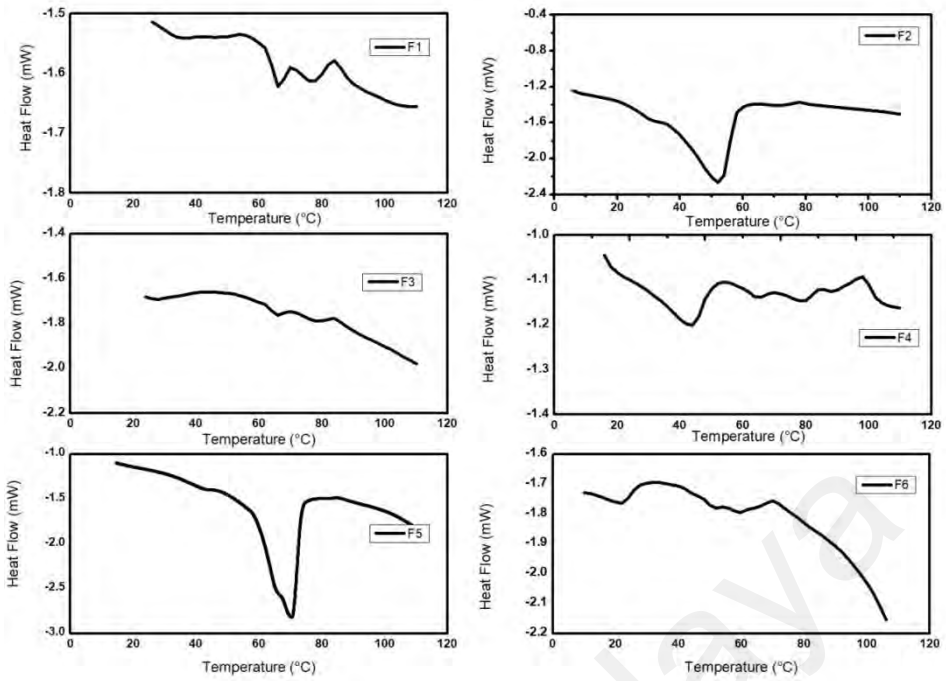

Figure 4.13: Thermal behavior of freeze dried liposomes using DSC. Thermograms were recorded at a rate of 2 ºC min^{-1}.

These transitions may include either a gel to lipid-crystalline transition (T_m), or a pretransition (T_p). During DSC experiments, T_m is considered a rather rapid transition which has been described in equilibrium thermodynamic terms. A pretransition may occur some 5 – 10 °C below T_m and mostly not considered to be equilibrium data being much lower than the main transition temperature. These temperatures, however, are important to characterize each of the transitions and are related to the purity of the system and nature of transitions. Presence of double bonds in the acyl chains may also play an important role in explaining the phase transition temperatures of phospholipids. Location of *cis* double bonds in the middle of the chains will significantly decrease the phase transition temperatures of lipids whereas those closer to head groups or near the end of acyl chain will melt at temperatures similar to the phospholipids with saturated chains. In case of presence of asymmetric acyl chains in phospholipids, a decrease in T_m has also been reported. In addition to dependence of T_m on chain length and saturation (as a reflection of interaction between the non-polar acyl-chains in gel and liquid-

crystilline states), the head groups may also have considerable affect the thermotropic behavior of phospholipids which will depend on the ionic strength, pH and exact ion composition of the solution (Biltonen *et al.*, 1993). Phase diagram of phospholipids with identical acyl chains but different head groups in a mixture deviates from an ideal phase diagram (Liang *et al.*, 2015). Many practically important preparations involve mixtures of phospholipids which may have dramatic influence on the thermotropic behavior of the system. If the phospholipids in a mixture possess similar thermotropic behavior, their effect on DSC results will not be much affected whereas addition of phospholipids with dissimilar thermotropic behavior will depend upon the details of the head group capacity and the exact composition of the lipids (Biltonen *et al.*, 1993).

4.6 Encapsulation Efficiency Determination

It is expressed in terms of amount of the drug incorporated into the liposomes, either inside the core or in between the lipid bilayers. Its determination generally requires separation of free drug from the liposomal formulations and the analysis of drug in both the free and encapsulated drug fraction may help in calculations of encapsulation efficiency. The efficacy of the treatment is enhanced by using liposome nanocarriers as they have the capability of carrying both lipophilic and hydrophilic drugs. The optimized liposome formulation (F1) was loaded with 1-5 mg of the active ingredient insulin in order to have an overview of the liposomal % EE. The usual method of analyzing insulin in the supernatant after centrifugation was not followed due to poor reproducibility. The precipitated liposomes containing insulin were dissolved in ethanol and the encapsulation efficiency was measured using UV absorption measurements. The % EE of insulin was quite low for 1 mg and increased with increasing amounts of insulin (Figure 4.14, a). This system requires quite large amounts of insulin for targeted drug delivery. It is well known that loading of any active ingredients in the liposomes leads to the knowledge of optimum efficacy, enhanced specific targeting and reduced

toxicity. Lipophilicity, a physicochemical property of encapsulated drugs, is of principal importance in determining its pharmaceutical and pharmacokinetic actions on targeted sites. Log *p* values are used to determine the partition characteristics of drugs in such biphasic systems. Therefore, in the current study four anticancer drugs were later selected as model drugs based on their log *p* values. Their log *P* values ranged from log *p* = -3 to log *p* = +3. Encapsulation efficiency of various drugs in all liposome formulations has been shown in Figure 4.14 (c). The anticancer drugs used were leucovorin calcium salt (log *p* = -2.67), methotrexate (log *p* = - 0.53), doxorubicin hydrochloride (log *p* = + 0.53) and irinotecan (log *p* = +2.78). The liposomes formed in the current study were able to encapsulate more than 60 % of the anticancer drugs.

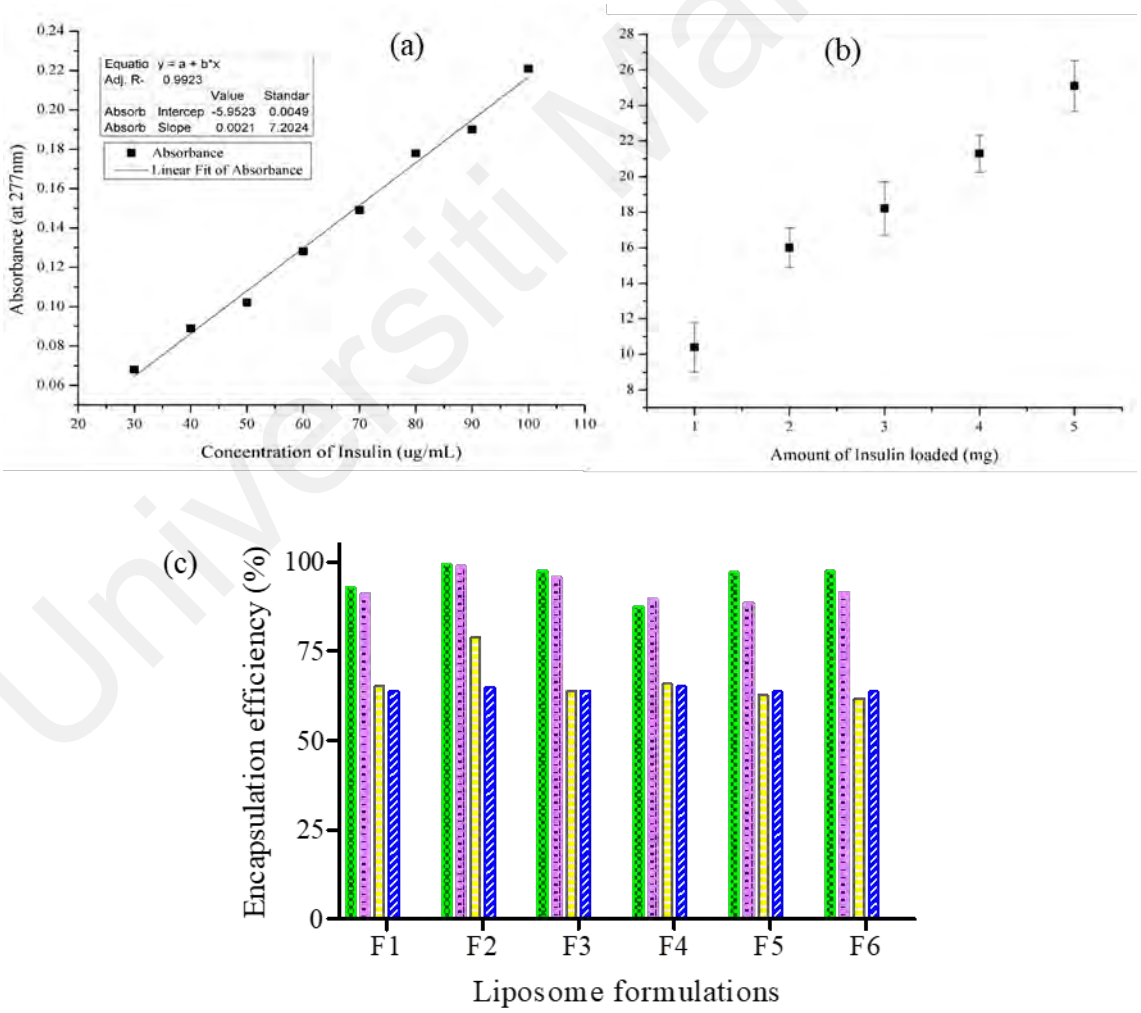

Figure 4.14: Encapsulation efficiency (%) of the liposomes: for insulin (a, b), for anticancer drugs (c) i.e DOX (green bar), MTX (purple bar), IRT (yellow bar), and LVC (blue bar) using UV/Vis spectrophotometer.

Hydrophilic drugs, Leucovorin calcium and methotrexate are usually assumed to be located in the aqueous part of the liposomes. On the other hand, lipophilic drugs i.e. doxorubicin and irinotecan are expected to be entrapped within the bilayers of the liposomes. From the study of drug encapsulation in the newly formed liposome formulations, however, it has been observed that the encapsulation of the more hydrophilic and more hydrophobic drugs was lower as compared to the drugs with intermediate log *p* values. Encapsulation efficiency of methotrexate and doxorubicin was observed to be more than 80 % whereas it was around 60 % in case of leucovorin calcium and irinotecan. The negative surface charge of the liposome formulations may be considered as one of the reasons for this change in the encapsulation efficiency of the highly hydrophilic leucovorin and highly hydrophobic drug irinotecan. The higher encapsulation efficiency may be attributed to the entrapment of the drug both in the aqueous core and within the lipid bilayer membranes. The highly hydrophilic drug was assumed to be entrapped only in the lipid bilayer and the highly hydrophobic drug only within the aqueous core of the liposomes. Thus, the high solubility of the leucovorin calcium in aqueous medium drove this drug to diffuse easily across the bilayers of the liposomes to the environment. Another possible explanation may be that incorporation of charged molecules in the bilayer membranes (especially containing lipophilic chains) would increase the hydrophilicity of the bilayers of liposomes. This will lead to enhanced bilayer water interaction.

4.7 *In vitro* Drug Release and Release Kinetics

The release profile of an entrapped drug predicts how a drug delivery system might function and gives valuable insight into its *in vivo* behavior. It is a process by which a drug is subjected to ADME (adsorption, distribution, metabolism, excretion) upon leaving a drug product and becomes available for pharmacological actions. The rate at which the drug is released from the liposomal carrier is an essential point in evaluating

liposomal drug delivery system. The efficacy of the treatment is enhanced by using liposome nanocarriers as they have the capability of carrying both lipophilic and hydrophilic drugs. Lipophilicity as an equilibrium property, describes a balance between the two contributions namely hydrophobicity (a bulk term reflecting cavity formation, hydrophobic and dispersive forces) and polarity (a polar term reflecting more directional electrostatic interactions and hydrogen bonds) (Lodish *et al.*, 2000; Rutkowska *et al.*, 2013; Simonsen *et al.*, 2011). Leucovorin calcium, methotrexate, doxorubicin hydrochloride, and irrinotecane, like many other anticancer drugs, have been reported to have severe side effects when injected directly in blood streams; however, while trapped in liposomes, these drugs offer much efficacy and shows sustained targeted release (Chen *et al.*, 2013; Lee *et al.*, 2016; Song *et al.*, 2016). In vitro release profiles help to distinguish whether the system portrays either slow or fast release depending upon the release mechanisms and kinetics. Being one of the most influential factors involved in biological activity, it helps in determining solubility, reactivity, degradation of drugs as well as formulation of pharmaceuticals.

4.7.1 *In vitro* Release Profile of Leucovorin Calcium

Therapeutic activity of active ingredients from different liposomal drug delivery systems was studies through in vitro release using Franz diffusion cell. A release medium of PBS (pH 7.4) was employed as a sink medium to mimic intravenous pH conditions. LVC loaded liposomes were allowed to diffuse through a 3500 Da MWCO cellulose dialysis membrane under osmotic pressure. Cumulative drug release values were plotted against time to calculate release rates for the drug. In order to understand the release kinetics and mechanism of anticancer drugs, various dissolution model methods were used. In the current study, different amphiphilic phospholipids have been used to formulate various liposomes that mimic the natural cell membranes whereby the fatty acid chains at one end and the hydrophilic ionized head regions at the other have

arranged spontaneously forming a lipid bilayer. *In vitro* diffusion of encapsulated anticancer drugs from the liposomes offers valuable information regarding drug release rates. Leucovorin calcium salt with log *p* value of –2.67 was chosen as model hydrophilic anticancer drug. Figure 4.15 shows the cumulative release of leucovorin calcium from liposomes for a period of 24 hours. The cumulative drug release rate was slower until 12 hours for all liposomes which gradually started increasing after that.

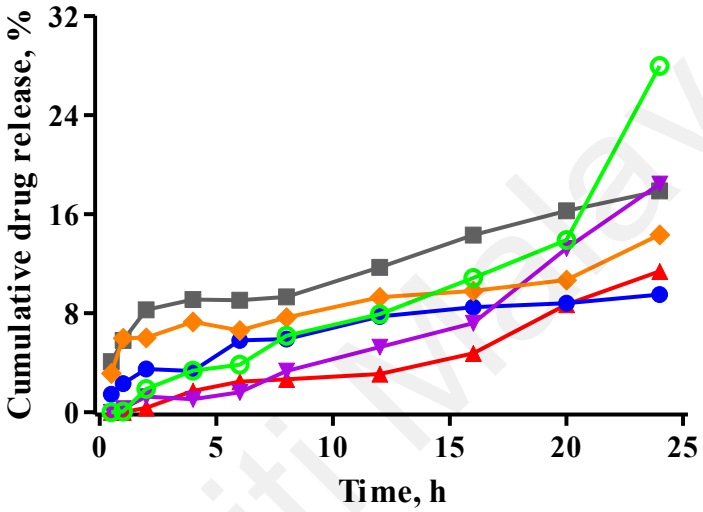

Figure 4.15: Cumulative release (%) of leucovorin calcium from different one day old liposome formulations in PBS of pH 7.4 after 24 h at 37 °C, where ■ = F1 (PC:Tween®80:DPPC:DSPC:PS), ■ = F1 (PC:Tween®80:DPPC:DSPC:PS), ▲= F2 (PC:Tween®80:DPPC:DSPC:PS:DCP), ● = F3 (PC:Tween®80:DPPC:DSPC:PS:PI), ▼= F4 (PC:Tween®80:DPPC:DSPC), ♦ = F5 (PC:Tween®80:DPPC:DSPC:DCP), ● = F6 (PC:Tween®80:DPPC:DSPC:PI).

After 24 hours, a controlled cumulative drug release of less than 20 % was observed from liposomes except for F6 liposomes at physiological pH 7.4 thus making them useful for drug delivery applications. Leucovorin calcium has high log *p* value and is expected to be located more in the aqueous core of the liposomes. Thus, it takes longer for the hydrophilic drug to come out of the inner core while crossing the hydrophobic bilayers. The diffusion of the leucovorin calcium through liposomal hydrophobic membrane was favorable due to the less affinity of this drug with the lipid bilayer membrane.

Table 4.3: Rate of release (K), and Regression coefficient (R^2) values of leucovorin calcium from one day old phospholipid liposomes.

Kinetic model		**Liposome formulations**					
		F1	F2	F3	F4	F5	F6
Zero order,	K_0	0.877	0.403	0.493	0.620	0.651	0.873
	R^2	0.187	0.923	0.541	0.898	-0.207	0.874
First order	K_1	0.010	0.004	0.005	0.007	0.007	0.009
	R^2	0.264	0.917	0.576	0.884	-0.141	0.856
Higuchi	K_H	3.690	1.518	2.057	2.289	2.764	3.275
	R^2	0.878	0.706	0.966	0.648	0.714	0.660
Gompertz	$K_{G\alpha}$	2.983	10.754	3.867	19.613	3.122	14.919
	$K_{G\beta}$	0.356	1.131	0.363	1.751	0.273	1.672
	R^2	0.913	0.935	0.973	0.967	0.842	0.878

*F1= PC: Tween® 80: DPPC: DSCP: PS, F2 = PC: Tween® 80: DPPC: DSCP: PS: DCP, F3= PC: Tween® 80: DPPC: DSCP: PS: PI, *F4= PC:Tween®80:DPPC:DSCP, F5= PC:Tween® 80:DPPC: DSCP:DCP, F6= PC:Tween® 80:DPPC:DSCP:PI.

However, nature of drugs in different pH gradients, nature of the membrane comprising phospholipids, interaction between drugs and liposomal membrane, and diffusion path lengths altogether play vital role in the release patterns of drugs through such delivery systems (Bally *et al.*, 2010).Application of mathematical models to drug release processes is termed as drug release kinetics. The release rate of leucovorin calcium as fitted into four dissolution models has been displayed in Table 4.3. Drug dissolution rate is the amount of the drug substance that goes in solution per unit time under standardized conditions of liquid/solid interface, temperature and solvent composition. An utmost requisite to establish an *in vitro-in vivo* correlation is the mathematical modeling of drug release process most of which rely on the diffusion equations based on composition of the liposomes and the conditions underlying such physicochemical release phenomenon. Four models namely Zero order, First order, Higuchi and Gompertz model were selected to find the one best fitted with drug release data under study. Zero order model is used to investigate if the release rate is concentration dependent or not. First order kinetic model is used to describe the

adsorption or elimination of drugs and explains that the rate of the drug release is proportional to its concentration. Higuchi model, being the first model to describe the drug release from a matrix system, is used to study the release of water soluble or less soluble drugs incorporated into semisolids of solid matrices. Comparisons of release profiles of drugs having good solubility and intermediate release rates can be best explained by Gompertz model (Dash *et al.*, 2010). The average release rate in all dissolution models was slower. The regression coefficient values showed that the release was to Gompertz dissolution models.

4.7.2 *In vitro* Release Profile of Methotrexate

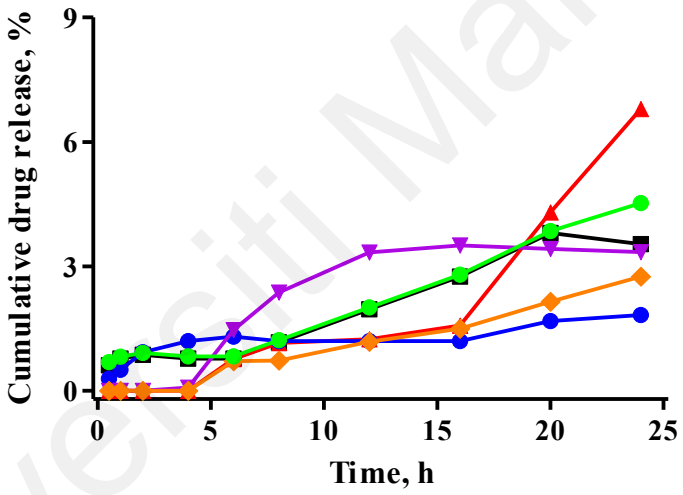

Figure 4.16: Cumulative release (%) of methotrexate from different one day old liposome formulations in PBS of pH 7.4 after 24 h at 37 °C, where ■ = F1 (PC:Tween®80:DPPC:DSPC:PS), ■ = F1 (PC:Tween®80:DPPC:DSPC:PS), ▲= F2 (PC:Tween®80:DPPC:DSPC:PS:DCP), ● = F3 (PC:Tween®80:DPPC:DSPC:PS:PI), ▼= F4 (PC:Tween®80:DPPC:DSPC), ♦ = F5 (PC:Tween®80:DPPC:DSPC:DCP), ● = F6 (PC:Tween®80:DPPC:DSPC:PI).

The release of methotrexate has been presented in Figure 4.16. Methotrexate exhibited slower and sustained release property in all MTX-loaded liposomal formulations where only less than 10 % of the drug was release after 24 h at 37 ºC. Methotrexate has an intermediate log *p* value which suggests the probability of the drug entrapment both in the aqueous and membrane phase.

Table 4.4: Rate of release (K), and Regression coefficient (R^2) values of methotrexate from one day old phospholipid liposomes.

Kinetic model		**Liposome formulation**					
		F1	F2	F3	F4	F5	F6
Zero order,	K_0	0.233	0.202	0.091	0.182	0.105	0.184
	R^2	0.933	0.796	-0.277	0.814	0.960	0.926
First order	K_1	0.002	0.002	0.001	0.002	0.001	0.002
	R^2	0.932	0.791	-0.271	0.819	0.959	0.925
Higuchi	K_H	0.898	0.731	0.389	0.725	0.97	0.720
	R^2	0.769	0.544	0.681	0.785	0.744	0.798
Gompertz	$K_{G\alpha}$	8.146	37.938	5.092	6.119	9.151	7.446
	$K_{G\beta}$	0.756	1.912	0.160	0.468	0.670	0.626
	R^2	0.923	0.949	0.847	0.879	0.979	0.895

*F1= PC: Tween® 80: DPPC: DSCP: PS, F2 = PC: Tween® 80: DPPC: DSCP: PS: DCP, F3= PC: Tween® 80: DPPC: DSCP: PS: PI, *F4= PC:Tween®80:DPPC:DSCP, F5= PC:Tween® 80:DPPC: DSCP:DCP, F6= PC:Tween® 80:DPPC:DSCP:PI.

Though, there was some variation in the cumulative drug release rate, however, slower and sustained release of methotrexate make liposomes useful carriers in drug delivery application. However, nature of drugs in different pH gradients, nature of the membrane comprising phospholipids, interaction between drugs and liposomal membrane, and diffusion path lengths altogether play vital role in the release patterns of drugs through such delivery systems (Bally *et al.*, 2010).

The release data of methotrexate was fitted to zero-order, First-order, Higuchi and Gompertz dissolution models and has been displayed in Table 4.4. The coefficient regression values from the curve fittings showed that the dissolution was most fitted to Gompertz model. The fitting data reveals that the release route of methotrexate was ruled by the nature of drug which has an intermediate release rate and good solubility (Dash *et al.*, 2010).

4.7.3 *In vitro* Release Profile of Doxorubicin

Figure 4.17 represents the release of doxorubicin from liposomes F1-F6. Doxorubicin, having log p value of + 0.53, has the tendency to incorporate in the bilayer membrane more than the aqueous core of liposomes. Cumulative release rate for F3, F4, and F6 was below 20 % even after 24 hours. However, cumulative release was below in first 12 hours in case of F4, F2 and F5 which increased up to 30 % after 24 hours.

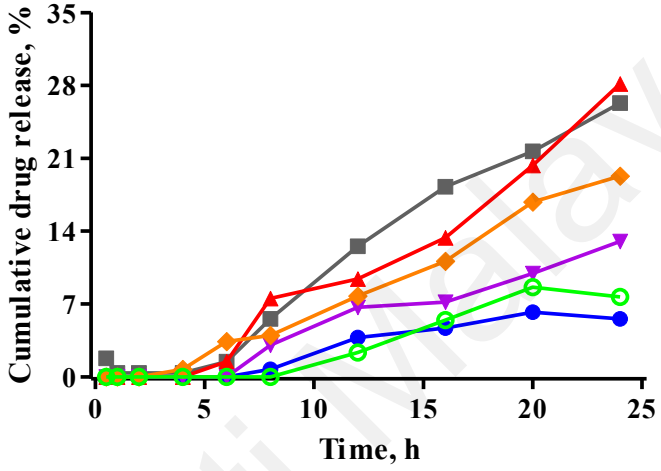

Figure 4.17: Cumulative release (%) of doxorubicin hydrochloride from different one day old liposome formulations in PBS of pH 7.4 after 24 h at 37 °C, where ■ = F1 (PC:Tween®80:DPPC:DSPC:PS), ■ = F1 (PC:Tween®80:DPPC:DSPC:PS), ▲= F2 (PC:Tween®80:DPPC:DSPC:PS:DCP), ● = F3 (PC:Tween®80:DPPC:DSPC:PS:PI), ▼= F4 (PC:Tween®80:DPPC:DSPC), ♦ = F5 (PC:Tween®80:DPPC:DSPC:DCP), ● = F6 (PC:Tween®80:DPPC:DSPC:PI).

Because of the less steric hindrance on the surface of F1, F2, F4 and F5, some of the molecules get attached to the surface of the liposomes as it is slightly positively charged drug. This rendered the high release of doxorubicin as compared with the other formulations F3 and F6 which contain phosphatidylinositol having bulky head groups. Addition of charged molecules like DCP may add to more hydrophilic character in the bilayers of liposomes. Furthermore, Presence of such charged molecules may separate the adjacent bilayers in the vesicles due to charge repulsion, producing larger vesicles (Chaw *et al.*, 2013) and encouraging vesicle leakage (Dousset *et al.*, 1981).

Table 4.5: Rate of release (K), and Regression coefficient (R^2) values of doxorubicin hydrochloride from one day old phospholipid liposomes.

Kinetic model							
		Liposome formulation					
		F1	F2	F3	F4	F5	F6
Zero order,	K_0	1.045	0.987	0.256	0.488	0.752	0.315
	R^2	0.939	0.918	0.874	0.920	0.956	0.822
First order	K_1	0.012	0.011	0.003	0.005	0.008	0.003
	R^2	0.924	0.898	0.872	0.913	0.945	0.816
Higuchi	K_H	3.899	3.634	0.949	1.803	2.802	1.135
	R^2	0.703	0.665	0.651	0.677	0.718	0.564
Gompertz	$K_{G\alpha}$	12.634	16.053	9.706	11.016	11.261	15.503
	$K_{G\beta}$	1.638	1.797	0.925	1.216	1.393	1.352
	R^2	0.990	0.974	0.926	0.975	0.992	0.939

*F1= PC: Tween® 80: DPPC: DSCP: PS, F2 = PC: Tween® 80: DPPC: DSCP: PS: DCP, F3= PC: Tween® 80: DPPC: DSCP: PS: PI, *F4= PC:Tween®80:DPPC:DSCP, F5= PC:Tween® 80:DPPC: DSCP:DCP, F6= PC:Tween® 80:DPPC:DSCP:PI.

Table 4.5 represents the drug release data fitting to zero-order, first-order, Higuchi and Gompertz dissolution models. The regression data reveals the Gomperts model as the best fitted model which relveals an intermediate drug release and good solubility of the drug.

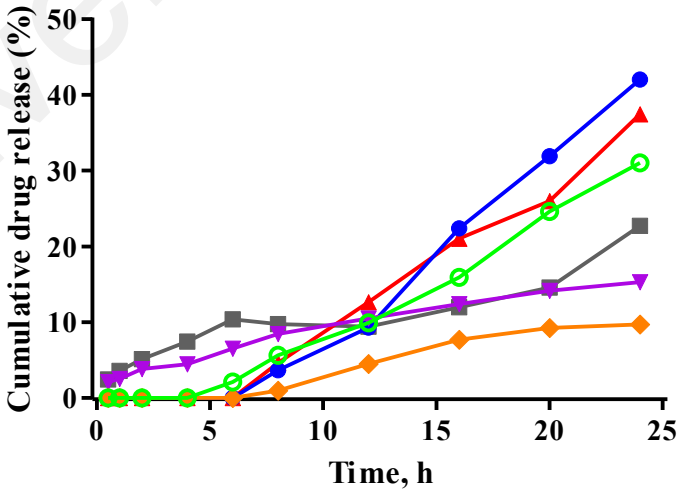

Figure 4.18: Cumulative release (%) of irinotecan from different one day old liposome formulations in PBS of pH 7.4 after 24 h at 37 °C, where ■ = F1 (PC:Tween®80:DPPC:DSPC:PS), ■ = F1 (PC:Tween®80:DPPC:DSPC:PS), ▲= F2 (PC:Tween®80:DPPC:DSPC:PS:DCP), ● = F3 (PC:Tween®80:DPPC:DSPC:PS:PI), ▼= F4 (PC:Tween®80:DPPC:DSPC), ♦ = F5 (PC:Tween®80:DPPC:DSPC:DCP), ● = F6 (PC:Tween®80:DPPC:DSPC:PI).

4.7.4 *In vitro* Release Profile of Irinotecan

The cumulative release rate for irinotecan loaded liposomes has been displayed in Figure 4.18. Liposomes containing these drugs may circulate in bloodseam for extended periods in comparison to the same drug in a non-liposomal form and may result in extended treatment covering simplified dosage regimen. This way the liposomes help to accumulate drugs in higher concentrations to disease target and play a vital role in reducing their harmful effects on healthy tissies. The cumulative release of hydrophobic irinotecan was slower until first 12 hour. After 24 hours, F2, F3, and F6 have shown an increase in cumulative drug release up to approximately 40 % However it was found to be less than 30 % for F1, F4 and F5 liposomes The increased release of irinotecan can be attributed to its log *p* value of + 2.78 which render it to incorporate in liposome bilayers. This shows that hydrophobic drugs are expected to be released more for the given liposome formulations in the current study. Table 4.6 shows that Gompertz model best fits to the release rate of the irinotecan which depicts the intermediate drug release from the liposomes.

Table 4.6: Rate of release (K), and Regression coefficient (R2) values of irinotecan from one day old phospholipid liposomes.

Kinetic model		**Liposome formulation**					
		F1	F2	F3	F4	F5	F6
Zero order,	K_0	0.639	1.298	1.433	0.741	0.402	0.113
	R^2	0.123	0.893	0.858	0.842	0.888	0.916
First order	K_1	0.007	0.014	0.016	0.008	0.004	0.012
	R^2	0.174	0.863	0.819	0.869	0.883	0.891
Higuchi	K_H	2.704	4.711	5.138	3.016	1.473	4.073
	R^2	0.788	0.625	0.582	0.979	0.640	0.653
Gompertz	$K_{G\alpha}$	3.303	28.540	68.113	4.024	11.898	21.716
	$K_{G\beta}$	0.320	2.406	3.154	0.544	1.216	2.099
	R^2	0.853	0.992	0.998	0.981	0.965	0.993

*F1= PC: Tween® 80: DPPC: DSCP: PS, F2 = PC: Tween® 80: DPPC: DSCP: PS: DCP, F3= PC: Tween® 80: DPPC: DSCP: PS: PI, *F4= PC:Tween®80:DPPC:DSCP, F5= PC:Tween® 80:DPPC: DSCP:DCP, F6= PC:Tween® 80:DPPC:DSCP:PI.

4.8 Chemical Activity of Drugs

Chemical and biological activity of drugs after release into the body is the most critical parameter. Sometimes, chemical reactions of the drugs with carriers may cause some detrimental outcomes after release. In order to avoid such issues, the drug must not react with the carrier and should be delivered without undergoing any chemical transformation in this regard. Chemical activity of pure leucovorin calcium and leucovorin calcium after release from phospholipid liposomes F1-LVC, F2-LVC, F3-LVC, F4-LVC, F5-LVC and F6-LVC was studied using UV/Vis spectrophotometer (Cary 50, Agilent technologies, USA). The spectra were recorded at wavelength of 288 nm. The spectra of pure leucovorin calcium and in the release medium were recorded and are shown in the Figure 4.18. Chemical activity of methotrexate before and after release of the drug from phospholipid liposomes namely F1-MTX, F2-MTR, F3-MTR, F4-MTR, F5-MTR and F6-MTR was investigated using UV/Vis spectrophotometer.

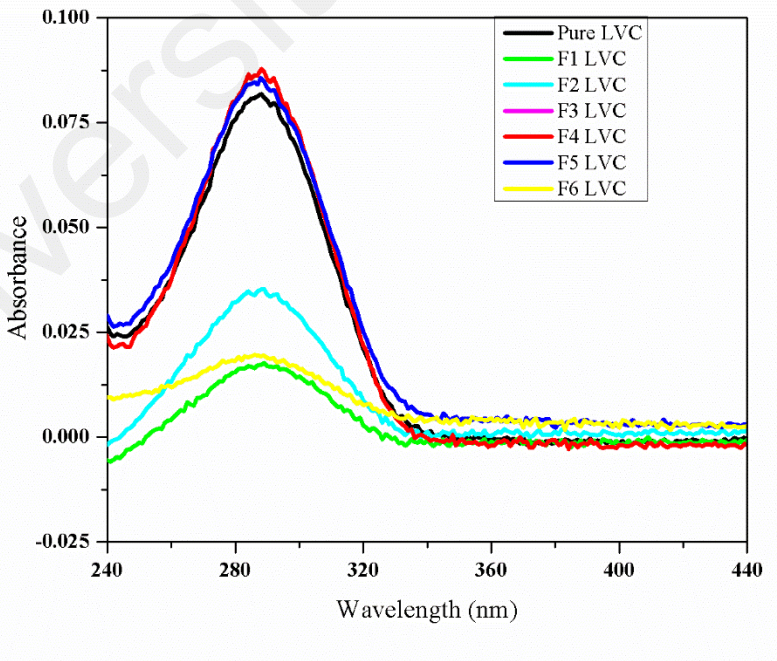

Figure 4.19: Chemical activity of pure LVC and LVC after release from phospholipids F1, F2, F3, F4, F5 and F6. F1 (PC:Tween®80: DPPC:DSPC:PS), F2 (PC:Tween®80: DPPC:DSPC:PS:DCP), F3 (PC:Tween®80: DPPC:DSPC:PS:PI), F4 (PC:Tween®80: DPPC:DSPC), F5 (PC:Tween®80: DPPC:DSPC:DCP), F6 (PC:Tween®80: DPPC:DSPC:PI).

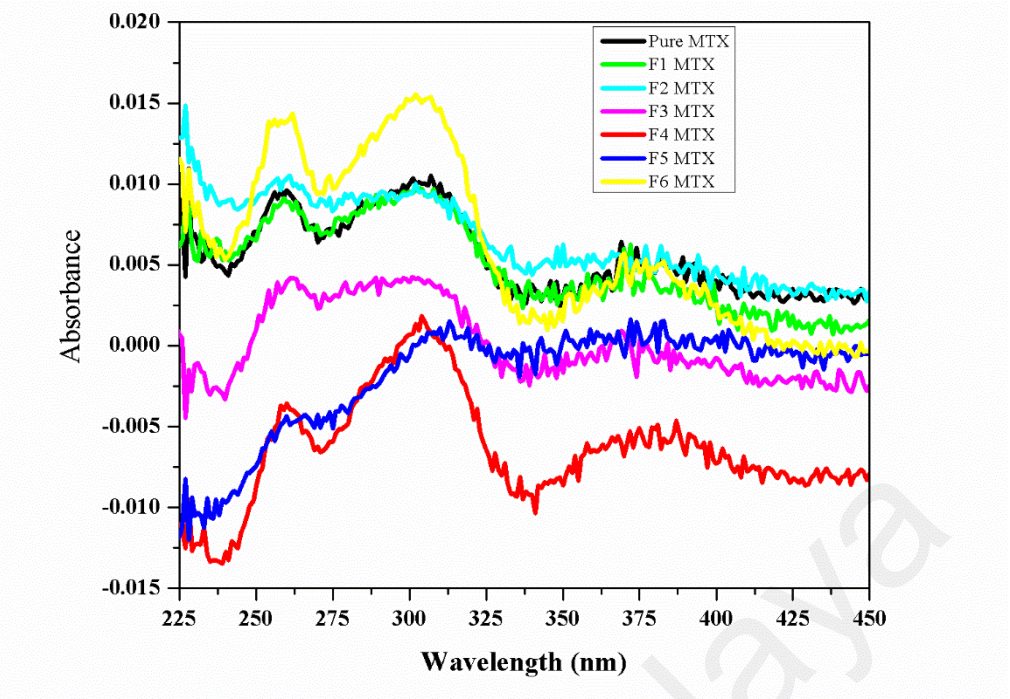

Figure 4.20: Chemical activity of pure MTX and MTX after release from phospholipids F1, F2, F3, F4, F5 and F6, where F1 (PC:Tween®80: DPPC:DSPC:PS), F2 (PC:Tween®80: DPPC:DSPC:PS:DCP), F3 (PC:Tween®80: DPPC:DSPC:PS:PI), F4 (PC:Tween®80: DPPC:DSPC), F5 (PC:Tween®80: DPPC:DSPC:DCP), F6 (PC:Tween®80: DPPC:DSPC:PI).

The analysis was carried out by comparing the pure drug with the drug released in the release medium PBS (pH 7.4) at a wavelength of 303 nm. The spectra recorded are shown in Figure 4.19. Furthermore, the chemical activity of doxorubicin hydrochloride was also investigated using UV/Vis spectrophotometer. The spectra were recorded for the pure doxorubicin hydrochloride and doxorubicin hydrochloride after release in the buffer medium (PBS, pH 7.4). The spectra were recorded at a wavelength of 485 nm and are shown in Figure 4.20. Chemical activity of the irinotecan anticancer drug was also investigated using UV/Vis spectrophotometer. The spectra were recorded at a wavelength of 255 nm for pure irinotecan and irinotecan released in release medium of PBS (pH 7.4). It was observed in each case that there was no significant difference in the spectra of drugs before and after encapsulation in the carriers. This depicted that the drugs did not show any chemical transformation after release from the phospholipid liposomes.

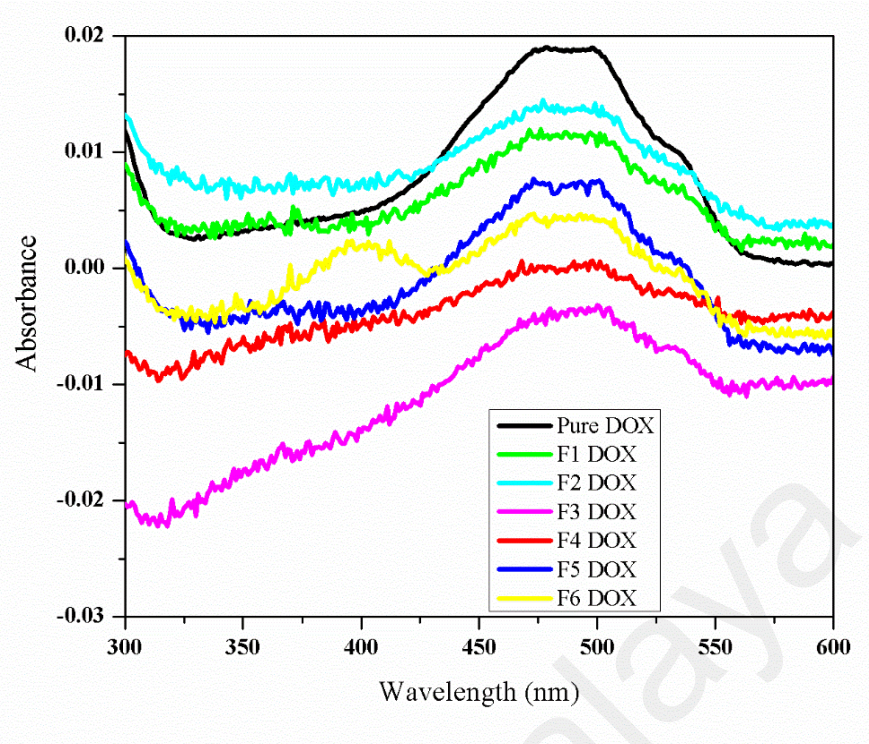

Figure 4.21: Chemical activity of pure DOX and DOX after release from phospholipids F1, F2, F3, F4, F5 and F6. F1 (PC:Tween®80: DPPC:DSPC:PS), F2 (PC:Tween®80: DPPC:DSPC:PS:DCP), F3 (PC:Tween®80: DPPC:DSPC:PS:PI), F4 (PC:Tween®80: DPPC:DSPC), F5 (PC:Tween®80: DPPC:DSPC:DCP), F6 (PC:Tween®80: DPPC:DSPC:PI).

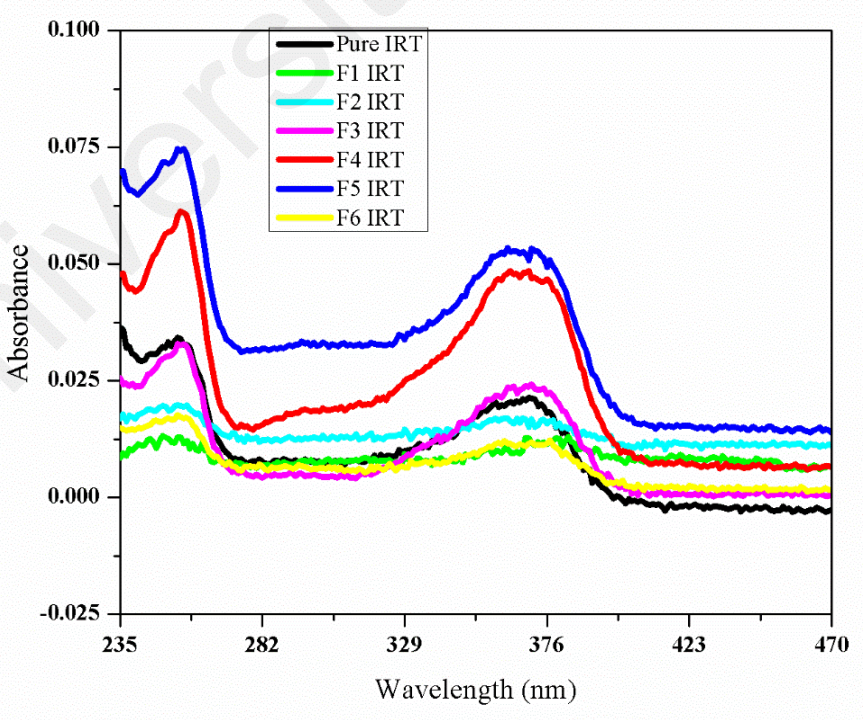

Figure 4.22: Chemical activity of pure IRT and IRT after release from phospholipids F1, F2, F3, F4, F5 and F6., where F1 (PC:Tween®80: DPPC:DSPC:PS), F2 (PC:Tween®80: DPPC:DSPC:PS:DCP), F3 (PC:Tween®80: DPPC:DSPC:PS:PI), F4 (PC:Tween®80: DPPC:DSPC), F5 (PC:Tween®80: DPPC:DSPC:DCP), F6 (PC:Tween®80: DPPC:DSPC:PI).

4.9 Haemocompatibilty Studies and Cell Cytotoxicity Analysis

For many years, drug delivery strategies have been developed to improve the effectiveness and reduce the cardiotoxicity of doxorubicin. In a first approach, association with colloidal nanosystems such as liposomes and nanoparticles allows the drug distribution route to be modified avoiding serious side effects. In a second step, carrier targeting specificity toward cancer cells have been developed. DOX has highest encapsulation efficiency. From the release kinetics data, it is evident that DOX showed the best and superior results in terms of slow and stable release when monitored upto 24 hours. DOX is one of the most commonly used in Chemotherapy today and hence chose that for in vitro studies. Among the six formulations, we did investigate three representative formulations F1, F2 and F3 and DOX for the preliminary in vitro studies. However it is apparent that further studies need to be conducted for all the formulations to make a conclusive final assessment of the best formulation.

4.9.1 Haemolysis Tests

Both qualitative and quantitative compositions of the liposomes have been long been considered important aspect for intravenous anticancer drug delivery applications (Edwards *et al.,* 2006). In pharmacology and toxicology, the path by which the fluid, drug or any other relevant substance is taken into the body is termed as the route of administration, and is generally classified based on their applied locality. These may be classified according to the targeted action such as topical (on the skin surface or mucous membrane), transdermal (absorbed through the skin or mucous membrane), enteral (delivered through the gut) or parenteral (delivered by routes other than the gut). Liposomes have been designed and used for different modes of applications such as transportation of oral (Nguyen *et al.*, 2016), transdermal (Agarwal *et al.*, 2016) and intravenous drug payloads (Gref *et al.*, 2012).

The most critical of all is their use in intravenous drug delivery. The intravenous route is believed to be the fastest way of delivering fluids (Gref *et al.*, 2012) and other medications throughout the body with a medication bioavailability of ideally, although not practically, 100 % (Allen *et al.*, 2013; Durymanov *et al.*, 2016). The infusion is made directly into a vein to ensure its maximum bioavailability. Anything administered through the intravenous route must not be harmful to the blood, especially red blood cells, which are the only means of delivering oxygen to the body tissues via circulatory system (Biagiotti *et al.*, 2011; Muzykantov, 2010). The phenomenon of rupturing the red blood cells by any means is called hemolysis (Ji *et al.*, 2014). As a result of hemolysis, the contents of the red blood cells are released into the surrounding fluid and accelerated hemolysis rates lead to anemia, jaundice and reticulocytosis (Han *et al.*, 2012; Shalel *et al.*, 2002). Hence, carriers administered via the blood route must be evaluated according to their hemolytic potentials using pharmacology and toxicity assays (Elmowafy *et al.*, 2013; Feng *et al.*, 2016; Roggers *et al.*, 2014). Hemolysis may be studied both by *in vitro* or *in vivo* methods In the present study, the principle of hemolysis test for unloaded liposomes (blank liposomes) was based on the measurement of supernatant of RBCs using UV/Vis spectrophotometer. After the liposomes were incubated with red blood cells for 5 h, the samples were subjected to centrifugation to separate the undamaged red blood cells from the supernatant. The supernatant quantified by the absorbance using UV/Vis spectrophotometer. To be considered as blood compatible, the liposomes under study must not cause the event of hemolysis Triton® X 100 solution, a detergent that is capable of destabilizing membranes of red blood cells, was used to generate the positive control. A 100 % hemolysis was observed when the liposomes were incubated with red blood cells in the presence of 1 % v/v Triton® X 100 solution (El-Far *et al.*, 2018; Somaglino *et al.*, 2011). On the other hand, a non-hemolytic medium known as negative control was prepared by incubating with

PBS. Based on the calculations, the percentage of hemolysis was found more than 15 % for 20 mg/ml sample whereas all liposomes treated sample with concentrations 10 mg/ml and below showed less than 15 % hemolysis over 5 hours of incubation. Percentage hemolysis observed in the samples was significantly lower compared to the positive control. According to the reported literature, substances with less than 15 % hemolysis are still considered non-hemolytic (Petersen *et al.*, 2002). The low hemolysis may be due to experimental errors during pipetting and centrifugation steps.

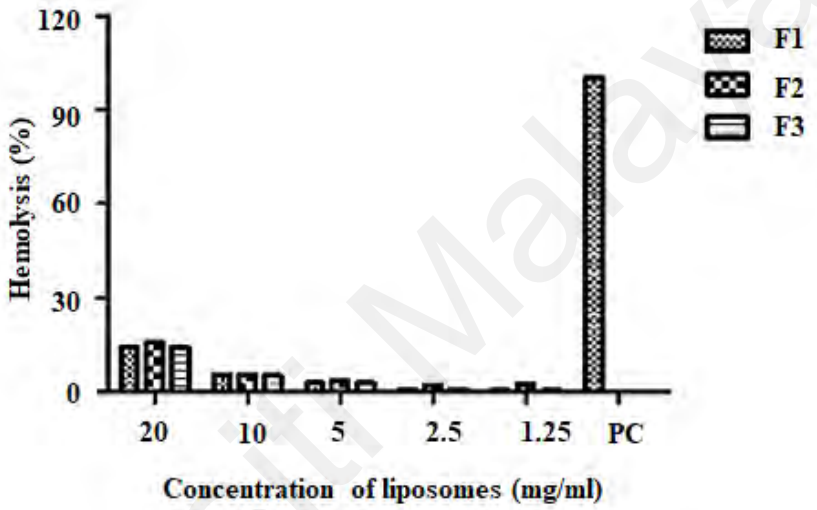

Figure 4.23: Determination of hemolytic activity in liposome formulations with reference to positive control (PC).

The results demonstrated that the liposomes formulated as F1, F2 and F3 were non-hemolytic up the concentration of 10 mg/ml. Our modified liposomes were considered suitable for intravenous administration based on this hemocompatibility data. All the data was expressed in the form of the mean ± standard deviation (Iman *et al.*, 2017). In case of 20 mg/ml, the hemolytic activity was more obvious and ranged from 15 % to 20 % owing to the previously reported studies on the hemolysis on human RBCs (Lange *et al*., 1983*). In vitro* incubation of liposomes has been reported to result in an exchange of membrane components (Rindlisbacher & Zahler, 1983) whereby increasing the fragility of the cells towards the liposomes (Quirion & St-Pierre, 1991; Tokumasu *et al*., 2012).

4.9.2 Red Blood Cell Aggregation Test

In order to investigate whether liposomes induce aggregation of red blood cells, red blood cell aggregation test was performed on fresh human blood. To prevent the occurance of coagulation, Ringer‘s solution containing sodium citrate was used during this analysis (Petersen *et al.*, 2002).

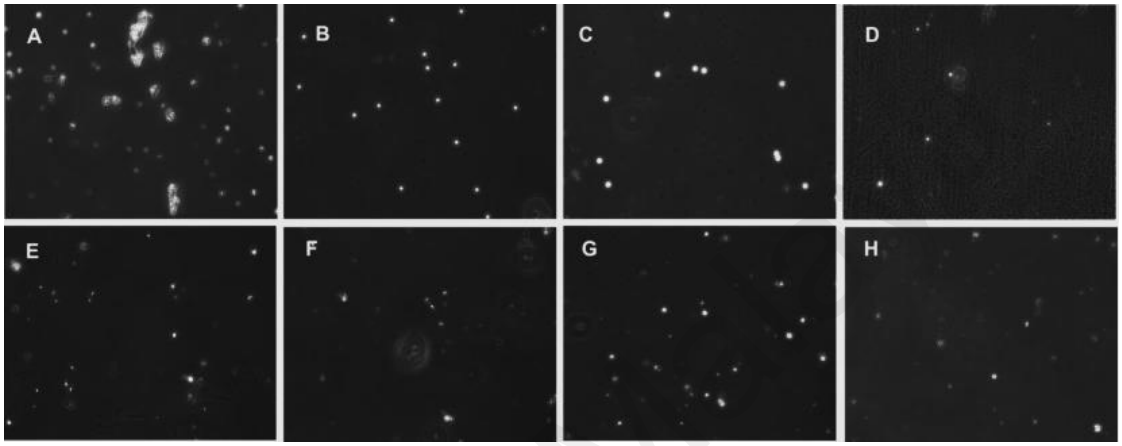

Figure 4.24: Aggregation studies of liposomes using fresh human blood. (A) Positive control (RBCs suspended in modified Ringer‘s solution(without sodium citrate)); (B) Negative control (RBCs suspended in Ringers‘ solution (with sodium citrate)); (C) F1, 1 mg/ml; (D) F1, 10 mg/ml; (E) F2, 1 mg/ml; (F) F2 10 mg/ml; (G) F3, 1 mg/ml; (H) F3, 10 mg/ml.

Sodium citrate as an anticoagulant, binds to calcium ions to prevent blood clotting. Therefore, to induce red blood cell aggregation, the ringer‘s solution was modified without addition of sodium citrate and was used as positive control. Based on the images obtained from microscope, negative control showed no red blood cell aggregation whereas positive control showed aggregation of red blood cells. Our modified liposomes were considered suitable for intravenous administration based on the good biocompatibility of liposomes as they do not induce red cell aggregation for up to concentration of 10 mg/ml.

This study involved the preparation of negatively charged particles mimicking red blood cell surface charge based on the hypothesis that these modified liposomes will be biocompatible similar to red blood cells. Hence, based on these results, the modified

liposomes were found to be blood compatible with no significant hemolysis and red cell aggregation was observed. It was important to evaluate their biocompatibility in order to avoid any complications later when administered into the human body. This technique is highly beneficial in early detection and timely treatment of breast cancer as it is the most commonly diagnosed cancers among women. The results have been shown in the Figure 4.23.

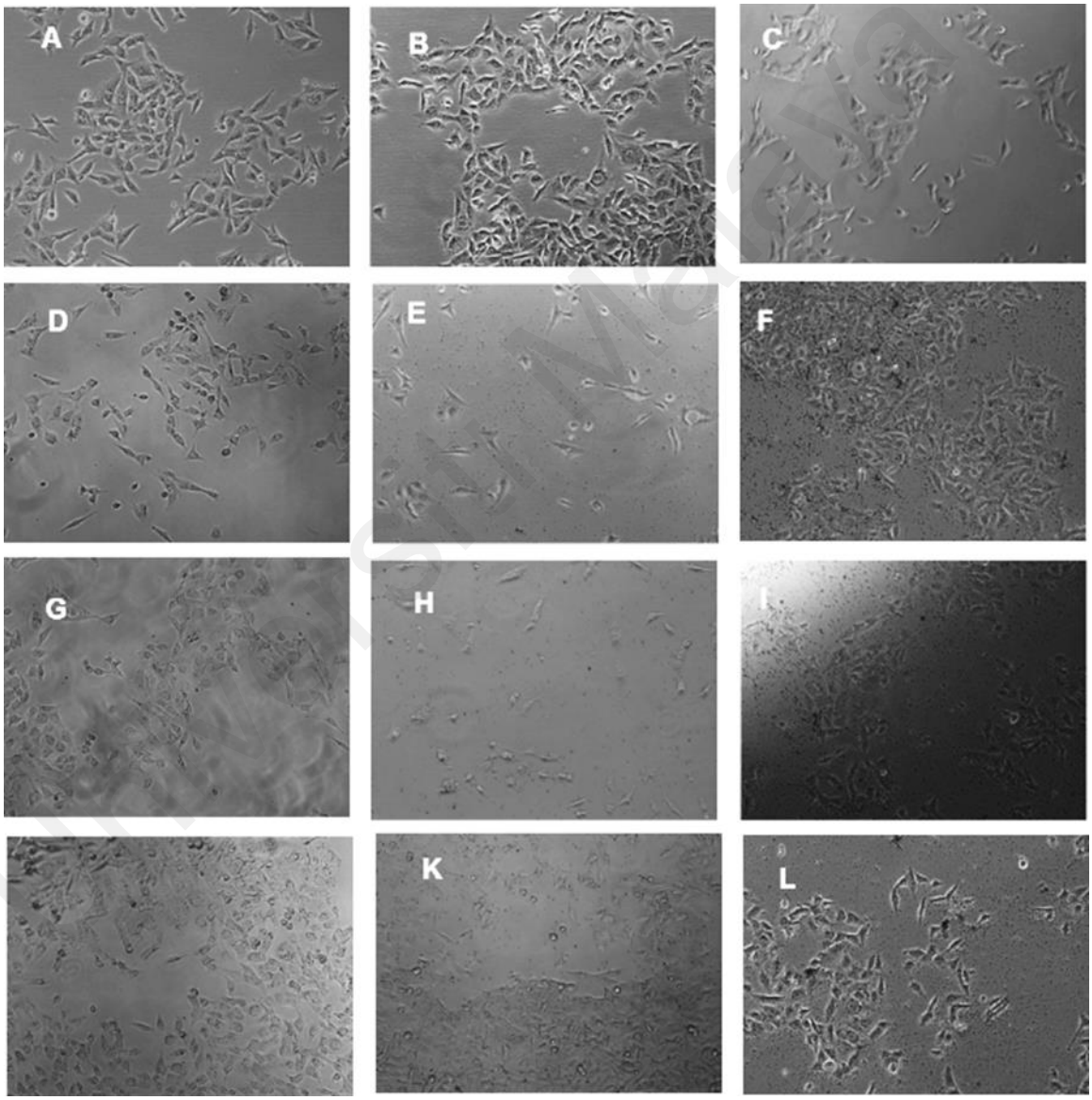

Figure 4.25: Microscope images of MDA-MB-231 cancer cell at 4 h following different treatments: untreated (A); treated with free DOX, 1 µg (B); treated with free DOX,10 µg (C); treated with blank liposomes (10 µg): F1 (D), F2 (G), F3 (J); treated with DOX-loaded liposomes 1 µg, : DOX-F1 (E), DOX-F2 (H), DOX-F3 (K); treated with DOX loaded liposomes, 10 µg: DOX-F1 (F), DOX-F2 (I), DOX-F3 (L).

4.9.3 Effect of DOX-Loaded Nanoparticles on Suppression of Cellular Growth and Cell Uptake

The effects of free and liposome-encapsulated DOX on the viability of MDA-MB-231 cells were compared. The Studies were done after 4 hours (Figure 4.24) and 48 hours (Figure 4.25) of incubation after treatment of MDA-MB-231 cells with blank and DOX-loaded liposomes. The cells incubated with blank liposomes and loaded ones showed no cell suppression after 4 hours. After 48 hours of incubation, the cells in untreated wells (Figure 4.25, A) and with blank liposomes (Figure 4.25, D, E, and F) remained alive and their growth was no significant suppression in the cell growth at all. The cells treated with free DOX showed that no cell could survive even with concentration as low as 1 µg/ml (Figure 4.25, C). The cells treated with 1 µg/ml and 10 µg/ml of the DOX-loaded liposomes revealed an obvious cell death as depicted in Figure 4.25 (E, F, H, I, K and L). That showed that the DOX was released from the liposomes after 48 hours incubation and suppressed the cell growth to a higher extent. The nano-drug carriers should be nontoxic and biocompatible in order to be used for *in vivo* applications.

Doxorubicin, an anthracycline antitumor antibiotic, is commonly used in chemotherapy for wide range of cancers. Breast, overran, sarcoma, leukemia and lung cancers are treated widely with doxorubicin. Two main mechanisms have been proposed for mode of action of doxorubicin. It works through the inhibition of topoisomerase II according to the first mechanism whereas the second proposed mechanism is by free radical generation (Thorn *et al.*, 2011).

The main mechanism underlying doxorubicin mode of action is linked with the intercalation of doxorubicin into DNA which contributes to the inhibition of topoisomerase II, which eventually leads to DNA damage and cell death.

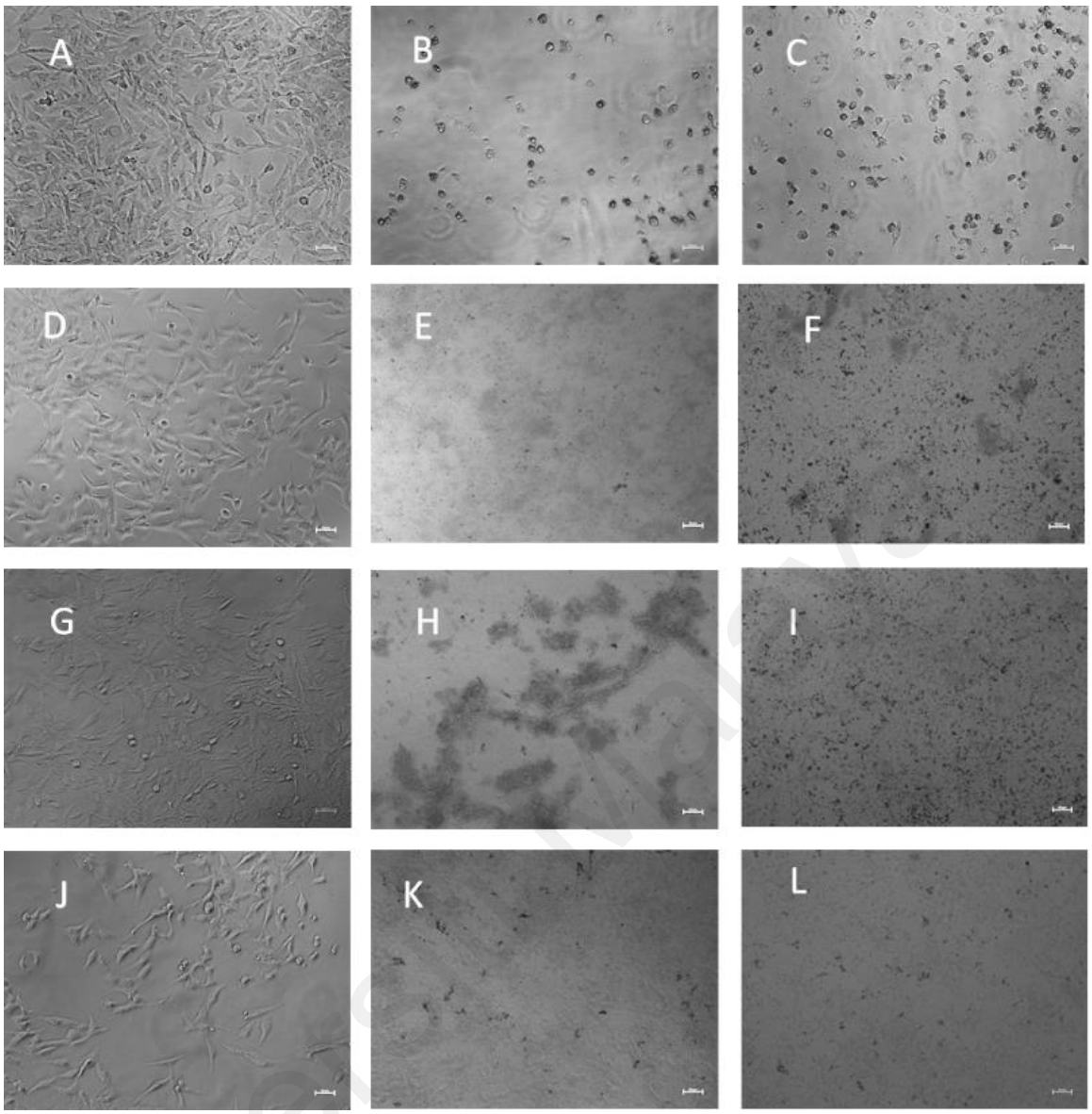

Figure 4.26: Microscope images of MDA-MB-231 cancer cell at 48 h following different treatments: untreated (A); treated with free DOX, 1 µg (B); treated with free DOX,10 µg (C); treated with blank liposomes (10 µg): F1 (D), F2 (G), F3 (J); treated with DOX-loaded liposomes 1 µg, : DOX-F1 (E), DOX-F2 (H), DOX-F3 (K); treated with DOX loaded liposomes, 10 µg: DOX-F1 (F), DOX-F2 (I), DOX-F3 (L).

Besides, binding of doxorubicin to cell membrane generates free radicals and also contributes to the DNA and cell membrane damage (Mohan *et al.*, 2010). Even though, doxorubicin is water soluble, its log p value depicts that it exhibits amphiphilic nature. It can exist in either hydrophilic or hydrophobic environment. Thus, doxorubicin is expected to be loaded in inner core and lipid bilayer of the liposomes. Fluorescence microscopy can easily detect tumors on account of altered fluorescence properties.

4.9.4 Cell Uptake Analysis by Flow Cytometry

The fluorescent properties of doxorubicin were used to investigate its uptake by the MDA-MB-231 cells when it was presented as free drug or as liposomes, by flow cytometry experiments.

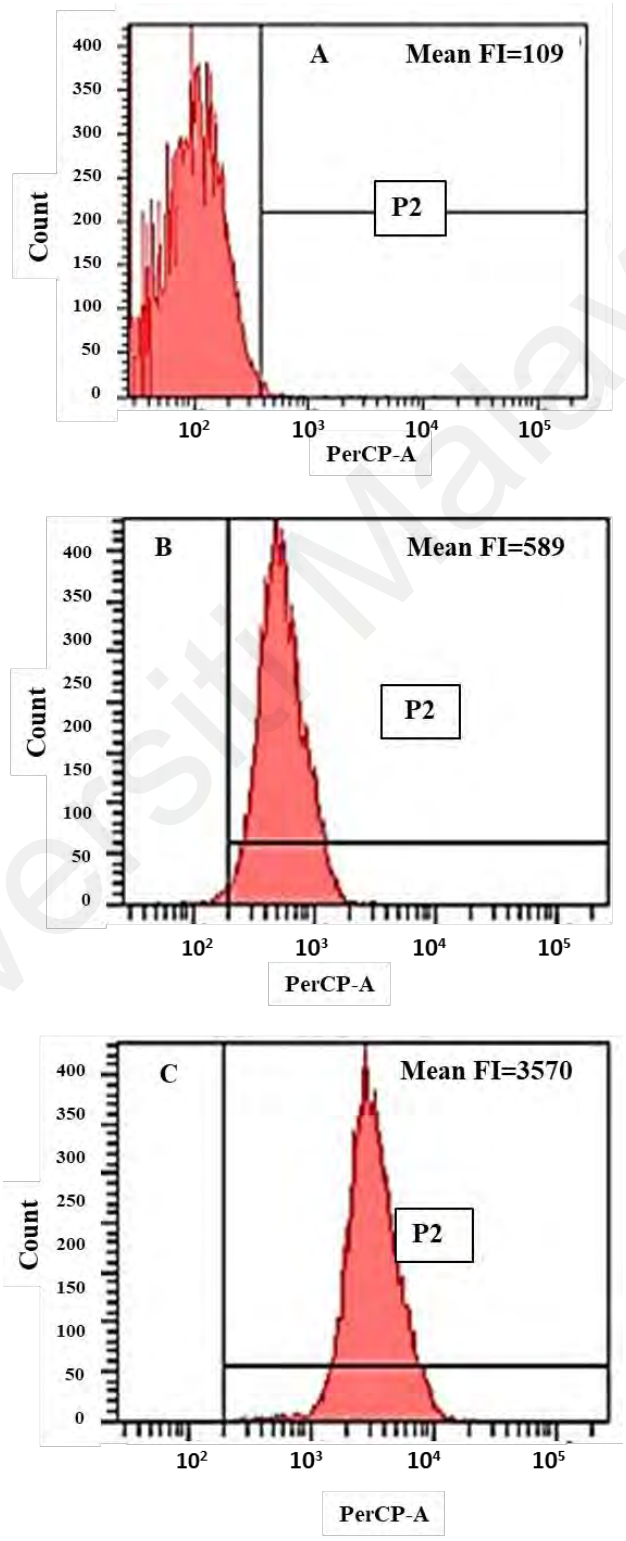

Figure 4.27: Cell uptake of free DOX after incubation with MDA-MB-231 cells for 3 h by flow cytometry. (A) Untreated Control; (B) free DOX, 1 µg; (C) free DOX, 10 µg.

Flow cytometery is a techniques used to obtain quantitative information by comparing fluorescence intensity and a calibration standard. Treatment with 10 µg free doxorubicin (Figure 4.26 C) led to a high level of cell-associated fluorescence after 3 hours. When the doxorubicin was incubated with the cells in the form of liposomes the mean fluorescence intensity was lower than that of free doxorubicin with a slight variation among the three formulations. The fluorescence intensity was quite lower in the untreated cells at 3 h.

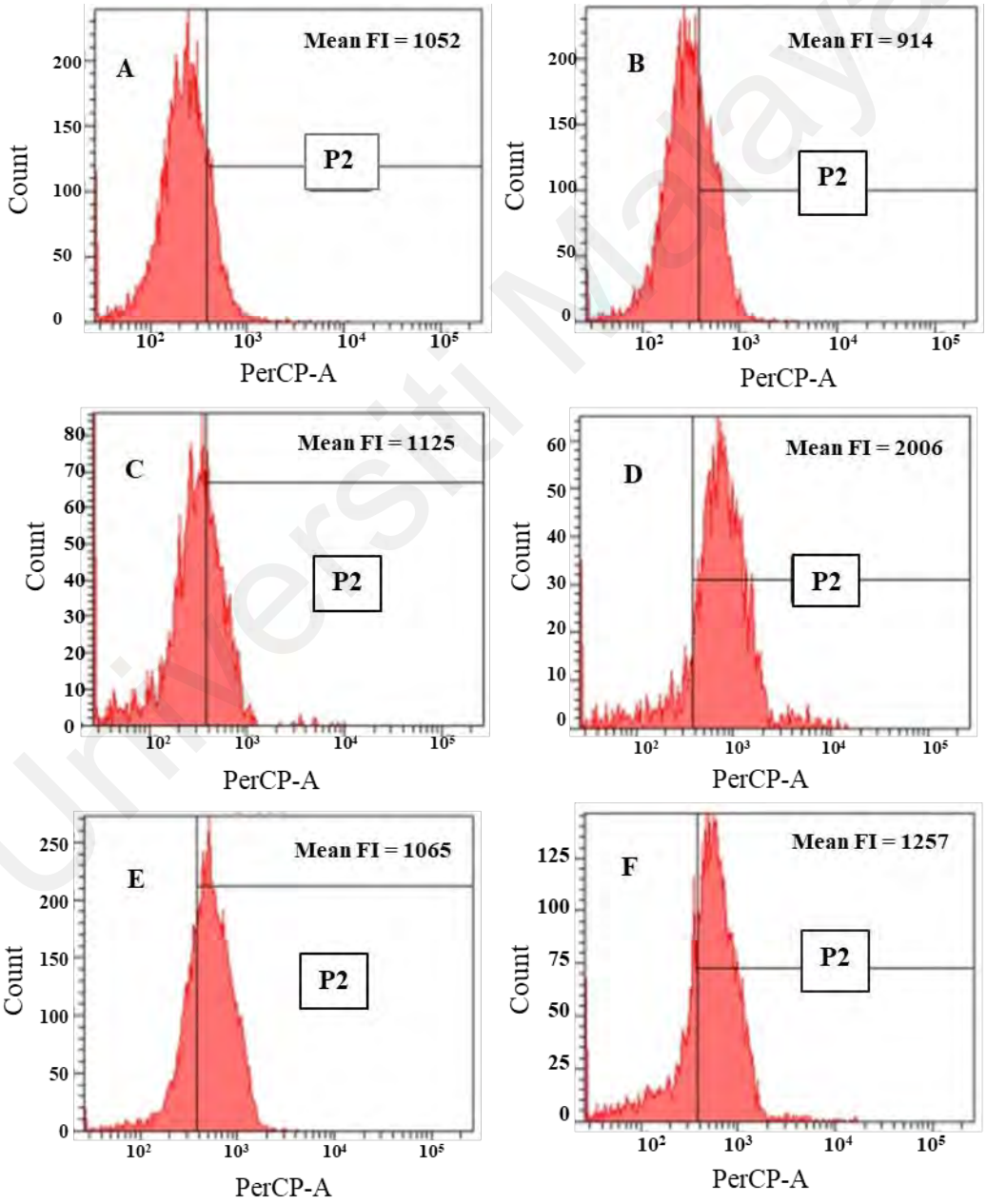

Figure 4.28: Cell uptake of DOX-NP after incubation with MDA-MB-231 cells for 3 h by flow cytometry. (A) F1-DOX, 1 µg; (B) F2-DOX, 1µg; (C) F3-DOX, 1 µg(D) F1-DOX, 10 µg; (E) F2-DOX, 10 µg; (F) F3-DOX, 10 µg.

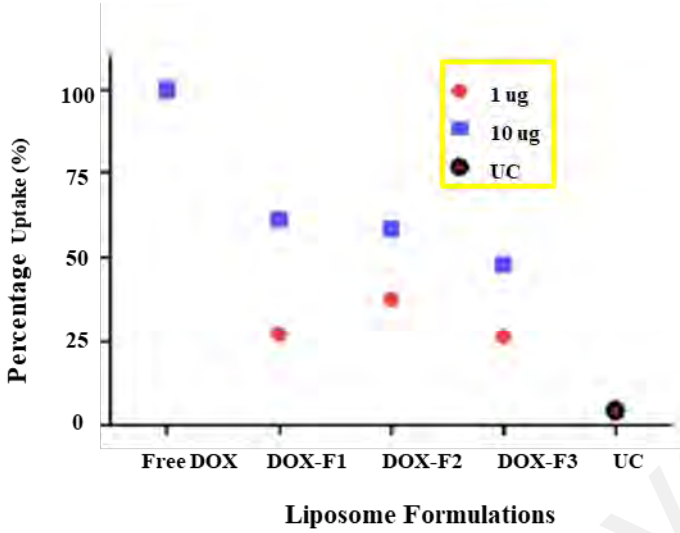

Figure 4.29: Per cent uptake of DOX-NP after incubation with MDA-MB-231 cells for 3 h by flow cytometry. (UC= untreated Control)

But a gradual more accumulation of the DOX-liposomes is required to be observed at different time intervals in order to evaluate a much promising formulations under study. The % uptake among the three formulations has been compared and given in Figure 4.27. This technique is a laser based technology which measures and analyses various physicomechmical properties of the breast cancer cells flowing in a stream of fluid through a beam of light.

4.9.5 Confocal Microscopy

Confocal microscopy is an optical imaging technique which was used to examine liposome–cell interactions in more detail as the term confocal refers to two lenses that are arranged to focus on the same point. It allows 3D analysis of fluorescent labeled thick specimens without its physical sectioning. Cellular uptake of liposomes F1-DOX, F2-DOX, F3-DOX and free doxorubicin was analysed by using confocal microscopy. DAPI (4,6-diamidino-2-phenylindole) was used to stain the cancer cells. It is the most commonly used DNA stain. Phase contrast images of MDA-MB-231 cells adhering to glass coverslips and incubated for 3 h are shown in Figure 4.29.

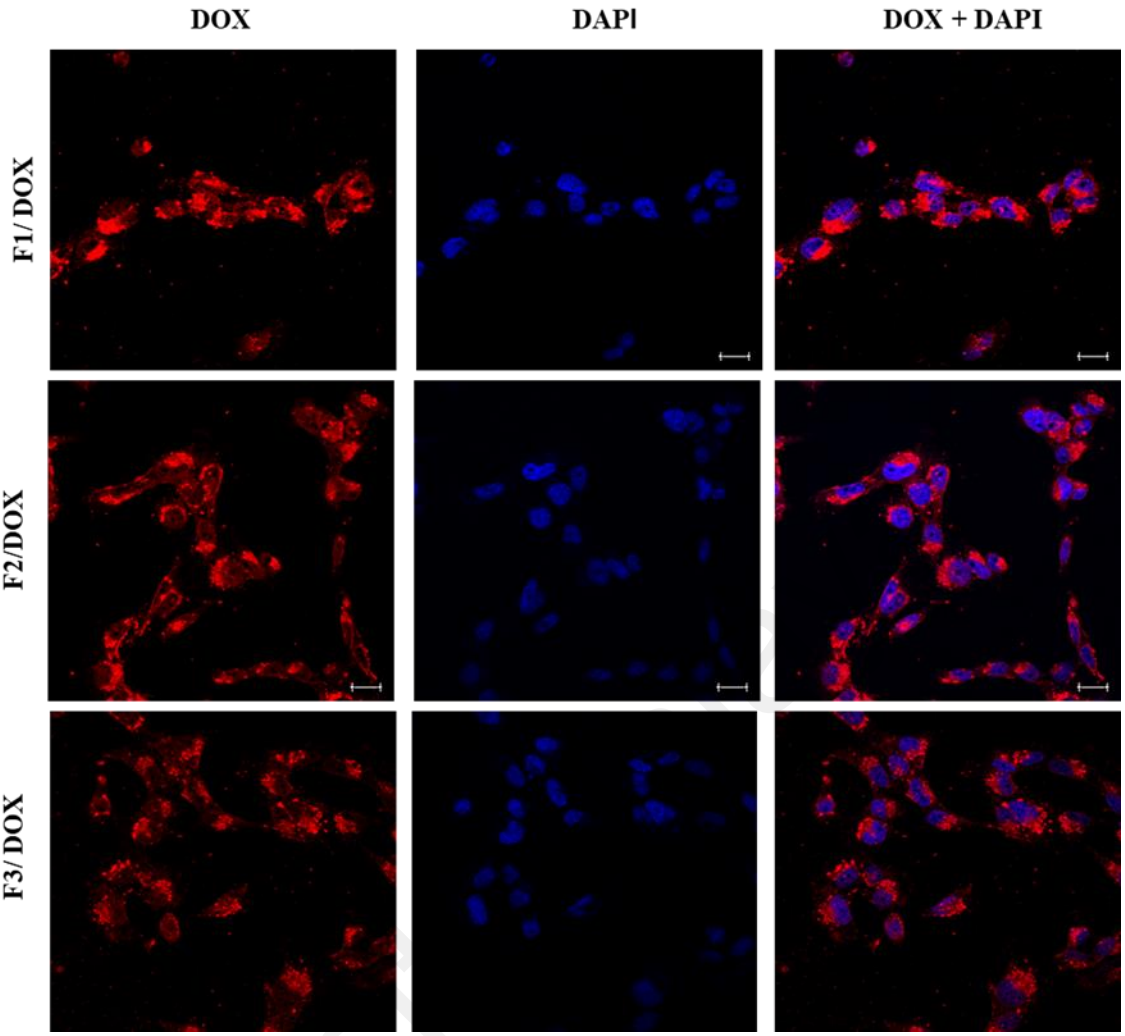

Figure 4.30: Confocal images of MDA-MB-231 cells treated with DOX-loaded fluorescent liposomes. Phase-contrast images of are shown after 3 hour incubation. The scale bars indicate 20 μm.

Besides, its most common use as anticancer drug in chemotherapy, it is also preferably used in research due to its inherent fluorescence which is related to the central anthracyclic chromophore group. This feature allows its visualization and localization in cancer cells by using fluorescence imaging. The uptake of doxorubicin into MDA-MB-231 breast cancer cells was assessed by its intrinsic fluorescence.

It is a well-established fact that binding of the doxorubicin to DNA will dramatically quench its fluorescence (Mohan *et al.*, 2010). An increased intensity of fluorescence of DAPI will be observed once it binds to DNA. A blue fluorescence is observed when

DAPI is bound to AT region of DNA. Thus, staining of nucleus of the cells with DAPI allows investigations of doxorubicin localization inside the cells. The main mechanism of doxorubicin is thought to be trough intercalation of doxorubicin with DNA (Anders *et al.*, 2013; Mohan *et al.*, 2010).

As shown in the Figure 4.29, red fluorescence of doxorubicin was observed in the nuclear apartment of the cells. Thus, intact liposomes are able to cross the nuclear membrane. The accumulation of fluorescence associated with the cells was quite good in DOX-F1, DOX-F2 and DOX-F3 liposomes. This indicates that the doxorubicin was released from the DOX-loaded liposomes and diffused into the nucleus of the cancer cells.

Furthermore, the fluorescence was not limited to the cytoplasm but was clearly observed in the nuclei which are shown as stained in DAPI and DOX/DAPI images. Intense fluorescence can be observed in the nucleus, with only diffuse staining in the cytoplasm. This shows that our modified liposomes can deliver its doxorubicin payloads into the MDA-MB-231 cells in an efficient manner.

CHAPTER 5: CONCLUSION

In this study, different type liposomes from phospholipids, lecithin, dipalmitoyl phosphatidylcholine, distearoylphosphatidylcholin, phosphatidylserin, and phosphatidylinositol were investigated. Since, average particle size and zeta potential play a key role in drug delivery, therefore, Tween 80 and dicetyl phosphate was also used in liposome formulations to get optimum particle size and zeta potentials for efficient drug delivery applications. The mean particle size is in range of 70 nm – 80 nm and zeta potential is in -3 mV to -14 mV.

All the liposomes were prepared by dry lipid hydration method. Three different types of liposomes were investigated in this study. Each type was further into two different formulations based on their composition. F1 and F4 liposome compositions were with zeta potential near zero in order to investigate their role in drug delivery and to compare their physicochemical characterization with other two types of liposomes containing DCP (F2 and F5) and PI (F3 and F6) for inducing red blood cell zeta potentials on the surface of formulated liposomes. These liposomes were having zeta potential in the range of -9 mV to -14 mV. Before formulation of the liposomes, lecithin (phosphatidylcholine) was investigated for its critical vesiculation concentration (CVC) in PBS at pH 7.4. Lecithin, above its CVC, was then mixed with other phospholipids to formulate F1-F6 liposome suspensions.

The liposomes were investigated further for stability at body‘s temperature i.e., 37 °C in terms of particle size and zeta potential over five days. It was important to investigate stability of the liposomes in PBS of pH 7.4 as these liposomes were prepared for *in vitro* anticancer drug delivery applications. Drug unloaded formulations were stable at 37 °C for five days except for F5. The changes in mean particle size and zeta potentials were more obvious in anticancer drug loaded formulations F2, F4 and F5. Liposomes were

also evaluated for their storage stability at 4 °C and 28 °C (room temperature) with respect to the average particle size and zeta potential over 28 days. Stability of formulated liposomes was found to be better at 4 °C compared to their stability at 28 °C where coagulation and fusion disturbed their particle size and zeta potential. The storage stability revealed that the liposomal formulations can be well stored for at least one month at 4 °C.

Loading efficiency of leucovorin calcium and irinotecan in liposomes was found to be lower compared to methotrexate, doxorubicin hydrochloride. It is understood that liposomes are amphiphilic carriers and loading efficiency for drugs with intermediate log p values has been found to be better because of the possibility of their retention in both hydrophobic lipid bilayer and hydrophilic core. The prepared liposomes also exhibited excellent biocompatibility and robust phospholipid structure under the physiological conditions. A high drug-loading capability and an intracellular drug release capability were observed for this system, revealing its great potential for delivering anticancer drugs. Three formulations namely F1-DOX, F2-DOX and F3-DOX were chosen as model formulations to investigate hemocompatibility via hemolytic activity assay and cell aggregation. The confocal laser scanning microscopy and flow cytometry assays showed that DOX-loaded liposomes had a high level of uptake in MDA-MB-231 human breast cancer cells. The *in-vitro* cytotoxicity studies confirmed that DOX-NP exhibited higher inhibition of tumor cell growth and proliferation. Thus the formulated liposomes may be a promising system for delivering anticancer drugs. Furthermore, formulation F3-DOX was found to be the best among all six liposome formulations after obtaining successful results of cell uptake studies using confocal microscopy and flow cytometry and can be used for sustained *in vitro* drug delivery applications. So, mimicking RBC membrane will shape the present goals and will influence the future of drug delivery.

5.1 The Future Research Plan

This study developed a new thought to use phospholipids as potential drug delivery carriers. Although, the stability data obtained suggests that formulations may further need to be modified, however the information provided may be helpful in identifying the factors which may contribute to stabilization and destabilization of the liposomes.

The ability of the liposomes to encapsulate anticancer drugs with intermediate log p value may render them to be applied in the field of drug delivery by either using other similar drugs or to investigate the combined effect of two drugs loaded in same system at the same time.

This study may help in identifying the possible *in vitro* and *in vivo* drug delivery applications with other such formulations- using different anticancer drugs. Further studies on the drug release mechanisms and cell cytotoxicity may be performed to be applied in the field of drug delivery. MTT assay for cancer cell viability in MDA-MB-231 and more specific uptake studies using other cancer cell lines of different origin and tissues will be conducted in future.

REFERENCES

Agarwal, R., Iezhitsa, I., Agarwal, P., Abdul Nasir, N. A., Razali, N., Alyautdin, R., & Ismail, N. M. (2016). Liposomes in topical ophthalmic drug delivery: An update. *Drug Delivery, 23*(4), 1075-1091.

Adelantado, C., Rodríguez-Fariñas, N., Martín-Doimeadios, R. C. R., Zougagh, M., & Ríos, Á. (2016). Analysis of silica nanoparticles by capillary electrophoresis coupled to an evaporative light scattering detector. *Analytica Chimica Acta*, *923*, 82-88.

Ahmad, A., Mondal, S. K., Mukhopadhyay, D., Banerjee, R., & Alkharfy, K. M. (2016). Development of liposomal formulation for delivering anticancer drug to breast cancer stem-cell-like cells and its pharmacokinetics in an animal model. *Molecular Pharmaceutics, 13*(3), 1081-1088.

Ahmed, M., Liu, Z., Lukyanov, A. N., Signoretti, S., Horkan, C., Monsky, W. L., Torchilin, V. P., & Goldberg, S. N. (2005). Combination radiofrequency ablation with intratumoral liposomal doxorubicin: Effect on drug accumulation and coagulation in multiple tissues and tumor types in animals 1. *Radiology, 235*(2), 469-477.

Akbarzadeh, A., Rezaei-Sadabady, R., Davaran, S., Joo, S. W., Zarghami, N., Hanifehpour, Y., Samiei, M., Kouhi, M., & Nejati-Koshki, K. (2013). Liposome: classification, preparation, and applications. *Nanoscale Research Letters, 8*(1), 102.

Akhtari, J., Rezayat, S. M., Teymouri, M., Alavizadeh, S. H., Gheybi, F., Badiee, A., & Jaafari, M. R. (2016). Targeting, bio distributive and tumor growth inhibiting characterization of anti-HER2 affibody coupling to liposomal doxorubicin using BALB/c mice bearing TUBO tumors. *International Journal of Pharmaceutics, 505*(1), 89-95.

Al Sabbagh, C., Tsapis, N., Novell, A., Calleja-Gonzalez, P., Escoffre, J.-M., Bouakaz, A., Chacun, H., Denis, S., Vergnaud, J., Gueutin, C. & Fattal, E. (2015). Formulation and pharmacokinetics of thermosensitive stealth® liposomes encapsulating 5-Fluorouracil. *Pharmaceutical Research, 32*(5), 1585-1603.

Albanese, A., Tang, P. S., & Chan, W. C. (2012). The effect of nanoparticle size, shape, and surface chemistry on biological systems. *Annual Review of Biomedical Engineering, 14*, 1-16.

Allen, T. M. (2002). Ligand-targeted therapeutics in anticancer therapy. *Nature Reviews Cancer, 2*(10), 750-763.

Allen, T. M., & Cullis, P. R. (2013). Liposomal drug delivery systems: from concept to clinical applications. *Advanced Drug Delivery Reviews, 65*(1), 36-48.

Al-Remawi, M., Elsayed, A., Maghrabi, I., Hamaidi, M., & Jaber, N. (2017). Chitosan/lecithin liposomal nanovesicles as an oral insulin delivery system. *Pharmaceutical Development and Technology*, *22*(3), 390-398.

Alves, A. C., Ramos, I. I., Nunes, C., Magalhães, L. M., Sklenářová, H., Segundo, M. A., & Reis, S. (2016). On-line automated evaluation of lipid nanoparticles transdermal permeation using Franz diffusion cell and low-pressure chromatography. *Talanta*, *146*, 369-374.

Amani, A., York, P., Chrystyn, H., & Clark, B. J. (2010). Factors affecting the stability of nanoemulsions-use of artificial neural networks. *Pharmaceutical Research, 27*(1), 37.

Amoozgar, Z., & Yeo, Y. (2012). Recent advances in stealth coating of nanoparticle drug delivery systems. *Wiley Interdisciplinary Reviews: Nanomedicine and Nanobiotechnology, 4*(2), 219-233.

Anders, C. K., Adamo, B., Karginova, O., Deal, A. M., Rawal, S., Darr, D., Schorzman, A., Santos, C., Bash, R., Kafri, T., Carey, L., Miller, R., Perou, M. C., Sharpless, N., & Kafri, T. (2013). Pharmacokinetics and efficacy of PEGylated liposomal doxorubicin in an intracranial model of breast cancer. *PLoS ONE, 8*(5), Article # e61359.

Apel, C. L., Deamer, D. W., & Mautner, M. N. (2002). Self-assembled vesicles of monocarboxylic acids and alcohols: conditions for stability and for the encapsulation of biopolymers. *Biochimica et Biophysica Acta (BBA)-Biomembranes, 1559*(1), 1-9.

Arvaniti, E. C., Juenger, M. C., Bernal, S. A., Duchesne, J., Courard, L., Leroy, S., & De Belie, N. (2015). Determination of particle size, surface area, and shape of supplementary cementitious materials by different techniques. *Materials and Structures*, *48*(11), 3687-3701.

Aryal, S., Hu, C.-M. J., Fang, R. H., Dehaini, D., Carpenter, C., Zhang, D.-E., & Zhang, L. (2013). Erythrocyte membrane-cloaked polymeric nanoparticles for controlled drug loading and release. *Nanomedicine, 8*(8), 1271-1280.

Attwood, S., Choi, Y., & Leonenko, Z. (2013). Preparation of DOPC and DPPC supported planar lipid bilayers for atomic force microscopy and atomic force spectroscopy. *International Journal of Molecular Sciences*, *14*(2), 3514-3539.

Baban, D. F., & Seymour, L. W. (1998). Control of tumour vascular permeability. *Advanced Drug Delivery Reviews, 34*(1), 109-119.

Bagalkot, V., Deiuliis, J. A., Rajagopalan, S., & Maiseyeu, A. (2016). –Eat me" imaging and therapy. *Advanced Drug Delivery Reviews, 99*, 2-11.

Bagatolli, L. A., & Needham, D. (2014). Quantitative optical microscopy and micromanipulation studies on the lipid bilayer membranes of giant unilamellar vesicles. *Chemistry and Physics of Lipids*, *181*, 99-120.

Bagatolli, L., Gratton, E., Khan, T. K., & Chong, P. L.-G. (2000). Two-photon fluorescence microscopy studies of bipolar tetraether giant liposomes from thermoacidophilic archaebacteria sulfolobus acidocaldarius. *Biophysical Journal, 79*(1), 416-425.

Bakker, H. E., Dussi, S., Droste, B. L., Besseling, T. H., Kennedy, C. L., Wiegant, E. I., & van Blaaderen, A. (2016). Phase diagram of binary colloidal rod-sphere mixtures from a 3D real-space analysis of sedimentation–diffusion equilibria. *Soft Matter*, *12*(45), 9238-9245.

Balzus, B., Colombo, M., Sahle, F. F., Zoubari, G., Staufenbiel, S., & Bodmeier, R. (2016). Comparison of different in vitro release methods used to investigate nanocarriers intended for dermal application. *International Journal of Pharmaceutics*, *513*(1-2), 247-254.

Bally, M., Bailey, K., Sugihara, K., Grieshaber, D., Vörös, J., & Städler, B. (2010). Liposome and lipid bilayer arrays towards biosensing applications. *Small*, *6*(22), 2481-2497.

Bangham, A., Standish, M. M., & Watkins, J. C. (1965). Diffusion of univalent ions across the lamellae of swollen phospholipids. *Journal of Molecular Biology, 13*(1), 238-IN227.

Bao, G., Mitragotri, S., & Tong, S. (2013). Multifunctional nanoparticles for drug delivery and molecular imaging. *Annual Review of Biomedical Engineering, 15*, 253-282.

Bareford, L. M., & Swaan, P. W. (2007). Endocytic mechanisms for targeted drug delivery. *Advanced Drug Delivery Reviews, 59*(8), 748-758.

Barenholz, Y. C. (2016). Doxil®–the First FDA-approved Nano-drug: from Basics via CMC, Cell Culture and Animal Studies to Clinical Use. In *Nanomedicines,* 315-345.

Berger, N., Sachse, A., Bender, J., Schubert, R., & Brandl, M. (2001). Filter extrusion of liposomes using different devices: comparison of liposome size, encapsulation efficiency, and process characteristics. *International Journal of Pharmaceutics*, *223*(1-2), 55-68.

Bhateria, M., Rachumallu, R., Singh, R., & Bhatta, R. S. (2014). Erythrocytes-based synthetic delivery systems: transition from conventional to novel engineering strategies. *Expert Opinion on Drug Delivery, 11*(8), 1219-1236.

Bhattacharjee, S. (2016). DLS and zeta potential–what they are and what they are not? *Journal of Controlled Release*, *235*, 337-351.

Bhattarai, N., Gunn, J., & Zhang, M. (2010). Chitosan-based hydrogels for controlled, localized drug delivery. *Advanced Drug Delivery Reviews, 62*(1), 83-99.

Biagiotti, S., Paoletti, M. F., Fraternale, A., Rossi, L., & Magnani, M. (2011). Drug delivery by red blood cells. *IUBMB Life, 63*(8), 621-631.

Bibi, S., Kaur, R., Henriksen-Lacey, M., McNeil, S. E., Wilkhu, J., Lattmann, E., Christensen, D., Mohammed, A. R., & Perrie, Y. (2011). Microscopy imaging of liposomes: from coverslips to environmental SEM. *International Journal of Pharmaceutics, 417*(1-2), 138-150.

Bigdeli, A., Palchetti, S., Pozzi, D., Hormozi-Nezhad, M. R., Baldelli Bombelli, F., Caracciolo, G., & Mahmoudi, M. (2016). Exploring cellular interactions of liposomes using protein corona fingerprints and physicochemical properties. *ACS Nano, 10*(3), 3723-3737.

Biltonen, R. L., & Lichtenberg, D. (1993). The use of differential scanning calorimetry as a tool to characterize liposome preparations. *Chemistry and Physics of Lipids, 64*(1-3), 129-142.

Boyer, C., Whittaker, M. R., Bulmus, V., Liu, J., & Davis, T. P. (2010). The design and utility of polymer-stabilized iron-oxide nanoparticles for nanomedicine applications. *NPG Asia Materials, 2*(1), 23-30.

Bozzuto, G., & Molinari, A. (2015). Liposomes as nanomedical devices. *International Journal of Nanomedicine*, *10*, 975.

Brannon-Peppas, L. (1995). Recent advances on the use of biodegradable microparticles and nanoparticles in controlled drug delivery. *International Journal of Pharmaceutics, 116*(1), 1-9.

Brannon-Peppas, L., & Blanchette, J. O. (2012). Nanoparticle and targeted systems for cancer therapy. *Advanced Drug Delivery Reviews, 64*, 206-212.

Bretscher, M. S. (1972). Phosphatidyl-ethanolamine: differential labelling in intact cells and cell ghosts of human erythrocytes by a membrane-impermeable reagent. *Journal of Molecular Biology, 71*(3), 523-528.

Brigger, I., Dubernet, C., & Couvreur, P. (2002). Nanoparticles in cancer therapy and diagnosis. *Advanced Drug Delivery Reviews, 54*(5), 631-651.

Brown, B. S., Patanam, T., Mobli, K., Celia, C., Zage, P. E., Bean, A. J., & Tasciotti, E. (2014). Etoposide-loaded immunoliposomes as active targeting agents for GD2-positive malignancies. *Cancer Biology & Therapy, 15*(7), 851-861.

Brown, R., & Links, M. (1999). Clinical relevance of the molecular mechanisms of resistance to anti-cancer drugs. *Expert Reviews in Molecular Medicine, 1*(15), 1-21.

Bunjes, H., & Kuntsche, J. (2016). Light and electron microscopy. In *Analytical Techniques in the Pharmaceutical Sciences* (pp. 491-522). Springer, New York, NY.

Carboni, E., Tschudi, K., Nam, J., Lu, X., & Ma, A. W. (2014). Particle margination and its implications on intravenous anticancer drug delivery. *American Association of Pharmaceutical Sciences, 15*(3), 762-771.

Casadó, A., Giuffrida, M. C., Sagristá, M. L., Castelli, F., Pujol, M., Alsina, M. A., & Mora, M. (2016). Langmuir monolayers and Differential Scanning Calorimetry for the study of the interactions between camptothecin drugs and biomembrane models. *Biochimica et Biophysica Acta (BBA)-Biomembranes*, *1858*(2), 422-433.

Chang, H.-I., & Yeh, M.-K. (2012). Clinical development of liposome-based drugs: formulation, characterization, and therapeutic efficacy. *International Journal of Nanomedicine, 7*(4), 49-60.

Choudhary, G. S., Al-Harbi, S., Mazumder, S., Hill, B. T., Smith, M. R., Bodo, J., His, E. D., & Almasan, A. (2015). MCL-1 and BCL-xL-dependent resistance to the BCL-2 inhibitor ABT-199 can be overcome by preventing PI3K/AKT/mTOR activation in lymphoid malignancies. *Cell Death & Disease*, *6*(1), Articl # e1593.

Chaudhary, S., Garg, T., Rath, G., Murthy, R. R., & Goyal, A. K. (2016). Enhancing the bioavailability of mebendazole by integrating the principles solid dispersion and nanocrystal techniques, for safe and effective management of human echinococcosis. *Artificial Cells, Nanomedicine, and Biotechnology, 44*(3), 937-942.

Chaw, C. S., & Ah Kim, K. Y. (2013). Effect of formulation compositions on niosomal preparations. *Pharmaceutical Development and Technology, 18*(3), 667-672.

Chen, J., Lu, W.-L., Gu, W., Lu, S.-S., Chen, Z.-P., Cai, B.-C., & Yang, X.-X. (2014). Drug-in-cyclodextrin-in-liposomes: a promising delivery system for hydrophobic drugs. *Expert Opinion in Drug Delivery, 11*(4), 565-577.

Chen, W., & Du, J. (2013). Ultrasound and pH dually responsive polymer vesicles for anticancer drug delivery. *Scientific Reports, 3*, 2162.

Chevalier, G., Sinatra, S. T., Oschman, J. L., & Delany, R. M. (2013). Earthing (grounding) the human body reduces blood viscosity-a major factor in cardiovascular disease. *The Journal of Alternative and Complementary Medicine, 19*(2), 102-110.

Chu, K. S., Schorzman, A. N., Finniss, M. C., Bowerman, C. J., Peng, L., Luft, J. C., Madden, A. J., Wang, A. Z., Zamboni, W. C., & DeSimone, J. M. (2013). Nanoparticle drug loading as a design parameter to improve docetaxel pharmacokinetics and efficacy. *Biomaterials, 34*(33), 8424-8429.

Chu, Z., Dreiss, C. A., & Feng, Y. (2013). Smart wormlike micelles. *Chemical Society Reviews, 42*(17), 7174-7203.

Cipolla, D., Wu, H., Eastman, S., Redelmeier, T., Gonda, I., & Chan, H. K. (2014). Development and characterization of an in vitro release assay for liposomal ciprofloxacin for inhalation. *Journal of Pharmaceutical Sciences, 103*(1), 314-327.

Cole, M. A., Voelcker, N. H., Thissen, H., & Griesser, H. J. (2009). Stimuli-responsive interfaces and systems for the control of protein-surface and cell-surface interactions. *Biomaterials, 30*(9), 1827-1850.

Crommelin, D. J. (1984). Influence of lipid composition and ionic strength on the physical stability of liposomes. *Journal of Pharmaceutical Sciences, 73*(11), 1559-1563.

Da Silva Malheiros, P., Daroit, D. J., & Brandelli, A. (2010). Food applications of liposome-encapsulated antimicrobial peptides. *Trends in Food Science & Technology, 21*(6), 284-292.

Dai, W., Yang, F., Ma, L., Fan, Y., He, B., He, Q., Wang, X., Zhang, H., & Zhang, Q. (2014). Combined mTOR inhibitor rapamycin and doxorubicin-loaded cyclic octapeptide modified liposomes for targeting integrin α3 in triple-negative breast cancer. *Biomaterials, 35*(20), 5347-5358.

Daraee, H., Etemadi, A., Kouhi, M., Alimirzalu, S., & Akbarzadeh, A. (2016). Application of liposomes in medicine and drug delivery. *Artificial Cells, Nanomedicine, and Biotechnology, 44*(1), 381-391.

Dash, S., Murthy, P. N., Nath, L., & Chowdhury, P. (2010). Kinetic modeling on drug release from controlled drug delivery systems. *Acta Poloniae Pharmaceutica, 67*(3), 217-223.

Da Silva, C. B., Groppo, F. C., Dos Santos, C. P., Serpe, L., Franz-Montan, M., de Paula, E., & Volpato, M. C. (2016). Anaesthetic efficacy of unilamellar and multilamellar liposomal formulations of articaine in inflamed and uninflamed tissue. *British Journal of Oral and Maxillofacial Surgery*, *54*(3), 295-300.

Dawidczyk, C. M., Kim, C., Park, J. H., Russell, L. M., Lee, K. H., Pomper, M. G., & Searson, P. C. (2014). State-of-the-art in design rules for drug delivery platforms: lessons learned from FDA-approved nanomedicines. *Journal of Controlled Release, 187*, 133-144.

Deamer, D., & Bangham, A. D. (1976). Large volume liposomes by an ether vaporization method. *Biochimica et Biophysica Acta (BBA)-Nucleic Acids and Protein Synthesis*, *443*(3), 629-634.

Deng, C., Zhang, Q., Fu, Y., Sun, X., Gong, T., & Zhang, Z. (2017). Coadministration of oligomeric hyaluronic acid modified liposomes with tumor penetrating peptide-iRGD enhances the antitumor efficacy of doxorubicin against melanoma. *ACS Applied Material & Interfaces*, *9*(2), 1280-1292.

Dhand, C., Prabhakaran, M. P., Beuerman, R. W., Lakshminarayanan, R., Dwivedi, N., & Ramakrishna, S. (2014). Role of size of drug delivery carriers for pulmonary

and intravenous administration with emphasis on cancer therapeutics and lung-targeted drug delivery. *RSC Advances, 4*(62), 32673-32689.

Discher, D., Mohandas, N., & Evans, E. (1994). Molecular maps of red cell deformation: hidden elasticity and in situ connectivity. *Science, 266*(5187), 1032-1035.

Domínguez, A., Fernández, A., González, N., Iglesias, E., & Montenegro, L. (1997). Determination of critical micelle concentration of some surfactants by three techniques. *Journal of Chemical Education, 74*(10), 1227.

Dondelinger, Y., Declercq, W., Montessuit, S., Roelandt, R., Goncalves, A., Bruggeman, I., Hulpiau, P., Weber, K., Sehon, C. A., Marquis, R. B., Bertin, J., Gough, P. J., Savvides, S., Martinou, J. C., Mertrand, M. J. M., & Vandenabeele P. (2014). MLKL compromises plasma membrane integrity by binding to phosphatidylinositol phosphates. *Cell Reports*, *7*(4), 971-981.

Doshi, N., & Mitragotri, S. (2010). Needle-shaped polymeric particles induce transient disruption of cell membranes. *Journal of the Royal Society Interface*, *7*(suppl_4), S403-S410.

Doshi, N., Zahr, A. S., Bhaskar, S., Lahann, J., & Mitragotri, S. (2009). Red blood cell-mimicking synthetic biomaterial particles. *Proceedings of National Academy of United States of America, 106*(51), 21495-21499.

Dousset, N., Dousset, J.-C., & Douste-Blazy, L. (1981). Influence of dicarboxylic phosphatidylcholines on the stability and phase transition of phosphatidylcholine liposomes. *Biochimica et Biophysica Acta (BBA)-Biomembranes, 641*(1), 1-10.

Drummond, D. C., Meyer, O., Hong, K., Kirpotin, D. B., & Papahadjopoulos, D. (1999). Optimizing liposomes for delivery of chemotherapeutic agents to solid tumors. *Pharmacological Reviews, 51*(4), 691-744.

Duncan, R. (2006). Polymer conjugates as anticancer nanomedicines. *Nature Reviews Cancer, 6*(9), 688-701.

Durymanov, M. O., Yarutkin, A. V., Bagrov, D. V., Klinov, D. V., Kedrov, A. V., Chemeris, N. K., Rosenkranz, A. A., & Sobolev, A. S. (2016). Application of vasoactive and matrix-modifying drugs can improve polyplex delivery to tumors upon intravenous administration. *Journal of Controlled Release*, *232,* 20-28.

Eberhard, A., Kahlert, S., Goede, V., Hemmerlein, B., Plate, K. H., & Augustin, H. G.(2000). Heterogeneity of angiogenesis and blood vessel maturation in human tumors: implications for antiangiogenic tumor therapies. *Cancer Research, 60*(5), 1388-1393.

Edwards, K. A., & Baeumner, A. J. (2006). Analysis of liposomes. *Talanta*, *68*(5), 1432-1441.

El-Far, S. W., Helmy, M. W., Khattab, S. N., Bekhit, A. A., Hussein, A. A., & Elzoghby, A. O. (2018). Phytosomal bilayer-enveloped casein micelles for codelivery of monascus yellow pigments and resveratrol to breast cancer. *Nanomedicine, 13*(5), 481-499.

Elmowafy, M., Viitala, T., Ibrahim, H. M., Abu-Elyazid, S. K., Samy, A., Kassem, A., & Yliperttula, M. (2013). Silymarin loaded liposomes for hepatic targeting: in vitro evaluation and $HepG_2$ drug uptake. *European Journal of Pharmaceutical Sciences, 50*(2), 161-171.

Evans, D. F., & Ninham, B. (1983). Ion binding and the hydrophobic effect. *The Journal of Physical Chemistry, 87*(24), 5025-5032.

Kind, M. (2000). The Colloidal Domain: Where Physics, Chemistry, Biology, and Technology Meet by D. Fennell Evans and Hakan Wennerstrom, Wiley-VCH, 1999, ISBN 0-471-24247-0;@ $58.50, Hardback, 632 pp., more than 250 figures, several tables. *Chemical Engineering & Processing: Process Intensification*, *6*(39), 549.

Fang, R. H., Hu, C. M., Chen, K. N., Luk, B. T., Carpenter, C. W., Gao, W., shulin Li., Zhang, D., Weiyue, Lu., & Zhang, L. (2013). Lipid-insertion enables targeting functionalization of erythrocyte membrane-cloaked nanoparticles. *Nanoscale, 5*(19), 8884-8888.

Fang, R. H., Hu, C.-M. J., Luk, B. T., Gao, W., Copp, J. A., Tai, Y., O'Connor, D. E., & Zhang, L. (2014). Cancer cell membrane-coated nanoparticles for anticancer vaccination and drug delivery. *Nano Letters, 14*(4), 2181-2188.

Fathi, S., & Oyelere, A. K. (2016). Liposomal drug delivery systems for targeted cancer therapy: is active targeting the best choice? *Future Medicinal Chemistry, 8*(17), 2091-2112.

Felnerova, D., Viret, J.-F., Glück, R., & Moser, C. (2004). Liposomes and virosomes as delivery systems for antigens, nucleic acids and drugs. *Current Opinion in Biotechnology, 15*(6), 518-529.

Feng, L., Gao, M., Tao, D., Chen, Q., Wang, H., Dong, Z., Chen, M., & Liu, Z. (2016). Cisplatin-Prodrug-Constructed Liposomes as a versatile theranostic nanoplatform for bimodal imaging guided combination cancer therapy. *Advanced Functional Materials, 26*(13), 2207-2217.

Feng, S.-s., & Huang, G. (2001). Effects of emulsifiers on the controlled release of paclitaxel (Taxol®) from nanospheres of biodegradable polymers. *Journal of Controlled Release, 71*(1), 53-69.

Fennell Evans, D., Wennerstrom, H., & Rajagopalan, R. (1995). The colloidal domain: where physics, chemistry, biology, and technology meet. *Journal of Colloid and Interface Science*, *172*(2), 541-541.

Filipović, M., Lukić, M., Krstonošić, V., Đorđević, S., Pantelić, I., Gledović, A., Vuleta, G., & Savić, S. (2016). Feasibility of a natural surfactant as a stabilizer for cosmetics with liposome-encapsulated plant stem cells: pre-formulation and formulation through stability studies. *Tenside Surfactants Detergents, 53*(3), 214-226.

Fontes, A., Fernandes, H. P., Barjas-Castro, M. L., de Thomaz, A. A., de Ysasa Pozzo, L., Barbosa, L. C., & Cesar, C. L. (2006, February). Red blood cell membrane viscoelasticity, agglutination, and zeta potential measurements with double optical tweezers. In *Imaging, Manipulation, and Analysis of Biomolecules, Cells, and Tissues IV* (Vol. 6088, p. 608811). International Society for Optics and Photonics.

Fox, C. B., Moutaftsi, M., Vergara, J., Desbien, A. L., Nana, G. I., Vedvick, T. S., Coler, R. N., & Reed, S. G. (2013). TLR4 ligand formulation causes distinct effects on antigen-specific cell-mediated and humoral immune responses. *Vaccine, 31*(49), 5848-5855.

Franssen, E. J., Koiter, J., Kuipers, C. A., Bruins, A. P., Moolenaar, F., De Zeeuw, D., & Meijer, D. K. (1992). Low-molecular-weight proteins as carriers for renal drug targeting. Preparation of drug-protein conjugates and drug-spacer derivatives and their catabolism in renal cortex homogenates and lysosomal lysates. *Journal of Medicinal Chemistry, 35*(7), 1246-1259.

Fröhlich, E. (2012). The role of surface charge in cellular uptake and cytotoxicity of medical nanoparticles. *International Journal of Nanomedicine, 7*, 5577-5591.

Fu, Q., Lv, P., Chen, Z., Ni, D., Zhang, L., Yue, H., Yue, Z., Wei, W., & Ma, G.-H. (2015). Programmed Co-delivery of Paclitaxel and Doxorubicin Boosted by Camouflaging with Erythrocyte Membrane. *Nanoscale*, *7*(9), 4020-4030.

Gao, W., & Zhang, L. (2015). Engineering red blood cell membrane-coated nanoparticles for broad biomedical applications. *AIChE Journal*, *61*(3), 738-746.

Garg, T., & K. Goyal, A. (2014). Liposomes: targeted and controlled delivery system. *Drug Delivery Letters, 4*(1), 62-71.

Garín, M.-I., López, R.-M., Sanz, S., Pinilla, M., & Luque, J. (1996). Erythrocytes as carriers for recombinant human erythropoietin. *Pharmaceutical Research, 13*(6), 869-874.

Geng, Y., Dalhaimer, P., Cai, S., Tsai, R., Tewari, M., Minko, T., & Discher, D. E. (2007). Shape effects of filaments versus spherical particles in flow and drug delivery. *Nature Nanotechnology, 2*(4), 249-255.

Gey, G. (1952). Tissue culture studies of the proliferative capacity of cervical carcinoma and normal epithelium. *Cancer Research.*, *12*, 264-265.

Gomez-Hens, A., & Fernandez-Romero, J. (2006). Analytical methods for the control of liposomal delivery systems. *TrAC Trends in Analytical Chemistry, 25*(2), 167-178.

Gordesky, S. E., Marinetti, G., & Love, R. (1975). The reaction of chemical probes with the erythrocyte membrane. *The Journal of Membrane Biology, 20*(1), 111-132.

Gref, R., Domb, A., Quellec, P., Blunk, T., Müller, R., Verbavatz, J., & Langer, R. (2012). The controlled intravenous delivery of drugs using PEG-coated sterically stabilized nanospheres. *Advanced Drug Delivery Reviews, 64*, 316-326.

Grit, M., & Crommelin, D. J. (1993). Chemical stability of liposomes: implications for their physical stability. *Chemistry of Physics and Lipids, 64*(1-3), 3-18.

Grumezescu, V., Socol, G., Grumezescu, A. M., Holban, A. M., Ficai, A., Truşcă, R., Bleotue, C., Balaure, P. C., Cristescu, R., & Chifiriuc, M. C. (2014). Functionalized antibiofilm thin coatings based on PLA–PVA microspheres loaded with usnic acid natural compounds fabricated by MAPLE. *Applied Surface Science*, *302*, 262-267.

Grumezescu, A. M., Andronescu, E., Oprea, A. E., Holban, A. M., Socol, G., Grumezescu, V., & Maniu, H. (2015). MAPLE fabricated magnetite@ Melissa officinalis and poly lactic acid: chitosan coated surfaces with anti-staphylococcal properties. *Journal of Sol-Gel Science and Technology*, *73*(3), 612-619.

Gui, R., Wang, Y., & Sun, J. (2014). Encapsulating magnetic and fluorescent mesoporous silica into thermosensitive chitosan microspheres for cell imaging and controlled drug release in vitro. *Colloids and Surfaces B: Biointerfaces, 113*, 1-9.

Guo, P., Yang, J., Di Jia, M. A. M., & Auguste, D. T. (2016). ICAM-1-Targeted, Lcn2 siRNA-Encapsulating Liposomes are Potent Anti-angiogenic Agents for Triple Negative Breast Cancer. *Theranostics, 6*(1), 1.

Hajizade, A., Ebrahimi, F., Salmanian, A.-H., Arpanae, A., & Amani, J. (2015). Nanoparticles in Vaccine Development. *Journal of Applied Biotechnology Reports, 1*(4), 125-134.

Haley, B., & Frenkel, E. (2008, January). Nanoparticles for drug delivery in cancer treatment. *Urologic Oncology: Seminars and Original Investigations*, *26*(1), 57-64.

Halwani, M., Hossain, Z., Khiyami, M. A., & Omri, A. (2015). Liposomal [Beta]-Glucan: Preparation, Characterization and Anticancer Activities. *Journal of Nanomedicine & Nanotechnology, 6*(5), 7.

Han, H. D., Jeon, Y. W., Kwon, H. J., Jeon, H. N., Byeon, Y., Lee, C. O., Cho, S. H., & Shin, B. C. (2015). Therapeutic efficacy of doxorubicin delivery by a CO 2 generating liposomal platform in breast carcinoma. *Acta Biomaterialia, 24*, 279-285.

Han, Y., Wang, X., Dai, H., & Li, S. (2012). Nanosize and surface charge effects of hydroxyapatite nanoparticles on red blood cell suspensions. *ACS Appied Material and Interfaces, 4*(9), 4616-4622.

Hanke, W. (1978). The adrenal cortex of Amphibia. In *General, Comparative and Clinical Endocrinology of the Adrenal Cortex* (pp. 419-495). Academic Press.

He, H., Li, Y., Jia, X.-R., Du, J., Ying, X., Lu, W.-L., Lou, J-N., & Wei, Y. (2011). PEGylated Poly (amidoamine) dendrimer-based dual-targeting carrier for treating brain tumors. *Biomaterials, 32*(2), 478-487.

Honary, S., & Zahir, F. (2013). Effect of zeta potential on the properties of nano-drug delivery systems-a review (Part 1). *Tropical Journal of Pharmaceutical Research, 12*(2), 255-264.

Holliday, D. L., & Speirs, V. (2011). Choosing the right cell line for breast cancer research. *Breast Cancer Research, 13*(4), 215.

Holthoff, H., Egelhaaf, S. U., Borkovec, M., Schurtenberger, P., & Sticher, H. (1996). Coagulation rate measurements of colloidal particles by simultaneous static and dynamic light scattering. *Langmuir*, *12*(23), 5541-5549.

Hsin-I, C., Ming-Yen, C., & Ming-Kung, Y. (2012). Clinically-proven liposome-based drug delivery: formulation, characterization and therapeutic efficacy. *Scientific. Reports, 1*(3), 1-8.

Hosseini, H., Li, Y., Kanellakis, P., Tay, C., Cao, A., Tipping, P., Bobik, A., Yoh, B. H., & Kyaw, T. (2015). Phosphatidylserine liposomes mimic apoptotic cells to attenuate atherosclerosis by expanding polyreactive IgM producing B1a lymphocytes. *Cardiovascular Research*, *106*(3), 443-452.

Hu, C.-M. J., Zhang, L., Aryal, S., Cheung, C., Fang, R. H., & Zhang, L. (2011). Erythrocyte membrane-camouflaged polymeric nanoparticles as a biomimetic delivery platform. *Proceedings of the National Academy of Sciences, 108*(27), 10980-10985.

Iman, M., Huang, Z., Alavizadeh, S. H., Szoka, F. C., & Jaafari, M. R. (2017). Biodistribution and in vivo antileishmanial activity of 1, 2-distigmasterylhemisuccinoyl-sn-glycero-3-phosphocholine liposome intercalated amphotericin B. *Antimicrobial Agents and Chemotherapy*, *61*(9), 2525-16.

Ishida, T., Jo, T., Takemoto, S., Suzushima, H., Uozumi, K., Yamamoto, K., ... & Tobinai, K. (2015). Dose-intensified chemotherapy alone or in combination with mogamulizumab in newly diagnosed aggressive adult T-cell leukaemia-lymphoma: a randomized phase II study. *British Journal of Haematology*, *169*(5), 672-682.

Ishida, T., Maeda, R., Ichihara, M., Irimura, K., & Kiwada, H. (2003). Accelerated clearance of PEGylated liposomes in rats after repeated injections. *Journal of Controlled Release, 88*(1), 35-42.

Jain, A. S., Goel, P. N., Shah, S. M., Dhawan, V. V., Nikam, Y., Gude, R. P., & Nagarsenker, M. S. (2014). Tamoxifen guided liposomes for targeting encapsulated anticancer agent to estrogen receptor positive breast cancer cells: In vitro and in vivo evaluation. *Biomedicine & Pharmacotherapy, 68*(4), 429-438.

Jain, A., & Jain, S. K. (2016). In vitro release kinetics model fitting of liposomes: An insight. *Chemistry of Physics and Lipids, 201*, 28-40.

Jain, R. K. (2001). Delivery of molecular and cellular medicine to solid tumors. *Advanced Drug Delivery Reviews, 46*(1), 149-168.

Jang, S. H., Wientjes, M. G., Lu, D., & Au, J. L.-S. (2003). Drug delivery and transport to solid tumors. *Pharmaceutical Research, 20*(9), 1337-1350.

Ji, X., Shi, C., Qi, L., Guo, Y., Li, N., Li, Z., & Luan, Y. (2014). Preparation, properties and in vivo pharmacokinetic study of drug vesicles composed of diphenhydramine and AOT. *RSC Advances, 4*(107), 62698-62707.

Jordheim, L. P., Durantel, D., Zoulim, F., & Dumontet, C. (2013). Advances in the development of nucleoside and nucleotide analogues for cancer and viral diseases. *Nature Reviews Drug Discovery, 12*(6), 447-464.

Joyce, J. A., & Fearon, D. T. (2015). T cell exclusion, immune privilege, and the tumor microenvironment. *Science, 348*(6230), 74-80.

Kanapathipillai, M., Brock, A., & Ingber, D. E. (2014). Nanoparticle targeting of anti-cancer drugs that alter intracellular signaling or influence the tumor microenvironment. *Advanced Drug Delivery Reviews, 79*, 107-118.

Kaoui, B., Biros, G., & Misbah, C. (2009). Why do red blood cells have asymmetric shapes even in a symmetric flow? *Physical Review Letters, 103*(18), 188101.

Karavas, E., Georgarakis, E., Sigalas, M. P., Avgoustakis, K., & Bikiaris, D. (2007). Investigation of the release mechanism of a sparingly water-soluble drug from solid dispersions in hydrophilic carriers based on physical state of drug, particle size distribution and drug–polymer interactions. *European Journal of Pharmaceutics and Biopharmaceutics, 66*(3), 334-347.

Kaushik, A., & Sharma, H. K. (2018). *In-vitro* and in vivo studies of cetuximab loaded polymeric nanoparticles. *Journal of Drug Delivery and Therapeutics*, *8*(5-S), 184-188.

Keefe, A. J., & Jiang, S. (2012). Poly (zwitterionic) protein conjugates offer increased stability without sacrificing binding affinity or bioactivity. *Nature Chemistry, 4*(1), 59-63.

Key, T. J., Verkasalo, P. K., & Banks, E. (2001). Epidemiology of breast cancer. *The Lancet Oncology, 2*(3), 133-140.

Khoshneviszadeh, R., Bazzaz, B. S. F., Housaindokht, M. R., Ebrahim-Habibi, A., & Rajabi, O. (2016). A Comparison of Explanation Methods of Encapsulation Efficacy of Hydroquinone in a Liposomal System. *Journal of Paramedical Sciences*, *7*(2), 23-28.

Khosravi-Darani, K., Pardakhty, A., Honarpisheh, H., Rao, V. M., & Mozafari, M. R. (2007). The role of high-resolution imaging in the evaluation of nanosystems for bioactive encapsulation and targeted nanotherapy. *Micron, 38*(8), 804-818.

Kieler-Ferguson, H. M., Chan, D., Sockolosky, J., Finney, L., Maxey, E., Vogt, S., & Szoka, F. C. (2017). Encapsulation, controlled release, and antitumor efficacy of cisplatin delivered in liposomes composed of sterol-modified phospholipids. *European Journal of Pharmaceutical Sciences*, *103*, 85-93.

Knopp, M. M., Löbmann, K., Elder, D. P., Rades, T., & Holm, R. (2016). Recent advances and potential applications of modulated differential scanning calorimetry (mDSC) in drug development. *European Journal of Pharmaceutical Sciences*, *87*, 164-173.

Kirch, J., Guenther, M., Doshi, N., Schaefer, U. F., Schneider, M., Mitragotri, S., & Lehr, C.-M. (2012). Mucociliary clearance of micro-and nanoparticles is independent of size, shape and charge—an ex vivo and in silico approach. *Journal of Controlled Release, 159*(1), 128-134.

Kozovska, Z., Gabrisova, V., & Kucerova, L. (2014). Colon cancer: Cancer stem cells markers, drug resistance and treatment. *Biomedicine & Pharmacotherapy, 68*(8), 911-916.

Kraft, J. C., Freeling, J. P., Wang, Z., & Ho, R. J. (2014). Emerging research and clinical development trends of liposome and lipid nanoparticle drug delivery systems. *Journal of Pharmaceutical Sciences, 103*(1), 29-52.

Kumar, B. S., & Bhat, K. I. (2011). In-vitro cytotoxic activity studies of clitoria ternatea linn flower extracts. *International Journal of Pharmaceutical Sciences Review & Research, 6*, 120-121.

Kume, Y., Maeda, F., Harashima, H., & Kiwada, H. (1991). Saturable, Non-Michaelis-Menten Uptake of Liposomes by the Reticuloendothelial System. *Journal of Pharmacy and Pharmacology*, *43*(3), 162-166.

Laouini, A., Jaafar-Maalej, C., Limayem-Blouza, I., Sfar, S., Charcosset, C., & Fessi, H. (2012). Preparation, characterization and applications of liposomes: state of the art. *Journal of colloid Science and Biotechnology*, *1*(2), 147-168.

Lange, L. G., & Sobel, B. E. (1983). Mitochondrial dysfunction induced by fatty acid ethyl esters, myocardial metabolites of ethanol. *The Journal of Clinical Investigation*, *72*(2), 724-731.

Laouini, A., Jaafar-Maalej, C., Limayem-Blouza, I., Sfar, S., Charcosset, C., & Fessi, H. (2012). Preparation, characterization and applications of liposomes: state of the art. *Journal of Colloid Science and Biotechnology, 1*(2), 147-168.

Lasic, D. (1990). On the thermodynamic stability of liposomes. *Journal of Colloid and Interface Science, 140*(1), 302-304.

Lasic, D. D. (1988). The spontaneous formation of unilamellar vesiscles. *Journal of Colloid and Interface Science, 124*(2), 428-435.

Lee, C. C., MacKay, J. A., Fréchet, J. M., & Szoka, F. C. (2005). Designing dendrimers for biological applications. *Nature Biotechnology, 23*(12), 1517-1526.

Lee, H.-S., Lee, N. C., Kouprina, N., Kim, J.-H., Kagansky, A., Bates, S., Trepel, J. B., Pommier, Y., Sackett, D., & Larionov, V. (2016). Effects of Anticancer Drugs on Chromosome Instability and New Clinical Implications for Tumor-Suppressing Therapies. *Cancer Research, 76*(4), 902-911.

Lejeune, A., Moorjani, M., Gicquaud, C., Lacroix, J., Poyet, P., & Gaudreault, R. (1993). Nanoerythrosome, a new derivative of erythrocyte ghost: preparation and antineoplastic potential as drug carrier for daunorubicin. *Anticancer Research, 14*(3A), 915-919.

Lejeune, F. J., Rüegg, C., & Liénard, D. (1998). Clinical applications of TNF-α in cancer. *Current Opinion in Immunology, 10*(5), 573-580.

Leventis, P. A., & Grinstein, S. (2010). The distribution and function of phosphatidylserine in cellular membranes. *Annual Review of Biophysics, 39*, 407-427.

Liang, C.-H., Yeh, L.-H., Liao, P.-W., & Chou, T.-H. (2015). Characterization and in vitro biocompatibility of catanionic assemblies formed with oppositely charged dicetyl amphiphiles. *Colloids and Surfaces B: Biointerfaces, 126*, 10-17.

Li, R.-J., Ying, X., Zhang, Y., Ju, R.-J., Wang, X.-X., Yao, H.-J., Men, Y., Tian, W., Yu, Y., Zhang, L., Huang R-J., & Zhang, L. (2011). All-trans retinoic acid stealth liposomes prevent the relapse of breast cancer arising from the cancer stem cells. *Journal of Controlled Release, 149*(3), 281-291.

Li, X., Rao, X., Cai, L., Liu, X., Wang, H., Wu, W., Zhu, C., Chen, M., Wang, P. G., & Yi, W. (2016). Targeting Tumor Cells by Natural Anti-Carbohydrate Antibodies Using Rhamnose-Functionalized Liposomes. *ACS Chemical Biology, 11(5), 1205-1209.*

Li, Y., Lin, J., Yang, X., Li, Y., Wu, S., Huang, Y., Ye, S., Xie, L., Dai, L., & Hou, Z. (2015). Self-Assembled Nanoparticles Based on Amphiphilic Anticancer Drug–Phospholipid Complex for Targeted Drug Delivery and Intracellular Dual-Controlled Release. *ACS Applied Material and Interfaces, 7*(32), 17573-17581.

Liu, Z., Xiong, M., Gong, J., Zhang, Y., Bai, N., Luo, Y., & Xiang, R. (2014). Legumain protease-activated TAT-liposome cargo for targeting tumours and their microenvironment. *Nature Communications*, *5*, 4280-4295.

Lodish, H., Berk, A., Zipursky, S. L., Matsudaira, P., Baltimore, D., & Darnell, J. (2000). Molecular cell biology 4th edition. *National Center for Biotechnology Information, Bookshelf*.

Longmire, M., Choyke, P. L., & Kobayashi, H. (2008). Clearance properties of nano-sized particles and molecules as imaging agents: considerations and caveats, *Future Medicine*, *3*(5) 703-717.

Lu, T., Wang, Z., Ma, Y., Zhang, Y., & Chen, T. (2012). Influence of polymer size, liposomal composition, surface charge, and temperature on the permeability of pH-sensitive liposomes containing lipid-anchored poly(2-ethylacrylic acid). *International Journal of Nanomedicine, 7*, 4917-4926.

Lynch, W. E., Sartiano, G. P., & Ghaffar, A. (1980). Erythrocytes as carriers of chemotherapeutic agents for targeting the reticuloendothelial system. *American Journal of Hematology, 9*(3), 249-259.

Manconi, M., Mura, S., Sinico, C., Fadda, A. M., Vila, A. O., & Molina, F. (2009). Development and characterization of liposomes containing glycols as carriers for diclofenac. *Colloids and Surfaces A: Physicochemical and Engineering Aspects*, *342*(1-3), 53-58.

Maeda, H. (2010). Tumor-selective delivery of macromolecular drugs via the EPR effect: background and future prospects. *Bioconjugate Chemistry, 21*(5), 797-802.

Maleknia, L., & Majdi, Z. R. (2014). Electrospinning of Gelatin Nanofiber for biomedical Application. *Oriental Journal of Chemistry, 30*(4), 2043-2048.

Markman, J. L., Rekechenetskiy, A., Holler, E., & Ljubimova, J. Y. (2013). Nanomedicine therapeutic approaches to overcome cancer drug resistance. *Advanced Drug Delivery Reviews, 65*(13-14), 1866-1879.

Matthews, J. R., Payne, C. M., & Hafner, J. H. (2015). Analysis of phospholipid bilayers on gold nanorods by plasmon resonance sensing and surface-enhanced raman scattering. *Langmuir*, *31*(36), 9893-9900.

McDougall, S. R., Anderson, A. R., & Chaplain, M. A. (2006). Mathematical modelling of dynamic adaptive tumour-induced angiogenesis: clinical implications and therapeutic targeting strategies. *Journal of Theoretical Biology, 241*(3), 564-589.

McNamara, R. K., Jandacek, R., Rider, T., Tso, P., Dwivedi, Y., & Pandey, G. N. (2010). Selective deficits in erythrocyte docosahexaenoic acid composition in adult patients with bipolar disorder and major depressive disorder. *Journal of Affective Disorders, 126*(1), 303-311.

Metaxa, A.-F., Efthimiadou, E. K., & Kordas, G. (2014). Cellulose-based drug carriers for cancer therapy: Cytotoxic evaluation in cancer and healthy cells. *Materials Letters, 132*, 432-435.

Meyer, O. (1998). Cationic liposomes coated with polyethylene glycol as carriers for oligonucleotides. *Journal of Biological Chemistry, 273*(25), 15621-15627.

Millan, C. G., Marinero, M. a. L. S., Castaneda, A. Z., & Lanao, J. M. (2004). Drug, enzyme and peptide delivery using erythrocytes as carriers. *Journal of Controlled Release, 95*(1), 27-49.

Mitragotri, S., & Lahann, J. (2009). Physical approaches to biomaterial design. *Nature Materials, 8*(1), 15-23.

Mitragotri, S., & Stayton, P. (2014). Organic nanoparticles for drug delivery and imaging. *MRS Bulletin, 39*(03), 219-223.

Moghimi, S. M., Hunter, A. C., & Murray, J. C. (2001). Long-circulating and target-specific nanoparticles: Theory to practice. *Pharmacol Reviews, 53*(2), 283-318.

Mohan, P., & Rapoport, N. (2010). Doxorubicin as a molecular nanotheranostic agent: effect of doxorubicin encapsulation in micelles or nanoemulsions on the ultrasound-mediated intracellular delivery and nuclear trafficking. *Molecular Pharmaceutics, 7*(6), 1959-1973.

Mohandas, N. A. R. L. A., & Chasis, J. A. (1993, July). Red blood cell deformability, membrane material properties and shape: regulation by transmembrane, skeletal and cytosolic proteins and lipids. *Seminars in Hematology*, *30(3),* 171-192.

Mohandas, N., & Gallagher, P. G. (2008). Red cell membrane: past, present, and future. *Blood, 112*(10), 3939-3948.

Moser, C., Metcalfe, I. C., & Viret, J.-F. (2003). Virosomal adjuvanted antigen delivery systems. *Expert Review of Vaccines*, *2*(2), 189-196.

Mousa, S. A., Chidlowsky, E., Bawarski, W. E., & Bharali, D. J. (2017). Emerging Nanopharmaceuticals. In *Nanomedicine in Cancer* (pp. 125-154). Pan Stanford.

Muro, S., Garnacho, C., Champion, J. A., Leferovich, J., Gajewski, C., Schuchman, E. H., Muzykantov, V. R. (2008). Control of endothelial targeting and intracellular delivery of therapeutic enzymes by modulating the size and shape of ICAM-1-targeted carriers. *Molecular Therapy, 16*(8), 1450-1458.

Muzykantov, V. R. (2010). Drug delivery by red blood cells: vascular carriers designed by mother nature. *Expert Opinion on Drug Delivery, 7*(4), 403-427.

Muzykantov, V. R. (2013). Drug delivery carriers on the fringes: natural red blood cells versus synthetic multilayered capsules. *Expert Opinion on Drug Delivery, 10*(1), 1-4.

Naeem, S., Kiew, L. V., Chung, L. Y., Suk, V. R. E., Mahmood, A., & Misran, M. B. (2016). Optimization of phospholipid nanoparticle formulations using response surface methodology. *Journal of Surfactants and Detergents*, *19*(1), 67-74.

Nel, A. E., Mädler, L., Velegol, D., Xia, T., Hoek, E. M., Somasundaran, P., Klaessig, F., Castranova, V., & Thompson, M. (2009). Understanding biophysicochemical interactions at the nano–bio interface. *Nature Materials, 8*(7), 543-557.

Nguyen, T. X., Huang, L., Gauthier, M., Yang, G., & Wang, Q. (2016). Recent advances in liposome surface modification for oral drug delivery. *Nanomedicine, 11*(9), 1169-1185.

Nielsen, C. K., Kjems, J., Mygind, T., Snabe, T., & Meyer, R. L. (2016). Effects of Tween 80 on growth and biofilm formation in laboratory media. *Frontiers in Microbiology, 7*, 1878.

Ninham, B., Evans, D., & Wei, G. (1983). The curious world of hydroxide surfactants. Spontaneous vesicles and anomalous micelles. *The Journal of Physical Chemistry, 87*(24), 5020-5025.

Nounou, M. M., El-Khordagui, L. K., Khalafallah, N. A., & Khalil, S. A. (2006). In vitro release of hydrophilic and hydrophobic drugs from liposomal dispersions and gels. *Acta Pharmaceutica-Zagreb-, 56*(3), 311-324.

Parhi, P., Mohanty, C., & Sahoo, S. K. (2012). Nanotechnology-based combinational drug delivery: an emerging approach for cancer therapy. *Drug Discovery Today, 17*(17), 1044-1052.

Padamwar, M. N., & Pokharkar, V. B. (2006). Development of vitamin loaded topical liposomal formulation using factorial design approach: drug deposition and stability. *International Journal of Pharmaceutics*, *320*(1-2), 37-44.

Park, J.-H., Cho, H.-J., Yoon, H. Y., Yoon, I.-S., Ko, S.-H., Shim, J.-S., Cho, J-H., Park, H. J., Kim, K., Kwon, C. I., & Kim, D. D. (2014). Hyaluronic acid derivative-coated nanohybrid liposomes for cancer imaging and drug delivery. *Journal of Controlled Release, 174*, 98-108.

Parodi, A., Quattrocchi, N., van de Ven, A. L., Chiappini, C., Evangelopoulos, M., Martinez, J. O., Brown, S. B., Khaled, Z. S., Yazdi, K. I., Enzo, V. M., Isenhart, L., Ferrari, M., & Enzo, M. V. (2013). Synthetic nanoparticles functionalized with biomimetic leukocyte membranes possess cell-like functions. *Nature Nanotechnology, 8*(1), 61-68.

Pattni, B. S., Chupin, V. V., & Torchilin, V. P. (2015). New developments in liposomal drug delivery. *Chemical Reviews, 115*(19), 10938-10966.

Petersen, H., Fechner, P. M., Martin, A. L., Kunath, K., Stolnik, S., Roberts, C. J., Fischer, D., Davies, M. C., & Kissel, T. (2002). Polyethylenimine-graft-poly (ethylene glycol) copolymers: influence of copolymer block structure on DNA complexation and biological activities as gene delivery system. *Bioconjugate Chemistry, 13*(4), 845-854.

Petros, R. A., & DeSimone, J. M. (2010). Strategies in the design of nanoparticles for therapeutic applications. *Nature Reviews Drug Discovery, 9*(8), 615-627.

Płaczek, M., & Kosela, M. (2016). Microscopic methods in analysis of submicron phospholipid dispersions. *Acta Pharmaceutica, 66*(1), 1-22.

Polyak, B., & Friedman, G. (2009). Magnetic targeting for site-specific drug delivery: applications and clinical potential. *Expert Opinion on Drug Delivery*, *6*(1), 53-70.

Prat, A., Parker, J. S., Karginova, O., Fan, C., Livasy, C., Herschkowitz, J. I., He, X., & Perou, C. M. (2010). Phenotypic and molecular characterization of the claudin-low intrinsic subtype of breast cancer. *Breast Cancer Research, 12*(5), R68.

Preté, P., Gomes, K., Malheiros, S., Meirelles, N., & De Paula, E. (2002). Solubilization of human erythrocyte membranes by non-ionic surfactants of the polyoxyethylene alkyl ethers series. *Biophysical Chemistry, 97*(1), 45-54.

Psarros, C., Lee, R., Antonopoulos, A., & Margaritis, M. (2016). Nanomedicine in cardiovascular disease. In *Nanotechnology and Drug Delivery, Vol. 2* (pp. 270-296). CRC Press.

Quail, D. F., & Joyce, J. A. (2013). Microenvironmental regulation of tumor progression and metastasis. *Nature Medicine, 19*(11), 1423-1437.

Quirion, F., & St-Pierre, S. (1991). Reduction of the in vitro hemolytic activity of soybean lecithin liposomes by treatment with a block copolymer. *Biophysical Chemistry*, *40*(2), 129-134.

Ramadass, S. K., Anantharaman, N. V., Subramanian, S., Sivasubramanian, S., & Madhan, B. (2015). Paclitaxel/Epigallocatechin gallate coloaded liposome: A synergistic delivery to control the invasiveness of MDA-MB-231 breast cancer cells. *Colloids and Surfaces B: Biointerfaces, 125*, 65-72.

Ramalingam, N., Natarajan, T., & Rajiv, S. (2015). Preparation and characterization of electrospun curcumin loaded poly (2-hydroxyethyl methacrylate) nanofiber—A biomaterial for multidrug resistant organisms. *Journal of Biomedical Materials Research Part A, 103*(1), 16-24.

Rengan, A. K., Jagtap, M., De, A., Banerjee, R., & Srivastava, R. (2014). Multifunctional gold coated thermo-sensitive liposomes for multimodal imaging and photo-thermal therapy of breast cancer cells. *Nanoscale, 6*(2), 916-923.

Reza Mozafari, M., Johnson, C., Hatziantoniou, S., & Demetzos, C. (2008). Nanoliposomes and their applications in food nanotechnology. *Journal of Liposome Research, 18*(4), 309-327.

Rindlisbacher, B., & Zahler, P. (1983). Interaction of phosphatidylcholine liposomes and plasma lipoproteins with sheep erythrocyte membranes: Preferential transfer of phosphatidylcholine containing unsaturated fatty acids. *Biochimica et Biophysica Acta (BBA)-Biomembranes*, *732*(3), 485-491.

Ripple, D. C., Montgomery, C. B., & Hu, Z. (2015). An interlaboratory comparison of sizing and counting of subvisible particles mimicking protein aggregates. *Journal of Pharmaceutical Sciences*, *104*(2), 666-677.

Roggers, R. A., Joglekar, M., Valenstein, J. S., & Trewyn, B. G. (2014). Mimicking red blood cell lipid membrane to enhance the hemocompatibility of large-pore mesoporous silica. *ACS Applied Materil and Interfaces, 6*(3), 1675-1681.

Ruan, S., Qian, J., Shen, S., Chen, J., Cun, X., Zhu, J., Jiang, X., He, Q., & Gao, H. (2015). Non-invasive imaging of breast cancer using RGDyK functionalized fluorescent carbonaceous nanospheres. *RSC Advances, 5*(32), 25428-25436.

Rutkowska, E., Pajak, K., & Jóźwiak, K. (2013). Lipophilicity--methods of determination and its role in medicinal chemistry. *Acta Poloniae Pharmaceutica, 70*(1), 3-18.

Sala, M., Miladi, K., Agusti, G., Elaissari, A., & Fessi, H. (2017). Preparation of liposomes: A comparative study between the double solvent displacement and the conventional ethanol injection—From laboratory scale to large scale. *Colloids and Surfaces A: Physicochemical and Engineering Aspects*, *524*, 71-78.

Sawdon, A., & Peng, C.-A. (2013). Engineering antiphagocytic biomimetic drug carriers. *Therapeutic Delivery, 4*(7), 825-839.

Scherließ, R. (2015). Nasal administration of vaccines. In *Subunit Vaccine Delivery* (pp. 287-306). Springer, New York, NY.

Schieren, H., Rudolph, S., Finkelstein, M., Coleman, P., & Weissmann, G. (1978). Comparison of large unilamellar vesicles prepared by a petroleum ether vaporization method with multilamellar vesicles: ESR, diffusion and entrapment analyses. *Biochimica et Biophysica Acta (BBA)-General Subjects*, *542*(1), 137-153.

Sercombe, L., Veerati, T., Moheimani, F., Wu, S. Y., Sood, A. K., & Hua, S. (2015). Advances and challenges of liposome assisted drug delivery. *Frontiers in Pharmacology, 6*(127*)*, 1-13.

Shabnama, P. S., & Babu, d. R. (2014). Formulation and evaluation of parenteral methotrexate nanoliposomes. *International Journal of Pharmacy and Pharmaceutical Sciences, 6*(11), 295-300.

Shah, S. (2011). Novel drug delivery carrier: resealed erythrocytes. *International Journal of Pharma and Bio Sciences, 2*(1), 395-406.

Shalel, S., Streichman, S., & Marmur, A. (2002). The mechanism of hemolysis by surfactants: effect of solution composition. *Journal of Colloid and Interface Science, 252*(1), 66-76.

Shamsi, M., & Islamian, J. P. (2017). Breast cancer: early diagnosis and effective treatment by drug delivery tracing. *Nuclear Medicine Review, 20*(1), 45-48.

Sharma, P., Banerjee, R., & Narayan, K. P. (2016). Mineralocorticoid receptor mediated liposomal delivery system for targeted induction of apoptosis in cancer cells. *Biochimica et Biophysica Acta (BBA)-Biomembranes, 1858*(2), 415-421.

Shemesh, C. S., Hardy, C. W., David, S. Y., Fernandez, B., & Zhang, H. (2014). Indocyanine green loaded liposome nanocarriers for photodynamic therapy using human triple negative breast cancer cells. *Photodiagnosis and Photodynamic Therapy, 11*(2), 193-203.

Shen, Y.-X., Saboe, P. O., Sines, I. T., Erbakan, M., & Kumar, M. (2014). Biomimetic membranes: A review. *Journal of Membrane Science, 454*, 359-381.

Shi, J., Kantoff, P. W., Wooster, R., & Farokhzad, O. C. (2017). Cancer nanomedicine: progress, challenges and opportunities. *Nature Reviews Cancer, 17*(1), 20-37.

Shroff, K., & Kokkoli, E. (2012). PEGylated liposomal doxorubicin targeted to α5β1-expressing MDA-MB-231 breast cancer cells. *Langmuir, 28*(10), 4729-4736.

Shroff, K., Liu, D., Aravalli, R. N., Forster, C. L., Pengo, T., Sanders, M. A., Ebbini, S. E., & Kokkoli, E. (2016). Design principles for peptide-amphiphile-induced liposomal receptor-targeting with intracellular thermosensitivity. *Chemistry of Nanomaterials, 2*(1), 42-48.

Sikora, A., Bartczak, D., Geißler, D., Kestens, V., Roebben, G., Ramaye, Y., ... & Minelli, C. (2015). A systematic comparison of different techniques to determine the zeta potential of silica nanoparticles in biological medium. *Analytical Methods*, *7*(23), 9835-9843.

Sikora, A., Shard, A. G., & Minelli, C. (2016). Size and ζ-potential measurement of silica nanoparticles in serum using tunable resistive pulse sensing. *Langmuir*, *32*(9), 2216-2224.

Simone, E. A., Dziubla, T. D., & Muzykantov, V. R. (2008). Polymeric carriers: role of geometry in drug delivery. *Expert Opinion on Drug Delivery*, *5*(12), 1283-1300.

Simonsen, L. O., Harbak, H., & Bennekou, P. (2011). Passive transport pathways for $Ca^{(2+)}$ and $Co^{(2+)}$ in human red blood cells. $_{(57)}Co^{(2+)}$ as a tracer for $Ca^{(2+)}$ influx. *Blood Cells, Moecules and Diseases, 47*(4), 214-225.

Sine, J., Urban, C., Thayer, D., Charron, H., Valim, N., Tata, D. B., Schiff, R., Blumenthal, R., Joshi, A., & Puri, A. (2015). Photo activation of HPPH encapsulated in –Pocket" liposomes triggers multiple drug release and tumor cell killing in mouse breast cancer xenografts. *International Journal of Nanomedicine, 10*, 125-145.

Skibinski, C. G., Das, A., Chen, K.-M., Liao, J., Manni, A., Kester, M., & El-Bayoumy, K. (2016). A novel biologically active acid stable liposomal formulation of docosahexaenoic acid in human breast cancer cell lines. *Chemico-Biological Interactions, 252*, 1-8.

Somaglino, L., Bouchoux, G., Mestas, J.-L., & Lafon, C. (2011). Validation of an acoustic cavitation dose with hydroxyl radical production generated by inertial cavitation in pulsed mode: Application to in vitro drug release from liposomes. *Ultrasonics Sonochemistry, 18*(2), 577-588.

Song, W.-Y., Yang, Q.-L., Zhao, W.-L., Jin, H.-X., Yao, G.-D., Peng, Z.-F., Shi, S.-L., Yang, H.-Y., Zhang, X.-Y., & Sun, Y.-P. (2016). The effects of anticancer drugs TSA and GSK on spermatogenesis in male mice. *American Journal of Translational Research, 8*(1), 221-229.

Spangler, R. S. (1990). Insulin administration via liposomes. *Diabetes Care*, *13*(9), 911-922.

Spill, F., Guerrero, P., Alarcon, T., Maini, P. K., & Byrne, H. M. (2015). Mesoscopic and continuum modelling of angiogenesis. *Journal of Mathematical Biology, 70*(3), 485-532.

Stetefeld, J., McKenna, S. A., & Patel, T. R. (2016). Dynamic light scattering: a practical guide and applications in biomedical sciences. *Biophysical Reviews*, *8*(4), 409-427.

Sun, W., Zhang, N., Li, A., Zou, W., & Xu, W. (2008). Preparation and evaluation of N3-O-toluyl-fluorouracil-loaded liposomes. *International Journal of Pharmaceutics*, *353*(1-2), 243-250.

Sun, X., Wang, C., Gao, M., Hu, A., & Liu, Z. (2015). Remotely controlled red blood cell carriers for cancer targeting and near-infrared light-triggered drug release in combined photothermal–chemotherapy. *Advanced Functional Materials*, *25*(16), 2386-2394.

Sun, Y., Kim, H. S., Saw, P. E., Jon, S., & Moon, W. K. (2015). Targeted therapy for breast cancer stem cells by liposomal delivery of siRNA against fibronectin EDB. *Advanced Healthcare Materials, 4*(11), 1675-1680.

Suzuki, R., Omata, D., Oda, Y., Unga, J., Negishi, Y., & Maruyama, K. (2016). Cancer therapy with nanotechnology-based drug delivery systems: applications and challenges of liposome technologies for advanced cancer therapy. In *Nanomaterials in Pharmacology* (pp. 457-482). Humana Press, New York, NY.

Szeto, G. L., & Lavik, E. B. (2016). Materials design at the interface of nanoparticles and innate immunity. *Journal of Materials Chemistry B*, *4*(9), 1610-1618.

Tacar, O., Sriamornsak, P., & Dass, C. R. (2013). Doxorubicin: an update on anticancer molecular action, toxicity and novel drug delivery systems. *Journal of Pharmacy and Pharmacology, 65*(2), 157-170.

Tanford, C. (1980). *The Hydrophobic Effect: Formation of Micelles and Biological Membranes (2nd ed.)*: J. Wiley.

Tang, C. Y., Zhao, Y., Wang, R., Hélix-Nielsen, C., & Fane, A. G. (2013). Desalination by biomimetic aquaporin membranes: Review of status and prospects. *Desalination, 308*, 34-40.

Tang, L., Yang, X., Yin, Q., Cai, K., Wang, H., Chaudhury, I., Yao, C., Zhou, Q., Kwon, M., Hartman, A. J., Dobrucki, T. I., Dobrucki, W. L., Brost, B. L., Lezmi, S., Helferich, G. W., Ferguson, L. A., Fan, M. T., & Cheng, J., (2014). Investigating the optimal size of anticancer nanomedicine. *Proceedings of the National Academy of Sciences, 111*(43), 15344-15349.

Tardieu, A., Luzzati, V., & Reman, F. (1973). Structure and polymorphism of the hydrocarbon chains of lipids: a study of lecithin-water phases. *Journal of Molecular Biology, 75*(4), 711-733.

Thorn, C. F., Oshiro, C., Marsh, S., Hernandez-Boussard, T., McLeod, H., Klein, T. E., & Altman, R. B. (2011). Doxorubicin pathways: pharmacodynamics and adverse effects. *Pharmacogenetics and Genomics, 21*(7), 440-446.

Tian, G., Zheng, X., Zhang, X., Yin, W., Yu, J., Wang, D., & Zhao, Y. (2015). TPGS-stabilized NaYbF 4: Er upconversion nanoparticles for dual-modal fluorescent/CT imaging and anticancer drug delivery to overcome multi-drug resistance. *Biomaterials, 40*, 107-116.

Tokumasu, F., Ostera, G. R., Amaratunga, C., & Fairhurst, R. M. (2012). Modifications in erythrocyte membrane zeta potential by Plasmodium falciparum infection. *Experimental Parasitology*, *131*(2), 245-251.

Torchilin, V. P. (2005). Recent advances with liposomes as pharmaceutical carriers. *Nature Reviews Drug Discovery, 4*(2), 145-160.

Tsai, M.-J., Huang, Y.-B., Fang, J.-W., Fu, Y.-S., & Wu, P.-C. (2015). Preparation and characterization of naringenin-loaded elastic liposomes for topical application. *PLoS ONE, 10*(7), Article # e0131026.

Tsai, W. C., & Rizvi, S. S. (2016). Liposomal microencapsulation using the conventional methods and novel supercritical fluid processes. *Trends in Food Science & Technology*, *55*, 61-71.

Ulusoy, U., & Igathinathane, C. (2016). Particle size distribution modeling of milled coals by dynamic image analysis and mechanical sieving. *Fuel Processing Technology*, *143*, 100-109.

Urbinati, G., Marsaud, V., Plassat, V., Fattal, E., Lesieur, S., & Renoir, J.-M. (2010). Liposomes loaded with histone deacetylase inhibitors for breast cancer therapy. *International Journal of Pharmaceutics, 397*(1), 184-193.

Vahidkhah, K., & Bagchi, P. (2015). Microparticle shape effects on margination, near-wall dynamics and adhesion in a three-dimensional simulation of red blood cell suspension. *Soft Matter*, *11*(11), 2097-2109.

Valbonesi, M., Bruni, R., Florio, G., Zanella, A., & Bunkens, H. (2001). Cellular contamination of plasma collected with various apheresis systems. *Transfusion and Apheresis Science, 24*(1), 91-94.

Van den Bogaart, G., Meyenberg, K., Diederichsen, U., & Jahn, R. (2012). Phosphatidylinositol 4, 5-bisphosphate increases Ca^{2+} affinity of synaptotagmin-1 by 40-fold. *Journal of Biological Chemistry*, *287*(20), 16447-16453.

Van der Geest, T., Laverman, P., Metselaar, J. M., Storm, G., & Boerman, O. C. (2016). Radionuclide imaging of liposomal drug delivery. *Expert Opinion on Drug Delivery, 13*(9), 1231-1242.

Varenne, F., Rustique, E., Botton, J., Coty, J.-B., Lanusse, G., Lahcen, M. A., Rio, L., Zandanel, C., Lemarchand, C., & Germain, M. (2017). Towards quality assessed characterization of nanomaterial: Transfer of validated protocols for size measurement by dynamic light scattering and evaluation of zeta potential by electrophoretic light scattering. *International Journal of Pharmaceutics, 528*(1-2), 299-311.

Vasir, J. K., & Labhasetwar, V. (2005). Targeted drug delivery in cancer therapy. *Technology in Cancer Research & Treatment, 4*(4), 363-374.

Vercauteren, D., Vandenbroucke, R. E., Jones, A. T., Rejman, J., Demeester, J., De Smedt, S. C., Sanders, N. N. & Braeckmans, K. (2009). The use of inhibitors to study endocytic pathways of gene carriers: Optimization and pitfalls. *Molecular Therapy, 18*(3), 561-569.

Verma, A., & Stellacci, F. (2010). Effect of surface properties on nanoparticle–cell interactions. *Small, 6*(1), 12-21.

Virtanen, J. A., Cheng, K. H., & Somerharju, P. (1998). Phospholipid composition of the mammalian red cell membrane can be rationalized by a superlattice model. *Proceedings of the National Academy of Sciences, 95*(9), 4964-4969.

Viswanathan, G., Hsu, Y. H., Voon, S. H., Imae, T., Siriviriyanun, A., Lee, H. B., Kiew, L. V., Chung, L. Y., & Yusa, S. i. (2016). A comparative study of cellular uptake and subcellular localization of doxorubicin loaded in self-assemblies of amphiphilic copolymers with pendant dendron by MDA-MB-231 human Breast Cancer Cells. *Macromolecular Bioscience, 16*(6), 882-895.

Wahajuddin, S. A. (2012). Superparamagnetic iron oxide nanoparticles: magnetic nanoplatforms as drug carriers. *International Journal of Nanomedicine, 7*, 3445-3471.

Wan, C., Allen, T. M., & Cullis, P. R. (2013). Lipid nanoparticle delivery systems for siRNA-based therapeutics. *Drug Delivery and Translational Research, 4*(1), 74-83.

Wan, J., Forsyth, A. M., & Stone, H. A. (2011). Red blood cell dynamics: from cell deformation to ATP release. *Integrative Biology, 3*(10), 972-981.

Wang, C.-J., Chen, T.-C., Lin, J.-H., Huang, P.-R., Tsai, H.-J., & Chen, C.-S. (2015). One-step preparation of hydrophilic carbon nanofiber containing magnetic Ni nanoparticles materials and their application in drug delivery. *Journal of Colloid and Interface Science, 440*, 179-188.

Wang, F., Jiang, X., & Lu, W. (2003). Profiles of methotrexate in blood and CSF following intranasal and intravenous administration to rats. *International Journal of Pharmaceutics, 263*(1-2), 1-7.

Wang, H., Zhao, P., Su, W., Wang, S., Liao, Z., Niu, R., & Chang, J. (2010). PLGA/polymeric liposome for targeted drug and gene co-delivery. *Biomaterials, 31*(33), 8741-8748.

Wang, Q., Zhao, T., Liu, Y., Xing, S., Li, L., & Gao, D. (2016). An evaluation of anti-tumor effect and toxicity of PEGylated ursolic acid liposomes. *Journal of Nanoparticle Research, 18*(2), 1-13.

Wang, X. H., Cai, L. L., Zhang, X. Y., Deng, L. Y., Zheng, H., Deng, C. Y., & Chen, L. J. (2011). Improved solubility and pharmacokinetics of PEGylated liposomal honokiol and human plasma protein binding ability of honokiol. *International Journal of Pharmaceutics*, *410*(1-2), 169-174.

Wei, X., Patil, Y., Ohana, P., Amitay, Y., Shmeeda, H., Gabizon, A., & Barenholz, Y. (2017). Characterization of pegylated liposomal mitomycin C lipid-based prodrug (Promitil) by high sensitivity differential scanning calorimetry and cryogenic transmission electron microscopy. *Molecular Pharmaceutics*, *14*(12), 4339-4345.

Wang, Z., Yu, Y., Dai, W., Lu, J., Cui, J., Wu, H., Yuan, L., Zhang, H., Wang, X., Wang, J., Zhang, X., & Chang, Q. (2012). The use of a tumor metastasis targeting peptide to deliver doxorubicin-containing liposomes to highly metastatic cancer. *Biomaterials, 33*(33), 8451-8460.

Weingart, J., Vabbilisetty, P., & Sun, X. L. (2013). Membrane mimetic surface functionalization of nanoparticles: methods and applications. *Advances in Colloid and Interface Science, 197*, 68-84.

Wong, M.-Y., & Chiu, G. N. (2011). Liposome formulation of co-encapsulated vincristine and quercetin enhanced antitumor activity in a trastuzumab-insensitive breast tumor xenograft model. *Nanomedicine: Nanotechnology, Biology and Medicine, 7*(6), 834-840.

Woodle, M. C. (1998). Controlling liposome blood clearance by surface-grafted polymers. *Advanced Drug Delivery Reviews*, *32*(1-2), 139-152.

Xiao, D., Jia, H.-Z., Ma, N., Zhuo, R.-X., & Zhang, X.-Z. (2015). A redox-responsive mesoporous silica nanoparticle capped with amphiphilic peptides by self-assembly for cancer targeting drug delivery. *Nanoscale, 7*(22), 10071-10077.

Xiao, K., Li, Y., Luo, J., Lee, J. S., Xiao, W., Gonik, A. M., Rinik, G. A., & Lam, K. S. (2011). The effect of surface charge on *in vivo* biodistribution of PEG-oligocholic acid based micellar nanoparticles. *Biomaterials, 32*(13), 3435-3446.

Xing, J., Qi, X., Jiang, Y., Zhu, X., Zhang, Z., Qin, X., & Wu, Z. (2015). Topotecan hydrochloride liposomes incorporated into thermosensitive hydrogel for sustained and efficient in situ therapy of H22 tumor in Kunming mice. *Pharmaceutical Development and Technology, 20*(7), 812-819.

Xu, F., Weng, B., Gilkerson, R., Materon, L. A., & Lozano, K. (2015). Development of tannic acid/chitosan/pullulan composite nanofibers from aqueous solution for potential applications as wound dressing. *Carbohydrate Polymers, 115*, 16-24.

Xu, R. (2015). Light scattering: A review of particle characterization applications. *Particuology*, *18*, 11-21.

Xu, Z. P., Zeng, Q. H., Lu, G. Q., & Yu, A. B. (2006). Inorganic nanoparticles as carriers for efficient cellular delivery. *Chemical Engineering Science, 61*(3), 1027-1040.

Yadav, A., Murthy, M., Shete, A., & Sakhare, S. (2011). Stability aspects of liposomes. *Indian Journal of Pharmaceutical Education and Research, 45*(4), 402-413.

Yazdanbakhsh, K., Lomas-Francis, C., & Reid, M. E. (2000). Blood groups and diseases associated with inherited abnormalities of the red blood cell membrane. *Transfusion Medicine Reviews, 14*(4), 364-374.

Yoo, J. W., Doshi, N., & Mitragotri, S. (2011). Adaptive micro and nanoparticles: temporal control over carrier properties to facilitate drug delivery. *Advanced Drug Delivery Reviews, 63*(14-15), 1247-1256.

Yoshida, A., Shigekuni, M., Tanabe, K., & Fujita, A. (2016). Nanoscale analysis reveals agonist-sensitive and heterogeneous pools of phosphatidylinositol 4-phosphate in the plasma membrane. *Biochimica et Biophysica Acta (BBA)-Biomembranes, 1858*(6), 1298-1305.

Yuan, W., Kuai, R., Dai, Z., Yuan, Y., Zheng, N., Jiang, W., Noble, C., Hayes, M., Szoka, F. C., & Schwendeman, A. (2017). Development of a flow-through usp-4 apparatus drug release assay to evaluate doxorubicin liposomes. *The AAPS Journal, 19*(1), 150-160.

Yue, X., & Dai, Z. (2016). Multifunctional Liposomes for Imaging-Guided Therapy. In *Advances in Nanotheranostics I* (pp. 301-336). Springer, Berlin, Heidelberg.

Zahmatkeshan, M., Gheybi, F., Rezayat, S. M., & Jaafari, M. R. (2016). Improved drug delivery and therapeutic efficacy of PEgylated liposomal doxorubicin by targeting anti-HER2 peptide in murine breast tumor model. *European Journal of Pharmaceutical Sciences, 86*, 125-135.

Zarrin, A., Foroozesh, M., & Hamidi, M. (2014). Carrier erythrocytes: recent advances, present status, current trends and future horizons. *Expert Opinion on Drug Delivery, 11*(3), 433-447.

Zhang, Y., Huo, M., Zhou, J.,s Zou, A., Li, W., Yao, C., & Xie, S. (2010). DDSolver: an add-in program for modeling and comparison of drug dissolution profiles. *The AAPS Journal, 12*(3), 263-271.

Zhou, Y., Wong, C. O., Cho, K. J., Van Der Hoeven, D., Liang, H., Thakur, D. P., & Hu, H. (2015). Membrane potential modulates plasma membrane phospholipid dynamics and K-Ras signaling. *Science*, *349*(6250), 873-876.

Zlatev, H. P., Auriola, S., Mönkkönen, J., & Määttä, J. A. (2016). Uptake of free, calcium-bound and liposomal encapsulated nitrogen containing bisphosphonates by breast cancer cells. *European Journal of Pharmaceutical Sciences, 86*, 58-66.

Zylberberg, C., & Matosevic, S. (2017). Bioengineered liposome–scaffold composites as therapeutic delivery systems. *Therapeutic Delivery, 8*(6), 425-445.

LIST OF PUBLICATIONS & PAPERS PRESENTED

Published Articles

1. **Naeem, S.,** Viswanathan, G., & Misran, M. B. (2018). Liposomes as colloidal nanovehicles: on the road to success in intravenous drug delivery. *Reviews in Chemical Engineering*, *34*(3), 365-383.

2. **Naeem, S.,** Kiew, L. V., Chung, L. Y., Suk, V. R. E., Mahmood, A., & Misran, M. B. (2016). Optimization of phospholipid nanoparticle formulations using response surface methodology. *Journal of Surfactants and Detergents*, *19*(1), 67-74.

3. **Naeem, S.,** Kiew, L. V., Chung, L. Y., Fui, K. S., & Misran, M. B. (2015). A comparative approach for the preparation and physicochemical characterization of lecithin liposomes using chloroform and non-halogenated solvents. *Journal of Surfactants and Detergents*, *18*(4), 579-587.

4. **Naeem, S.,** Kiew, L. V., Yong, C. L., Yin, Y. T., & Misran, M. B. (2015). Drug delivery and innovative pharmaceutical development in mimicking the red blood cell membrane. *Reviews in Chemical Engineering*, *31*(5), 491-508.

Oral Presentations

1. Liposomes as amphiphilic carriers: encapsulation and stability aspects, *InternationalPolymer Conference of Thailand* (PCT-6), 30 June 2016, Pathumwan Princess Hotel, Bangkok, Thailand

2. *In vitro* blood compatibility of red blood cell mimics: surfactant effect on haemolysis, International conference on *Emerging Research in Science and Humanities* (ERSH-2016), 16 May 2016, Pearl International Hotel, Kuala Lumpur, Malaysia.

3. A comparative approach for the preparation and physicochemical characterization of lecithin liposomes using chloroform and non-halogenated solvents, *World Congress on Pharmacology*, 20-22 July 2015, Brisbane, Australia.

4. Advanced pharmaceutical development in mimicking red blood cell carriers and its applications, International conference on *Nanoscience, Nanoengineering and Applications*, 24- 25 April 2015, Penang, Malaysia.